

UNIVERSITY OF SOUTHAMPTON

**ENHANCED ACCURACY AND PRECISION OF ANALYSIS
OF SELENIUM IN CLINICAL MATRICES**

By
Christine Elizabeth Sieniawska

Doctor of Philosophy

Trace Element Unit
Institute of Human Nutrition

April 2001

UNIVERSITY OF SOUTHAMPTON
ABSTRACT
FACULTY OF MEDICINE
INSTITUTE OF HUMAN NUTRITION

Doctor of Philosophy
**ENHANCED ACCURACY AND PRECISION OF ANALYSIS
OF SELENIUM IN CLINICAL MATRICES**
by Christine Elizabeth Sieniawska

Conventional calibration procedures using external standards or standard additions provide sufficient precision and accuracy of selenium concentrations for clinical purposes, but an enhanced quality of analysis is required for accurate analysis of reference materials and for valid comparisons of inter-laboratory studies on a world-wide scale. Isotope Dilution (ID) mass spectrometry, a technique reputed for achieving high accuracy measurements, was investigated to improve the reproducibility and accuracy of selenium determinations by established methods. Low resolution inductively coupled plasma mass spectrometry (ICP-MS) using solution nebulisation (SN) was used for the accurate and precise determination of selenium isotopes. The addition of butan-1-ol to the samples reduced the interferences normally experienced by direct analysis of selenium in biological matrices, and also enhanced signal response. Samples were spiked with a ⁷⁴Se-enriched isotopic standard, and accurate determinations of ⁷⁸Se:⁷⁴Se ratios were converted into concentrations, using regression line equations obtained from calibrating solution ratios. This produced significant improvements in precision over conventional (single isotopic) ICP-MS analysis. Between-run relative standard deviations approached those obtained within-run, and were 1.0-6.0% for 0.25 - 1.90 $\mu\text{mol l}^{-1}$ selenium. An interlaboratory comparison showed improved accuracy, with a reduced overall spread of bias to $0.0 \pm 0.05 \mu\text{mol l}^{-1}$ selenium for ID, compared with $-0.01 \pm 0.07 \mu\text{mol l}^{-1}$ for conventional analysis.

Alternative methodologies/instrumentation for ICP-MS were investigated to establish the degree of accuracy and precision attainable for the measurement of selenium in serum. These techniques were compared to a method developed for conventional standard addition analysis of selenium, in which samples were diluted 1+14 in 0.5% v/v butan-1-ol and the signal at mass 78 monitored. The accuracy of the described method was demonstrated by the laboratory's excellent performance in two External Quality Control Assessment schemes, over 18 months. Hydride generation (HG) was evaluated as a method of sample introduction for ICP-MS. Multi-Collector magnetic field (ICP-MC-MS) and Dynamic Reaction Cell (DRC-ICP-MS) instrumentation, which use collision or reaction cells to destabilise any polyatomic argon adducts, were also assessed for their potential to enhance precision in quantitative isotopic analysis. The order of both precision and accuracy of analysis was found to be: ID-DRC-ICP-MS \approx ID-SN- ICP-MS > DRC-ICP-MS \approx SN-ICP-MS >> HG-ICP-MS.

The devised method was used to investigate the distribution of selenium amongst serum proteins separated by affinity chromatography. Overall recoveries were $101 \pm 4\%$. A limited study of patients on Total Parenteral Nutrition (TPN) indicated that the lower serum selenium concentrations found in TPN patients, were associated with a decreased binding to albumin ($3 \pm 2\%$ for TPN patients, compared with $10 \pm 7\%$ in control subjects). No significant changes were seen in either of the other two major selenium containing proteins: selenoprotein P ($53 \pm 3\%$ TPN, $50 \pm 4\%$ controls), and glutathione peroxidase ($45 \pm 7\%$ TPN, $42 \pm 7\%$ controls).

LIST OF CONTENTS

Abstract	Page no:	ii
List of contents		iii
List of tables		vi
List of figures		ix
Abbreviations used		xiii
Acknowledgements		xiv
Statement		xv
Chapter 1: Selenium		1
1.1. Biochemical function		1
1.2. Dietary selenium		2
1.3. Absorption, metabolism and homeostasis		3
1.4. Assessment of selenium status		4
1.5. Changes in selenium status in the British population		6
1.6. Methods of analysis		6
Chapter 2: Inductively coupled plasma mass spectrometry		8
2.1. The Inductively coupled plasma		10
2.2. The sampling interface		13
2.3. Quadrupole mass spectrometer		14
2.4. Ion detection		16
2.5. Data collection		17
2.6. Alternative mass spectrometers		17
2.7. Spectral interferences		18
Chapter 3: Selenium determination by Inductively coupled plasma spectrometry		20
3.1. Introduction		20
3.2. Instrumentation		22
3.3. Reagents		22
3.4. Quality control		23
3.5. Standards		24
3.6. Sample preparation		24
3.7. Establishing the optimum butan-1-ol concentration		24
3.8. Effect of rf power on selenium analysis		25
3.9. Accuracy of analysis		26
3.10. Calibration curves		28
3.11. Modification to sample preparation		29
3.12. Tellurium as an internal standard		30
3.12.1. Optimisation of nebuliser gas flow		31
3.12.2. Optimisation of scanning parameters		32
3.12.3. Calibration curves		32

	Page number:
3.13. Accuracy and precision of analysis	33
3.13.1. Internal quality control	33
3.13.2. Intra-laboratory comparison	34
3.13.3. External quality assessment	34
3.14. Selenium determination in whole-blood and erythrocytes	37
3.14.1. Modifications to the serum method	38
3.14.2. Sample preparation of red blood cells	38
3.14.3. Internal quality control	39
3.14.4. External quality assessment	40
3.15. Conclusion	40
 Chapter 4: Serum selenium proteins	41
4.1. Introduction	41
4.2. Separation procedure	42
4.2.1. Materials and reagents	43
4.2.2. Column separation procedure	43
4.2.3. Selenium determination in sub-fractions	45
4.3. Reducing the volume of serum applied to the column	46
4.4. Selenium measurement in Fraction D	48
4.5. Selenium distribution in healthy adults	51
4.6. Selenium distribution in TPN patients	52
4.7. Conclusion	52
 Chapter 5: Selenium determination by isotope dilution	53
5.1. Introduction	53
5.2. Isotope ratio measurement	55
5.2.1. Mass bias correction	55
5.2.2. Dead time correction	55
5.2.3. Optimal blend	56
5.3. Isotopically enriched selenium standards	57
5.4. IDMS equations employed	58
5.5. Method	59
5.6. Optimisation of the mass scanning conditions	60
5.7. Aqueous analysis	61
5.8. Serum analysis	62
5.9. Optimal blend for ^{78}Se : ^{74}Se analysis	64
5.10. Optimisation of scanning parameters	65
5.11. Artificial matrix for calibrating mass bias solutions	67
5.12. Accuracy and precision of IDMS using NaCl calibration	70
5.13. Conclusion	72
 Chapter 6: Selenium determination by flow-injection HG-ICP-MS	74
6.1. Introduction	74
6.2. Instrumentation	74
6.3. Reagents and equipment	76
6.4. Procedure for sample digestion	77
6.5. Method for selenium analysis	77

	Page number
6.6. Use of internal standard	78
6.7. Internal quality control	80
6.8. Intra-laboratory comparison	81
6.9. IDMS by hydride generation	82
6.10. Conclusion	84
Chapter 7: Selenium determination by collision and reaction cell ICP-MS instrumentation	85
7.1. Multicollector magnetic sector mass spectrometer	85
7.1.1. Instrumentation	85
7.1.2. Conventional analysis	87
7.1.3. Isotope dilution	88
7.2. Dynamic reaction cell ICP-MS	89
7.2.1. Instrumentation and reagents	91
7.2.2. DRC optimisation	92
7.2.3. Use of organic solvent	97
7.2.4. Choice of internal standard	100
7.2.5. Method	100
7.2.6. Accuracy and precision	102
7.2.7. Whole-blood analysis	105
7.2.8. Conclusion	106
Chapter 8: Selenium determination by ID-DRC-ICP-MS	107
8.1. Using the ^{77}Se -enriched selenium isotope standard	107
8.1.1. Instrumental scanning parameters	108
8.1.2. Method	108
8.1.3. Accuracy	108
8.1.4. Conclusion	110
8.2. Using the ^{74}Se -enriched selenium isotope standard	110
8.2.1. Scanning parameters	110
8.2.2. Accuracy and precision	112
8.2.3. Conclusion	114
Chapter 9: Comparison of ICP-MS methodologies	115
9.1. Methodology	115
9.2. Assessment of analytical performance	116
9.2.1. Calibration and sensitivity	117
9.2.2. Detection limits	117
9.2.3. Accuracy and precision	118
9.2.4. Intra-laboratory comparison of EQA samples	120
9.3. Conclusion	122
Overall conclusions and suggestions for further work	123
References	126
Appendix I	136
Appendix II	142
Publications in support of candidature	146

LIST OF TABLES

	Page no:
1.1. Selenium content of food.	2
3.1. Isobaric interferents on selenium determination by ICP-MS.	20
3.2. Operating conditions for the ICP-MS.	22
3.3. Endogenous concentration of selenium found in serum.	25
3.4. Reagent volumes used for sample dilution.	29
3.5. Internal quality control data for between assay serum analysis, using indium and tellurium as the internal standards.	33
3.6. Internal quality control data for selenium in whole-blood.	39
4.1. Operating conditions for the ICP-MS.	45
4.2. Inter-laboratory comparison of the selenium distribution associated with protein fractions of two serum samples.	46
4.3. Comparison of the protein distribution found for the Sigma serum at $38.5\mu\text{g l}^{-1}$ total selenium, when separated on columns with 8 ml and 2 ml bed volumes.	47
4.4. Selenium distribution in a healthy population, expressed as a percentage of total selenium and as a selenium concentration.	51
4.5. Selenium distribution in TPN samples, expressed as a percentage of total selenium and as a selenium concentration.	52
5.1. Isotopic abundances for the ^{74}Se and ^{77}Se -enriched selenium standards.	57
5.2. Operating conditions for the Elan 6100 ICP-MS.	59
5.3. Measurement of selenium in aqueous solutions by conventional and IDMS analysis using ^{77}Se and ^{74}Se -enriched isotope standards, with and without reference solution correction.	61
5.4. Comparison of measured aqueous and serum reference solution ratio values, obtained on spiking with $30\mu\text{g l}^{-1}$ $^{77}\text{Se}/3$ and $17\mu\text{g l}^{-1}$ ^{74}Se standard.	62
5.5. Major constituents of serum.	67
5.6. Internal quality control data for serum analysis by IDMS (NaCl calibration).	71
6.1. Operating conditions for the ICP-MS and the parameter file for the analysis of serum digests.	75
6.2. Fias programme.	76

6.3. Comparison of the RSDs obtained for five measurements of serum digest containing selenium at 80 $\mu\text{g l}^{-1}$ for ^{77}Se , ^{78}Se and ^{82}Se signals on normalisation to ^{128}Te and ^{131}Xe .	79
6.4. Internal quality control data for serum analysis by measurement of ^{77}Se , ^{78}Se and ^{82}Se , for ten determinations.	80
6.5. Comparison of the RSDs obtained for five measurements of serum digest containing selenium at 80 $\mu\text{g l}^{-1}$ for ^{77}Se , ^{78}Se and ^{82}Se signals, spiked with ^{77}Se -enriched standard at 20 $\mu\text{g l}^{-1}$.	83
7.1. Operating conditions for the ICP-MC-MS.	87
7.2. Observed concentrations obtained for IQCs by ICP-MC-MS.	88
7.3. Operating conditions for the DRC-ICP-MS	92
7.4. Comparison of parameter settings for optimal conditions for ^{78}Se determination with and without butan-1-ol, using a cross flow nebuliser.	98
7.5. Percentage relative standard deviation of the analysis of five dilutions of bovine serum (55 $\mu\text{g l}^{-1}$ endogenous selenium level) on increasing the dwell time and sweeps per reading, monitoring ^{78}Se .	101
7.6. Internal quality control data for serum analysis by DRC-ICP-MS.	103
7.7. Internal quality control data for selenium in whole-blood by DRC and direct ICP-MS detection.	105
8.1. Calculated and measured ratios for selenium isotopes at 80 $\mu\text{g l}^{-1}$ selenium spiked with the calculated optimal blend of ^{77}Se -enriched standard.	107
8.2. Comparison of aqueous, sodium chloride and serum ratio values obtained for ^{78}Se : ^{77}Se measurement.	109
8.3. Change of the isotopic ratios obtained by ^{74}Se IDMS with increasing q value, employing 100 $\mu\text{g l}^{-1}$ ^{74}Se spike.	111
8.4. Internal quality control data for serum analysis by ID-DRC-ICP-MS.	113
9.1. Internal quality control data for serum determination by conventional analysis using SN-ICP-MS (Series A IQCs employed).	118
9.2. Internal quality control data for serum determination by HG-ICP-MS, IDMS, conventional and ID analysis using DRC-ICP-MS (Series B IQCs employed).	119

Appendix I

1. Measurement of selenium in serum solutions by direct ICP-MS and HG-AAS.	136
2A. Measurement of selenium in serum solutions by IDMS and conventional analysis using ^{77}Se -enriched and ^{74}Se -enriched standards.	137
2B. Measurement of ^{77}Se : ^{74}Se ratio.	138
3. Measurement of selenium in serum solutions by IDMS and conventional analysis.	139
4. Measurement of selenium in serum solutions by HG-ICP-MS and conventional SN-ICP-MS analysis.	140
5. Measurement of selenium in serum solutions by DRC-ICP-MS, ^{78}Se : ^{74}Se ID-DRC-ICP-MS, and conventional SN-ICP-MS analysis.	141

Appendix II

6. Reagent volumes used for sample dilution for conventional and ID-ICP-MS analysis.	145
--	-----

LIST OF FIGURES

	Page no:
1.1. Whole-blood selenium concentrations in human populations world-wide.	5
2.1. Schematic representation of the Perkin-Elmer Sciex Elan 5000.	9
2.2. Mass stability diagram for ion transmission through the quadrupole field, showing the scan line at high and low resolution.	15
3.1. Change in signal intensities for selenium isotopes on increasing the butan-1-ol concentration; for aqueous blanks and a bovine serum sample.	24
3.2. Effect of rf power and of 1% butan-1-ol on ^{78}Se and ^{115}In signals.	26
3.3. Comparison of serum selenium concentrations observed with the target values for the three isotopes: ^{77}Se , ^{78}Se and ^{82}Se .	27
3.4. Aqueous, bovine serum and whole-blood calibration curves.	28
3.5. Regression lines for ^{78}Se measurement in bovine serum and plasma.	30
3.6. The change in signal intensity at m/z ratio 78, 115, 125, 126 and 128 with increasing concentration of butanol (at 1.0 l min^{-1} nebuliser gas flow).	31
3.7. The effect of the intensity of signals at m/z ratio 78, 115 and 128 with increasing nebuliser flow rate, in the presence of 0.5% butan-1-ol.	31
3.8. Aqueous, bovine serum and whole-blood calibration curves, using tellurium as the internal standard.	32
3.9. Comparison of within run and between run precision for analysis employing indium and tellurium as internal standards.	33
3.10. Bland Altman plot of the bias of measured serum samples determined by ICP-MS and HG-AAS, compared with target values.	34
3.11. Performance in EQA schemes for selenium in serum –January 1997 to December 1998, showing proximity to target values	35
3.12. Differences between reported and target values in the EQA schemes: Quebec and UK-TEQAS, from January 1997 to December 1998.	35
3.13. Performance in EQA schemes for selenium in serum –January 1999 to July 2000, showing proximity to target values.	36
3.14. Differences between reported and target values in the EQA schemes: Quebec and UK-TEQAS, from January 1999 to July 2000.	36
3.15. Standard additions calibration curves for ^{78}Se in whole-blood and red blood cells.	38

	Page no:
4.1. A schematic diagram showing the separation procedure for the heparin Sepharose and blue-Sepharose columns.	44
4.2. Profile of eluted sub-fractions of 8 ml columns, for 2.0 ml bovine serum.	47
4.3. Profile of eluted sub-fractions of 2 ml columns, for 500 µl bovine serum.	48
4.4. Selenium standard additions to ammonium acetate buffer, elution buffers 1 and 2.	49
4.5. Signal intensity at m/z 78 for two Seronorm serum aliquots, and at 82m/z for sample 2.	49
4.6. Selenium elution profiles of serum proteins, obtained using buffers containing increasing concentrations of NaCl from the blue-Sepharose column.	50
5.1. Log-log plot of the error magnification factor as a function of natural:spike selenium isotopic ratios (^{78}Se : ^{74}Se and ^{78}Se : ^{77}Se).	58
5.2. Percent relative standard deviation and the observed isotopic ratio (^{78}Se : ^{77}Se), as a function of dwell time.	61
5.3. Comparison of the bias from target values, of serum samples analysed by IDMS using the ^{74}Se -enriched standard of 80-corrected and 40/80/160 corrected results with aqueous and serum reference solution calibration.	63
5.4. Comparison of the bias from target values, of serum samples analysed by IDMS using the ^{77}Se -enriched standard of 80 corrected and 40/80/160 corrected results with aqueous and serum reference solution calibration.	63
5.5. Calculated and measured ^{78}Se : ^{74}Se ratios as a function of increasing levels of selenium, on addition of ^{74}Se -enriched standard at $17 \mu\text{g l}^{-1}$ and $100 \mu\text{g l}^{-1}$.	65
5.6. Percent relative standard deviation as a function of the number of ^{78}Se : ^{74}Se ratio measurement as a function of the dwell time.	66
5.7. Effect of albumin and NaCl on the observed ^{78}Se : ^{74}Se isotopic ratio, for reference solutions at 0, 40, 80, 160 $\mu\text{g l}^{-1}$ selenium.	68
5.8. Serum selenium concentrations determined using serum (graphical method and by 3 level correction), NaCl and aqueous reference solutions at 0, 40, 80, 160 $\mu\text{g l}^{-1}$, plotted against target values.	69
5.9. Comparison of the bias from target values, of serum samples determined by IDMS (NaCl calibration) with conventional quantitative analysis.	70
5.10. Comparison of within and between run precision data for IDMS with conventional ICP-MS analysis of IQC material.	71

	Page no:
6.1. Schematic diagram of FIAS-200	75
6.2. The signal response of the ICP-MS showing the peak profile obtained under optimised conditions for serum digest containing $150\mu\text{g l}^{-1}$ selenium.	78
6.3. Comparison of standard additions for ^{77}Se , ^{78}Se , ^{82}Se signals, without any normalisation and on normalisation to ^{128}Te and ^{131}Xe .	79
6.4. Comparison of within and between run precision data for HG-ICP-MS with conventional pneumatic ICP-MS analysis of IQC material.	80
6.5. Comparison of the bias from target values, of serum samples analysed by HG-ICP-MS using ^{77}Se , ^{78}Se , ^{82}Se isotopes.	86
6.6. Blank signals observed for ^{74}Se , ^{77}Se , ^{78}Se and ^{82}Se , pre and post analysis of spiked sample at $140\mu\text{g l}^{-1}$ natural selenium, giving 58000, 13500, 34800, 12250cps, respectively.	82
6.7. Measured ^{78}Se : ^{77}Se and ^{82}Se : ^{77}Se isotopic ratios as a function of increasing levels of selenium in the test sera, on addition of ^{77}Se -enriched standard at $20\mu\text{g l}^{-1}$.	83
7.1. Schematic representation of the Micromass Isoprobe.	86
7.2. Layout of the Perkin-Elmer Elan 6100DRC ICP-MS.	89
7.3. Methane gas flow optimisation plot showing signal profiles for background and $10\mu\text{g l}^{-1}$ Se as the gas flow is increased, for ^{78}Se .	93
7.4. Methane gas flow optimisation plot showing signal profiles for background and $10\mu\text{g l}^{-1}$ Se as the gas flow is increased, for ^{80}Se .	94
7.5. Signal profiles for background and $10\mu\text{g l}^{-1}$ Se for ^{77}Se , in a CaCl matrix as the methane gas flow is increased.	94
7.6. Selenium isotope scan of 1+14 dilution bovine serum with Se at $100\mu\text{g l}^{-1}$ in 0.5% butanol, $\alpha = 0$ and $q = 0.45$, showing interferences present at m/z of 77, 80, and 82.	95
7.7. Selenium isotope scan of 1+14 dilution bovine serum with Se at $100\mu\text{g l}^{-1}$ in 0.5% butan-1-ol, $\alpha = 0$ and $q = 0.7$, broad lines showing abundances with respect to the signal at ^{78}Se .	95
7.8. Selenium isotope scan of water, showing the presence of interferences in the analytical region of interest ($q = 0.6$).	96
7.9. Schematic diagram showing cell rod offset, cell path voltage, and quad rod offset parameters.	98
7.10. DRC nebuliser flow optimisation profiles for samples with and without butan-1-ol, showing the change in signal response with increased nebuliser flow rate.	99
7.11. The effect of the intensity of signals at m/z ratio 76, 78, 80, and 125 with increasing concentration of butan-1-ol.	99
7.12. Selenium standard additions to water, bovine serum (endogenous value = $10\mu\text{g l}^{-1}$ Se) and bovine blood ($55\mu\text{g l}^{-1}$ Se) in 0.5% butan-1-ol, using ^{125}Te internal standard.	101

7.13. Comparison of the bias from target values, of serum samples determined by DRC-ICP-MS.	103
7.14. Comparison of within and between run precision data for DRC-ICP-MS with conventional ICP-MS analysis of IQC material.	104
7.15. Performance in EQA schemes for selenium in serum, November 2000 to April 2001, showing proximity to target values.	104
8.1. Comparison of ^{78}Se : ^{77}Se isotopic ratios obtained for bovine serum, sodium chloride (140 mmol $^{-1}$) and aqueous reference solutions at 0, 40, 80, 160 $\mu\text{g l}^{-1}$.	109
8.2. Bias from target values of serum samples determined by ^{78}Se : ^{77}Se DRC-IDMS with serum calibration.	110
8.3. Comparison of ^{78}Se : ^{74}Se isotopic ratios obtained for serum, sodium chloride and aqueous reference solutions at 0, 40, 80, 160 $\mu\text{g l}^{-1}$, spiked with ^{74}Se standard at 100 $\mu\text{g l}^{-1}$, with q at 0.45 and 0.7.	112
8.4. Comparison of the bias from target values, of serum samples determined by ID-DRC-ICPMS, using ^{74}Se enriched standard at 100 $\mu\text{g l}^{-1}$, with NaCl calibration.	113
9.1. Standard addition calibration curves obtained for conventional analysis carried out by hydride generation and DRC-ICP-MS, compared to direct ICP-MS analysis.	116
9.2. Measured isotopic ratios as a function of increasing levels of selenium for direct and DRC-ICP-MS analysis, using 100 $\mu\text{g l}^{-1}$ ^{74}Se spike (NaCl calibration).	117
9.3. Comparison of within-run precision data for conventional and ID analysis by direct SN-ICP-MS and DRC, and for HG ICP-MS analysis	119
9.4. Comparison of between-run precision data for conventional and ID analysis by direct SN-ICP-MS and DRC, and for HG ICP-MS analysis.	120
9.5. Comparison of the bias from target values, of sera determined by conventional and ID analysis by direct (SN) and DRC-ICP-MS, and HG-ICP-MS.	121

ABBREVIATIONS

ac	Alternating current
dc	Direct current
CI	Confidence interval
cps	Counts per second
DRC	Dynamic reaction cell
DRC-ICP-MS	Dynamic reaction cell inductively coupled plasma mass spectrometry
EQA	External quality assessment
GFAAS	Graphite furnace atomisation absorption spectrometry
HG	Hydride generation
HG-AAS	Hydride generation atomisation absorption spectrometry
HG-ICP-MS	Hydride generation inductively coupled plasma mass spectrometry
ICP-MS	Inductively coupled plasma mass spectrometry
ICP-MC-MS	Inductively coupled plasma Multicollector mass spectrometry
ID	Isotope dilution
IDMS	Isotope dilution mass spectrometry
IQC	Internal quality control
LGC	Laboratory of the Government Chemist
rf	Radio frequency
r	Correlation coefficient
RSD	Relative standard deviation
sd	Standard deviation
SN-ICP-MS	Solution nebulisation inductively coupled plasma mass spectrometry
UK-NEQAS	National external quality assessment scheme

ACKNOWLEDGEMENTS

I would like to thank my supervisor Dr H. Trevor Delves for his guidance and encouragement during my research and in the preparation of this thesis. I am indebted to Dr Ben Fairman and Justine Turner of the Laboratory of the Government Chemist, for their advice and support, particularly with respect to the isotope dilution work.

I would like to extend my thanks to Maryanne Thomsen of Perkin-Elmer for technical support in the use of the Elan 6100DRC, and Prof. R. Nesbitt for the use of the Micromass Isoprobe at the Southampton Oceanography Centre, with technical help provided by Dr R. Taylor and Dr A. Milton.

A large part of the work carried out in this thesis was supported by the Department of Trade and Industry as part of the National Measurement System Valid Analytical Measurement Programme, funded by The Laboratory of the Government Chemist.

CHAPTER 1

SELENIUM

Concern over the overall health of the British population due to evidence of falling intakes of selenium, is initiating a large amount of interest in the measurement of the element in clinical matrices. Selenium is both an essential and a toxic element, with its beneficial effects occurring in a narrow range of concentrations. In this chapter, the nutritional importance of selenium is reviewed.

1.1 Biochemical function

Despite the awareness of selenium-dependent conditions in a variety of animal diseases since the 1930's, it was not until 1957, that selenium was first recognised as nutritionally important. Schwartz and Foltz¹ findings on the element's ability to prevent dietary liver necrosis in laboratory animals gave rise to the use of selenium supplementation to maintain the health of livestock. The realisation of selenium as an essential element for humans, however occurred when Rotruck et al.² presented evidence for it being an integral component of the enzyme, glutathione peroxidase (EC 1.11.1.9) in 1973. Catalysing the reduction of hydrogen peroxide and fatty acid hydroperoxides that would otherwise damage cell membranes, glutathione peroxidase, together with vitamin E, catalase and superoxide dismutase, is part of the antioxidant defence systems of the body. Having ascribed to selenium a specific biochemical function, dietary selenium has been studied as to its role in protecting the body from oxidative damage³. Selenium status has been linked with the risk of certain degenerative diseases, such as cancer⁴ and cardiovascular disease⁵, and recent studies have shown that oxidative stress induced by low selenium uptake, is implicated in the pathogenesis of several viral infections, including hepatitis and AIDS³.

A number of selenocysteine containing enzymes have now been identified, these include three other types of glutathione peroxidases, type I iodothyronine 5'-deiodinase, and thioredoxin reductase, which is involved in the formation of deoxyribonucleotides⁶. Selenium's role in thyroid hormone metabolism appears to be two-fold. The selenoenzyme, type I iodothyronine 5'-deiodinase converts thyroxine (T4) to the more metabolically active form triiodothyronine (T3)⁷, and glutathione peroxidase is involved in the detoxification of the hydrogen peroxide produced on the synthesis of hormones by the thyroid gland⁸. The

selenium deficiency in Central Africa has been found to be severe enough to induce disturbance of thyroid hormone metabolism⁸.

Another selenoenzyme system is the sperm specific selenoprotein. It is required for testosterone biosynthesis, and the normal development of spermatozoa⁹. Phospholipid hydroperoxide glutathione peroxidase acts as a soluble enzyme early in sperm development and later polymerises into a protein mesh that contributes to the structural integrity of the sperm¹⁰. Low selenium status has been associated with miscarriage, whereby deficiency concentrations of selenium dependent glutathione peroxidase are believed to induce early pregnancy loss, as a consequence of reduced antioxidant protection of biological membranes and DNA¹¹.

1.2. Dietary selenium

Selenium is typically found in protein fractions of foods, and is therefore present in muscle meat, organ meat such as liver and kidney, fish, nuts, beans and grains. Fish appears to be a good source of selenium. Although the bioavailability of the element from fish may be as low as half that of selenite, a change to a diet rich in fish has been found to increase the selenium content in the plasma of healthy subjects¹². Fruits and vegetables are poor sources of selenium (Table 1.1.).

Table 1.1. Selenium content of food¹³⁻¹⁵

Food	Selenium content µg /100g	Food	Selenium content µg /100g
Kidney	60 - 280	Brazil nuts	230 - 5300
Liver	6 - 140	Other nuts	<1 - 70
Fish	10 - 130	Cereals	2 - 50
Meat	<1 - 30	Fruit	<1
Dairy products	<1 - 14	Vegetables	<2
Tea/Coffee	4 - 12	Butter beans	2 - 45
Sugar	<1	Houmus	3 - 105

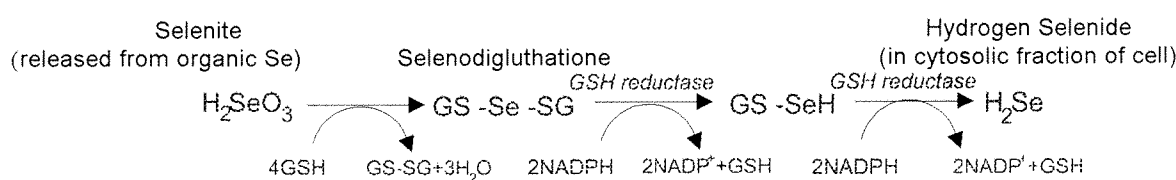
Although the selenium content of crops can depend on the nature of the soil in which they are grown (porous alkaline soils render the element more available), generally they correspond to soil levels¹⁶. In isolated rural communities, where there is little interchange of foods from different areas, a significant correlation exists between the soil levels and the

selenium status of the population¹⁷. This has been demonstrated by reports in dietary intake in China, which have varied from 11 µg (0.14 µmol l⁻¹) selenium per day, in areas where selenium deficiency has been located with a prevalence of a cardiomyopathy: Keshan disease, to an intake of greater than 750 µg (9.5 µmol)/day in high selenium areas¹⁸. The World Health Organisation has recommended a dietary range of 50-200 µg (0.63- 2.53 µmol) per day of selenium¹⁹.

1.3. Absorption, metabolism and homeostasis

Selenoamino acids, such as selenomethionine and selenocysteine, are the principle dietary forms of selenium. It is these organic forms that appear to be absorbed to a greater extent than the inorganic species, such as sodium selenite commonly used as a supplement²⁰. While selenite is reliant on passive diffusion, active absorption of selenomethionine is thought to be via the same mechanism as methionine. Selenium absorption in the gastrointestinal tract, has been found to be inhibited by methionine, cadmium, arsenic, mercury and lead, while vitamins A,C and E act as stimulators²¹. Once in the plasma, it binds to carrier proteins, such as albumin, to be distributed to tissues where it is incorporated in newly synthesised selenoproteins^{22,23}. Kinetic models based on findings obtained using stable isotopes of both inorganic selenium²⁴, and selenomethionine²⁵, have been proposed. These include selenium uptake by the liver-pancreas subsystem after passing through the gastrointestinal tract, enterohepatic recirculation, and slowly turning over tissue pools. Transport is through four components of the plasma pool, which may be selenium metabolites.

Metabolism of selenium involves the reduction of selenite to selenide, and a number of selenium metabolism pathways have been demonstrated relating to various cell fractions in laboratory animals²⁴. Erythrocytes have an active role in selenium's removal from the blood stream^{26,27}. A proposed mechanism for selenium metabolism in erythrocytes includes the process of its successive reduction catalysed by glutathione reductase, and its sequence is summarised by the following equation:



Selenide is incorporated into selenoprotein as selenocysteine. On selenium metabolism, toxic compounds with hydrogen are formed and released into the plasma where they can combine with proteins or be acted on by methyl-transferase, to convert these compounds into the corresponding less toxic methyl-derivatives. These include monomethylselenol, trimethylselenium, dimethyl selenide and dimethyl diselenide. While dimethyl diselenide is eliminated by expiration, these methyl-derivatives are excreted in the urine, and may play a significant role in the detoxification of excess selenium intake²⁸. 50-70% of selenium intake is excreted in the urine, mainly in the form of trimethylselenium but also as selenoaminoacids and selenite, thereby maintaining selenium homeostasis^{29,30}.

1.4. Assessment of selenium status

The preferred indexes of human selenium status are whole-blood, plasma/serum concentrations of the element, and the level of activity of the selenium-dependant enzyme, gluthathione peroxidase (GSH-Px) in erythrocytes¹⁸. Urinary excretion can vary considerably, 20-200µg selenium per day, depending on dietary habits²⁹, and therefore measurement is limited to monitoring occupational exposure. Increased urinary excretion of selenium has been reported in workers exposed to mercury²⁹, a consequence of the protective interactions that occur between selenium and several heavy toxic metals³¹. In assessing the selenium status of a population in remote parts of the world, nail and hair analysis employing strict standardisation (with the awareness of the selenium content of the shampoos³²) have been used as a convenient indicator of both deficiency and toxicity^{33,34}. These offer a long-term marker of selenium status, which have been shown to relate to geographical variations in selenium levels^{34,35}.

Blood levels show the geographical variation that is indicative of the differences in selenium availability (Figure 1.1.). Low blood selenium concentrations are associated with Keshan disease (a cardiomyopathy), Kashin-Beck disease (a deforming arthritis afflicting children)³⁶, and iodine-deficiency disorders particularly in areas of Zaire^{17,20}.

Selenium has a low threshold of toxicity commencing at ten times the dietary requirement. Chronic selenium poisoning is characterised by gastro-intestinal disturbance, 'garlic breath', hair loss, changes in fingernail morphology, skin lesions and nervous system abnormalities. These functional signs of excessive selenium intake were found to be

associated with regions of China where the daily selenium intake exceeded 850 μg (10.8 μmol)³⁷, and other seleniferous areas such as Venezuela¹⁷.

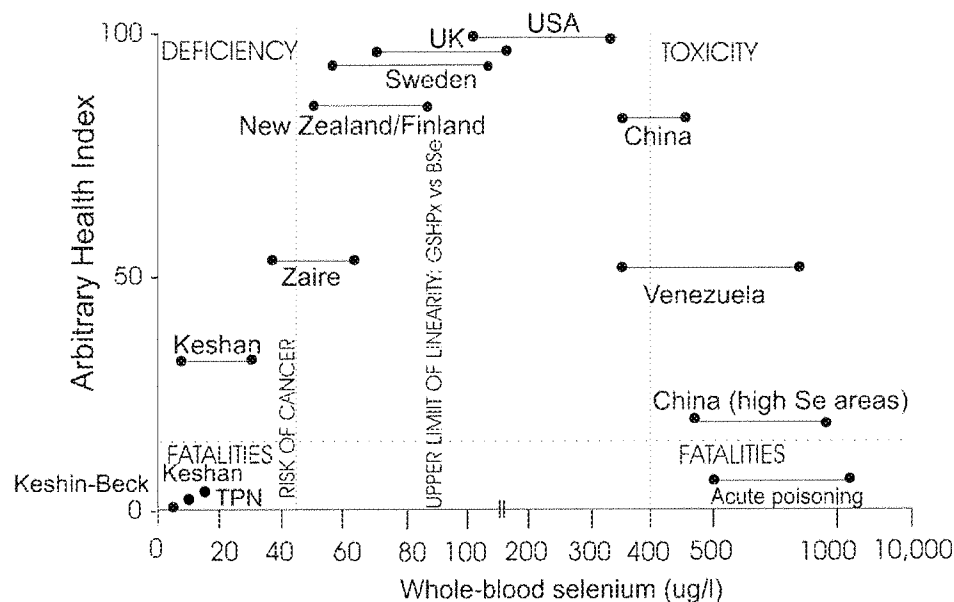


Figure 1.1. Whole-blood selenium concentrations in human populations world-wide¹⁷.
(Based on a figure produced by HTD Delves)

The lowest concentration of selenium in health have been found in infants of less than 4 months old, with milk generally being a poor source of selenium³⁸. However, a study to investigate the influence of maternal selenium status on the iodine content of breast milk demonstrated a regional variation of selenium in breast milk according to geographical location³⁹. The mean selenium content of breast milk in three groups of lactating mothers were $16\pm 4 \mu\text{g l}^{-1}$ ($0.20\pm 0.05 \mu\text{mol l}^{-1}$) for Europe, $42\pm 10 \mu\text{g l}^{-1}$ ($0.53\pm 0.13 \mu\text{mol l}^{-1}$) for Venezuela and $112\pm 40 \mu\text{g l}^{-1}$ ($1.42\pm 0.51 \mu\text{mol l}^{-1}$) for a seleniferous region in Venezuela. A positive correlation was found between selenium and iodine in all populations, although an inverse correlation was evident between the organic bound iodine and the selenium, at breast milk selenium levels higher than $70 \mu\text{g l}^{-1}$ ($0.89 \mu\text{mol l}^{-1}$).

Dietary supplements, until recently, contained insufficient levels of selenium giving rise to the low reference levels found in groups of patients on long-term parenteral nutrition (TPN)⁴⁰, and those suffering with phenylketonuria⁴¹. Low blood selenium levels have been observed as an effect of surgical stress, severe burns and a number of pathological

conditions including colonic, gastric and pancreatic carcinoma and cirrhosis^{40,42}.

Impairment of the antioxidative defences by the reduction of glutathione peroxide activity at low selenium levels is thought to promote viral propagation, which is implicated in the pathogenesis of myocardial viral infections and AIDS³, with selenium supplementation specifically aiding suppression of viral replication⁴³.

1.5. Changes in selenium status in the British population

The most recent determinations of the dietary intake of the British population were calculated to be 34 µg (0.43 µmol)/day in 1995¹⁵ and 49 µg (0.62 µmol)/day in 1997⁴⁴. These estimates are well below the government's defined reference nutrient intake at 75 µg (0.43 µmol) and 60 µg (0.76 µmol)/day for adult males and females, and ranks Britain as one of the countries of lowest measured selenium consumption. In 1978, the average British diet provided around 60µg (0.76µmol) of selenium/day¹⁵, of which half was derived from cereals and the remainder from meat and fish. The effects of the changed source of the higher protein flours during the past twenty years are responsible for much of this reduced intake, as home-grown and European flour with lower selenium content have replaced the Canadian flour used for bread making. These falling levels are reflected in reduced blood selenium concentrations monitored over several years. A 42% decrease over a period of eight years occurred in selenium whole-blood concentrations in Scotland⁴⁵, and an average drop of 6% was seen in a study carried out over two years in four regions of England⁴⁶.

Selenium deficiency is a widespread problem amongst crop production and grazing livestock in many areas of Britain⁴⁷, and the need for selenium supplementation is being assessed. New Zealand was the first country where selenium was added to fodder for livestock⁴⁸, and later supplementation studies gave support to the benefits of maintaining an adequate selenium status in humans⁴⁹. Concern that the lower reference range could be detrimental to the overall health of the population, a number of selenium surveys are being commissioned to assess the health significance of low selenium intake and the need for supplementation, in addition to cancer prevention and treatment trials⁵⁰.

1.6. Methods of analysis

Methods currently used in the analysis of selenium in clinical specimens have been reviewed by Sheehan and Halls⁵¹. Hydride generation atomic absorption spectrometry (HG-

AAS), graphite furnace atomic absorption spectrometry (GF-AAS), and molecular fluorescence spectrometry are widely used for the determination of the element in serum and urine. In molecular fluorescence spectrometry, selenium is complexed with 2,3-diamino-naphthalene to produce a fluorophore, the fluorescence of which can be measured⁵². Wet-digestion of the sample is necessary to convert all the selenium into the inorganic form, and the reduction of the element to the required valency, Se(IV), is usually carried out by heating with hydrochloric acid. This sample preparation is also necessary for HG-AAS analysis, whereby Se(IV) is converted to hydrogen selenide by reduction with sodium borohydride. The hydride is taken by a carrier gas to a cell (heated to 800°C) in the light beam of an atomic absorption spectrometer^{53, 54}. GF-AAS measures selenium directly without prior digestion, using nickel or palladium as chemical modifiers to stabilise the selenium during the ashing stage of analysis^{55,56}.

Inductively-coupled plasma mass spectrometry (ICP-MS) offers great sensitivity for the measurement of selenium, but with direct analysis on the low resolution instruments being subject to spectral interferences from polyatomic species, hydride generation, chromatography, or ion-exchange, have been used to isolate the analyte from matrix associated interferences⁵⁷⁻⁵⁹. The time consuming sample preparations that are required by these methods are a disadvantage, and qualifies the need for a direct procedure for selenium analysis in clinical samples. The development of such a method is described in Chapter 3 of this thesis, and Chapter 2 outlines the design and operation of a low resolution quadrupole ICP-MS, which was used for the majority of the analysis presented.

The recently commercially available ICP-MS instruments are now better suited to overcoming the problems of direct selenium determination. High-resolution magnetic sector instruments⁶⁰ are able to resolve the selenium response from the peaks produced by argon-adduct and matrix-related polyatomic species, but the high resolution setting required to give adequate separation, compromises the sensitivity of the analysis. The destabilisation of the interfering polyatomic ions is now possible with the ICP mass filter instruments, which incorporate hexapole collision cell⁶¹ or reaction cell⁶² technology. The theory and practicalities of these instruments, with respect to selenium analysis, are discussed in Chapter 7.

CHAPTER 2

INDUCTIVELY COUPLED PLASMA MASS SPECTROMETRY

In recent years, the Inductively coupled plasma mass spectrometry (ICP-MS) has proved to be one of the most convenient and versatile techniques for trace metal analysis, combining rapid analysis with low detection limits, a broad linear working range, multi-element and stable isotope ratio capabilities. Its application to selenium analysis offers better sensitivity than the established techniques used for routine clinical analysis. The ability to measure the individual isotopes is not only useful for metabolic studies, but enables the possibility of determination by isotope dilution (ID), a technique capable of achieving analysis of a high precision and accuracy⁶³. However, the relatively high ionisation potential of selenium and the presence of isobaric interferences, restrict the analytical performance of this technique when compared with that achieved for other elements.

The ICP-MS, consists of an ion source, a mass filter and a detector. A schematic diagram is presented in Figure 2.1. for the Elan 5000. The fundamental aspects of the instrument are outlined by Jarvis, Gray and Houk⁶⁴, and further details are found in published reviews⁶⁵⁻⁶⁷.

Alternate methods of ionisation to the inductively coupled plasma include the microwave-induced plasma (MIP) and glow discharge (GD), which enable selective element detection. These are characterised as harsh ionisation sources according to the extent to which they ionise or fragment the analyte compound. Chemical ionisation (CI), fast atom bombardment (FAB), and matrix-assisted laser desorption ionisation (MALDI), are soft ionisation sources yielding molecular ions, to enable the determination of fragment ions of long-chain molecules, and electron ionisation (EI) is used to gain structural information about a compound. In-situ determination of trace elements in solid materials is carried out by laser ionisation (LIMS) and secondary ion mass spectrometry (SIMS), where a primary ion beam at high current density is used for the layer erosion of the sample.

A well-established technique with a reputation as a reference method, is thermal ionisation mass spectrometry (TIMS). Analysis of small samples is enabled by an efficient thermal source that produces a highly stable ion beam. The element selective ionisation conditions avoid the generation of spectroscopic interferences, although the evaporation of the samples from the heated filament are subject to mass fractionation effects, caused by lighter isotopes being more volatile than the heavier isotopes of elements. Corrected for by scanning the mass spectrum repetitively to obtain time-dependent interpolation of the isotope peak heights, TIMS measurements are time consuming, requiring the initial chemical separation step to be carried out under very strict clean laboratory conditions to avoid contamination.

Advances in design and methodology of these and other ion sources are reviewed annually in an atomic mass spectrometry update in the *Journal of Analytical Atomic Spectrometry (JAAS)*^{68,69}.

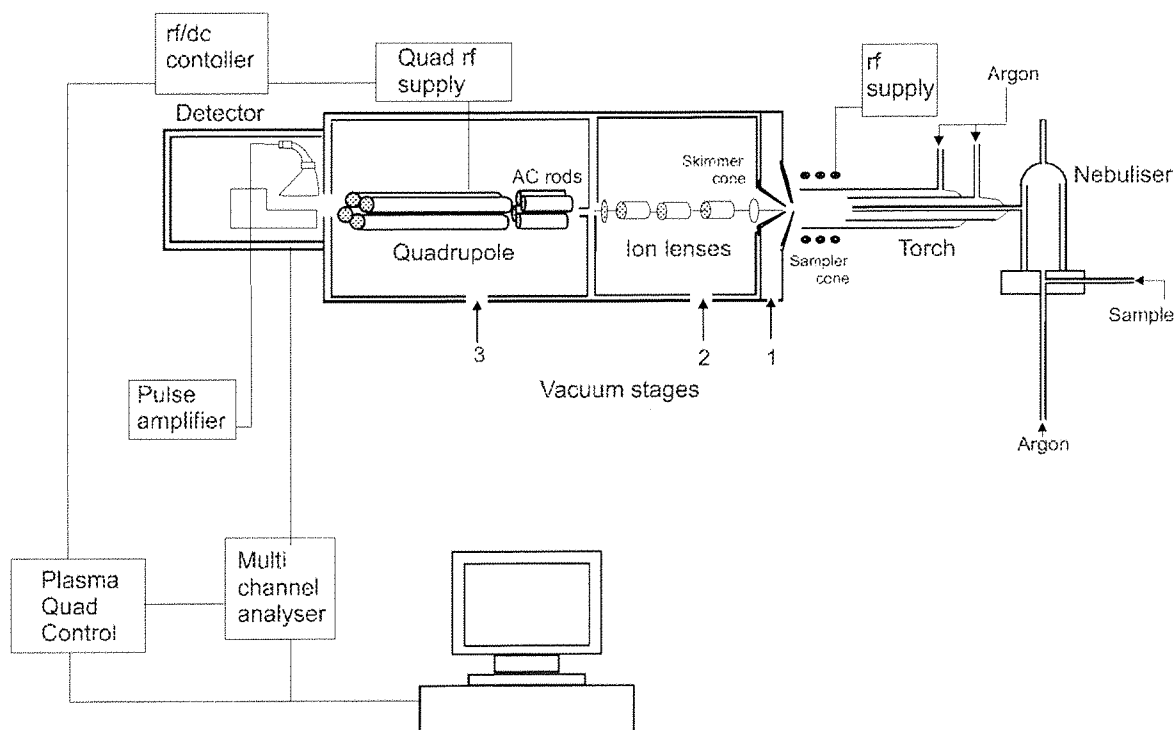


Figure 2.1. Schematic representation of the Perkin-Elmer Sciex Elan 5000

The Elan 5000 utilises a quadrupole mass filter and a single ion collector detection system. During the past ten years, advances in design have produced commercial instruments with alternate mass spectrometers and multicollector detection. Magnetic sector field instruments are now commonly used, and mass-selective devices such as time-of-flight mass spectrometers (TOF-MS), quadrupole ion traps and accelerator mass spectrometers represent a cross-section of the techniques that are employed for mass selection with a plasma source. These mass spectrometers are described in section 2.6.

2.1. The Inductively coupled plasma

The production of ions occurs in a high temperature plasma, at atmospheric pressure. Initiated by an electrical discharge from a Tesla coil, the plasma is sustained by the inductively coupling of radio frequency energy (rf) into a flowing gas which is frequently argon, but can be helium or an argon-oxygen or nitrogen mix. The plasma is generated at the end of a torch, consisting of two outer concentric quartz tubes and an inner alumina injector tube. An argon gas flow of $15 \text{ litres min}^{-1}$ provides the main plasma support, and an auxiliary gas flow (at $0.8 \text{ litres min}^{-1}$) controls the position of the plasma relative to the torch and protects the alumina tube from direct contact with the hot plasma. The nebuliser argon ($0.8\text{--}1.2 \text{ litres min}^{-1}$) carries the sample aerosol into the plasma. The argon flow through the assembly causes the plasma discharge to assume an annular configuration consisting of a cooler inner zone with most of the power confined to the outer layers. The torch is positioned along the central axis of copper tubing of a water-cooled coupling coil, with the end of the alumina tube located up to 5mm before the first turn. The supply of a rf current to the end of the coupling coil, generates a magnetic field along the axis of the torch, and free electrons derived from the spark produced by the Tesla coil, couple with the magnetic field producing local ionisation of the argon gas stream. Electrical energy within the plasma is converted to the kinetic energy of the electrons, which collide with the argon atoms to produce temperatures that are in excess of 6000K.

The introduction of the analyte into the plasma can be by dry sample input, such as electrothermal vaporisation, the generation of a gaseous hydride and laser ablation from a solid. In liquid sample introduction, a dilution of the sample is transferred to the plasma by pneumatic nebulisation into a spray chamber, using argon as the propellant gas to form an aerosol. Although nebulised water has a substantial effect on the mass spectra observed,

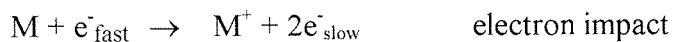
altering the ionisation conditions of the analytes and increasing the abundance of metal oxide ions, the convenience of simplified sample handling and few carryover problems, make this a popular mode of sample introduction.

The most common nebulisers used are crossflow, specifically used for biological samples as they are relatively resistant to clogging, and Meinhard for greater sensitivity, although susceptible to blockage. Ultrasonic nebulisers, which use a rapidly vibrating piezoelectric crystal to generate the aerosol, also offer high sensitivity. The increase efficiency in sample transport does require the use of a desolvator to remove the substantially higher water content which would otherwise cause plasma perturbation. This results in lower oxide formation but does necessitate longer washout times between samples. Microconcentric and direct injection nebulisers are specifically for small sample sizes, and are more easily clogged by particles.

The spray chamber separates the sample aerosol droplets by size. The standard device is a Scott dual pass spray chamber, made of “Ryton”, although glass cyclonic chambers are now more frequently being used, which offer better efficiency but produce higher oxide levels. Large droplets are removed by collision with the spray chamber walls, with only those of the appropriate diameter ($8\mu\text{m}$) and velocity being able to pass from the spray chamber. 99% of the original sample solution does not enter the plasma, and is drained to waste. As the aerosol travels through the inner cooler zone of the plasma, the droplets vaporise and the analyte molecules are progressively atomised and ionised.

The formation of singly charged ions is very efficient. Within the 2msec residence time all elements with a first ionisation potential below that of argon (15.8 eV) have become charged. 54 elements are ionised to 90% or more, although for elements with high ionisation potentials of between 9-11 eV, a higher proportion remains neutral. Selenium, arsenic, and tellurium which have ionisation potentials of 9.75, 9.81 and 9.01 eV, have ionisation efficiencies of only 33%, 52% and 66%, respectively. The extent of ion formation can be estimated using the Saha equation⁶², and is dependent on the ionisation potential of the element, partition function for both the ion and the neutral atom and the electron density of the plasma at a specific excitation temperature. The calculated value can only be an approximation because of the influences of the other ions present in the plasma, including the water making up the sample dilution. Water alters the thermal equilibrium of

the plasma and can contribute up to 17% of the total atom density present. The mechanism for ionisation is a non-selective process, believed to be by electron impact and charge transfer reactions.



Energy transfer to sample atoms can also occur via Penning ionisation-excitation mechanisms:



Where Ar^* is a highly argon atom and X is the sample atom.

Since second ionisation energies are greater than 10eV, the majority of elements do not produce doubly charged ions. The worst case of doubly charged population, exhibited by barium (with a second ionisation potential of 10.0 eV), is less than 2% of total ions.

This excitation zone of the plasma leads to the analytical area. The plasma tail contains the neutral atoms and oxides formed by reactions of the atomic ions with oxygen from the environment. As the degree of oxide formation is influenced by the input flux of the sample aerosol water, it can be reduced by dry sample introduction or by employing a nebuliser in conjunction with a desolvation system. Adjusting the instrumental parameters also affects the oxide levels. Increasing the rf power dissociates oxide ions more efficiently, although this can lead to an increase in doubly charged ions, and at a high nebuliser flow rate, the plasma temperature is reduced and oxides are increased. The analytical conditions imposed by the rf power setting, nebuliser flow rate and the positioning of the torch relative to the sampler cone, are interrelated and effectively move the excitation zone relative to the interface. Generally, the signal intensity from analyte ions is maximum when the sampling orifice is 2mm downstream from the tip of the excitation zone. The operating parameters can be selected to achieve the best compromise for sensitivity, noise, oxide and doubly charged ions.

2.2. The sampling interface

The mass spectrometer requires a high vacuum (operating pressure of 2×10^{-4} Pa [10^{-5} torr]) to minimise collision losses of ions with neutral gaseous species within the spectrometer. An interface separates the spectrometer from the inductively coupled plasma, operating under atmospheric pressure. This contains an outer shallow sampler cone and a conical skimmer cone, both made of either nickel or platinum, consisting of a central circular orifice of 0.5-1.0 mm in diameter, which are water-cooled. A central core of the plasma enters the sampler cone aperture, enabling the part of the argon gas that is richest in sample ions to reach the interface. The majority of argon gas in the interface is evacuated by a rotary vane pump, which maintains the pressure at 100 Pa (4 torr). The gate valve used to separate the high vacuum side of the instrument from the interface is withdrawn during operation, allowing ions to stream through the cone aperture into the second of the three distinct vacuum stages. Only 0.001% of the gas passes through the skimmer cone, with the remainder being removed from the interface.

On entering the initial low-pressure zone, the gas expands as a supersonic jet along the central axis, to form an ion beam. The plasma flows round the tip of the sampling cone forming a cold boundary layer of gas on the inside edge of the cone surface. During the initial stages of extraction, the ions collide with the cone wall, the boundary layer and argon atoms, while the random thermal motion of the plasma is being converted into directed flow. This can result in the loss of ions and induces the formation of oxide ions and polyatomic ions, before the reactions are frozen between the plasma species during the gas expansion.

A “photon stop” prevents photon emissions from the plasma to pass into the mass spectrometer, keeping the detector noise to a minimum. The plasma, which consisted of equal positively charged ions and negative electrons, now no longer maintains its charge neutrality as the ions are focused to the mass analyser by electrostatic lenses. For the Elan 5000, these consist of an Einzel lens, a three cylinder lens set, and a Bessel box, which have to be tuned with respect to each other to provide maximum transfer of the analyte. The transmission of an ion lens depends on the mass of the ions in the beam. Lighter ions are deflected more than those of a larger mass and are more influenced by the composition of the ion beam, whereas heavier ions stay closer to the beam centre. These ‘space charge effects’ contribute to matrix related changes of analyte sensitivity. Matrix elements can,

therefore, change the fraction of analyte ions that get through the lens, the effect being most severe when the analyte is of a low mass and the matrix is composed of heavy ions. The impact of these matrix effects can be lessened by using dilute solutions (with solute levels of less than 0.1%).

2.3. Quadrupole mass spectrometer

The final vacuum stage is maintained at 2×10^{-4} Pa by turbopumps, which provides a change in ion mean free path (ie. the average distance travelled between collisions) from 10^{-3} mm in the plasma to 1m in the spectrometer. The ion beam is directed first along a set of entrance alternating current (ac) rods, and then through the central axis of the main quadrupole, consisting of four independent cylindrical rods mounted in a square array and diagonally paired. The short pre-filter rods restrict the spread of kinetic energy of the ions when they leave the lens, to limit the range of speeds with which they enter the mass analyser quadrupole. This effectively improves the resultant peak shape of the response signal.

A positive direct current (dc) voltage is applied to one pair of the rods facing each other in the quadrupole array, and an equal but negative voltage is applied to the other pair. A rf voltage is superimposed on the paired rods, forming an electrical field between the rods at right angles to the central axis. This deflects the oncoming ions into oscillating paths through the rods. The ions follow a screw-type motion as they are first attracted to a positively charged rod, and then repelled away when the rod changes its polarity, with the acquired momentum driving the ion forwards. At any given set of applied voltages and frequencies, only ions of a certain charge to mass ratio will have stable trajectories and reach the detector. The trajectory followed by the ions can be described by Mathieu equations⁷⁰. Stability is affected by the amplitude and frequency of the applied rf voltage, the dc voltage, the mass of the ion and the number of pole pairs of rods.

A quadrupole is a second order multipole. Hexapole (third order) and octapole (fourth order) arrangement of paired rods are also used in mass spectrometers. The number of rod pairs characterise the shape of the effective potential well within the array, with a higher order multipole having a wider potential well near the axis and stronger field gradient closer to the rods. This efficient confinement of ions over a wide range of masses is particularly useful in studying the ion-molecule reactions - monitoring the product ions of

the reactions over a wide spectrum. However, the resultant stability boundaries are dependent on the initial position of the ion within the field, and are more diffuse with wide regions of partial stability being present⁶². In contrast, due to its symmetry, a quadrupole has well defined stability boundaries that are independent on the initial position of the ion, and so is well suited to it's role as a mass filter.

The Mathieu differential equations on being solved produce stability diagrams for ion transmission through the multipole. Figure 2.2. plots the stability of ions of increasing masses, M^+ , as a function of the amplitude of the applied dc and rf voltages for the transmission through a quadrupole. The shaded area defines the region of stable motion for M_n^+ , assuming collision-less conditions.

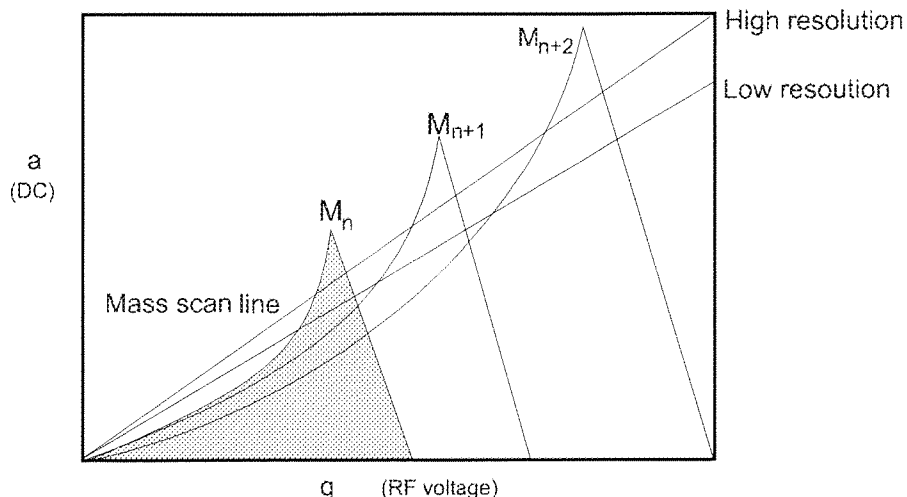


Figure 2.2. Mass stability diagram for ion transmission through the quadrupole field, showing the scan line at a high and low resolution.

The instrumental electronic parameters α and q control the rf frequency and the dc voltage, applied to the quadrupole rods. Lighter and heavier ions will adopt an unstable motion, and will effectively be filtered out as they strike the rods or pass out of the quadrupole field, to be pulled away by the turbopumps.

The degree of separation of neighbouring ions depends on the slope of the scan line, illustrated by the low and high resolution lines in Figure 2.2. The gradient is defined by α , a function of the rf voltage, which when increased improves the resolution (defined as the full

width at half maximum intensity) as the shape of the peak effectively becomes narrower with a corresponding deterioration in sensitivity. The resolving power of the quadrupole is capable of separating two peaks of a mass unit difference. The quadrupole operates by rapid sequential analysis, as only one ion of a given mass:charge ratio is transmitted at any one time. A complete mass spectrum can be obtained by scanning the quadrupole through the whole range of dc and rf voltages maintained at a constant ratio. The sensitivity of high mass elements is greater than the sensitivity of low mass elements by generally one order of magnitude.

2.4. Ion Detection

The most common detector used for ICP-MS is a channel electron multiplier. Positive ions set off a large cascade of electron discharges from the surface of a conical open glass tube, coated with a lead oxide semiconducting material. On application of a negative dc voltage across the tube, a continuous gradient of potential exists along the length, which produces a 10^6 amplification of the ion signal. These are processed by the detection electronics and sent to a computer for data processing. Registered as pulses, the signals are stored at each m/z unit. On current instruments, dual mode detectors are employed. When the pulse count exceeds about 2×10^6 counts per second (cps), the pulse mode detection is disabled, switching to analog detection, calibrated for the operating conditions. This extends the dynamic range of the detector up to 10^9 cps, enabling major and trace elements to be measured in the same solution in a single scan. The efficiency of the conversion of ions to pulses of electric current is maintained by adjustment of applied voltage as the detector ages.

The channel electron multiplier is also sensitive to photons. The majority of photons that are not removed by the photon stop within the Bessel box lens, are prevented from reaching the detector because of its right-angled alignment with respect to the quadrupole mass filter. Instead, a deflector lies in the ion path from the quadrupole, which induces a large positive voltage to direct the ions into the detector, allowing photons to pass through unaffected away from the detector. This arrangement prevents the contribution to the background noise by the majority of photons and neutral molecules.

2.5. Data collection

Continuous or segmented scans over selected portions of the spectrum offer a semi-quantitative analysis of samples, while quantitative analysis is achieved by monitoring of specific ion peaks. This utilises the peak-hopping mode of analysis, for which the rapid and repetitive data collection by the mass spectrometer at a number of fixed mass positions for each isotope of interest, limits the influence of plasma fluctuations. The computer drives the analyser to each mass in turn, storing the response in an appropriate memory address, and the number of sweeps per reading requested defines the number of times this is done. At each mass there is a settling time, to enable the physical change over of each population of ions to be stabilised within the mass analyser, before measurements are carried out. The dwell time entry determines the time spent integrating the data for a particular mass:charge ratio (m/z) during one sweep, and together with the number of repetitions, can be varied to obtain optimum counting statistics for a specific mass.

2.6. Alternative mass spectrometers

Magnetic sector ICP-MS, which include high resolution (HR-ICP-MS)⁷¹ and multicollector (MC-ICP-MS)⁶¹ instrumentation, incorporate a curved laminated magnet through which, ions in a focused beam are accelerated. As charged particles travel through a magnetic field, they are deflected at right angles to the lines of magnetic flux. The ion trajectories and radius of curvature are related to the accelerating voltage, magnetic field strength and mass to charge ratio. For ions with the same charge, the lightest are deflected to the greatest degree, resulting in a shorter flight path to the detector. These instruments can consist of a single-stage magnetic sector or more commonly, employ both a magnetic and an electric sector to achieve ion separation.

A detailed description of the multicollector technique is given in Chapter 7, which uses an array of ion detectors to enable simultaneous measurement of the ion currents of analytes within a limited mass range. For this reason, the technique specialises in high precision isotope ratio measurements. The HR-ICP-MS is more suited to multielement analysis⁷², with a resolving power adequate to solve most spectral interference problems occurring in the quadrupole, with a resolution capability of up to $M/\Delta M$ of 9,500 (ΔM being the mass difference between to singly charged ions of average mass M that produce peaks in the mass spectrum which overlap at 10% of the maximum peak height).

$M/\Delta M = 400$ at low resolution. Although capable of higher ion transmission when compared with quadrupole mass analyser in low-resolution mode, sensitivity does decline with resolution capacity.

Time-of-flight mass spectrometers also employ simultaneous sampling by the detector⁷³. Extracted ions are accelerated to a similar kinetic energy before entering the flight tube, with the time of arrival of an ion at the detector being proportional to the square root of its m/z ratio. The ions are deflected at the far end of the instrument by a reflectron, which doubles the flight path to increase resolution and is used to diminish small variations in kinetic energy acquired by the ions of the same mass to intensify signals. The production of ions is modulated, to ensure that the heaviest ion has reached the detector before the next batch of ions enters the flight tube. The measurement over the whole mass range is simultaneous and greater than 20,000 full mass spectra per second can be acquired. Although the sensitivity of analysis does not match that of the other techniques, short analysis times offer enhanced sample through-put, and is well suited to the analysis of transient signal obtained through dry sample introduction.

The ion trap spectrometer consists of a mass filter, which can be described as effectively a three-dimensional quadrupole, with similar equations applied for ion motion⁷⁴. It consists of a hyperbolic centre-ring electrode, to which a rf voltage is applied and two end-cap electrodes. The injection of a pulse of electrons into the ion trap ionises a gaseous sample. All ions above a certain m/z determined by the rf amplitude, have trajectories that keep them trapped within the electrodes, and on raising the rf amplitude, ions of increasing mass are sequentially ejected from the ion trap and detected with an electron multiplier. The introduction of helium causes collision damping of the ions, which maintains the trajectories of the ions towards the centre of the ion trap providing improved resolution and sensitivity.

2.7. Spectral interferences

A major problem associated with ICP-MS analysis has been its susceptibility to spectral interferences. The Sciex Elan 5000 software can correct for isobaric overlaps that are caused by the presence of metal isotopes of a similar m/z ratio to the analyte. For these elements, the scan parameters automatically include the measurement of an isotope from the interfering element, which has no isobaric overlap, and subsequently corrects for the elevation in analyte signal that has occurred. Other interferences for which the instrumental

software can not compensate for, include broad peaks due to the abundance of major matrix ions that overlap lower mass elements, such as experienced at ^{11}B by ^{12}C , and ^{39}K by ^{40}Ar , and the formation of polyatomic species. Argon-adducts and polyatomic ions produced after the ionisation of the sample by recombination reactions within the plasma, are derived from elements from the plasma support gas, atmospheric gases, water and sample matrix introduced into the plasma. Severe case examples include the $^{40}\text{Ar}^{12}\text{C}$ interference on the measurement of ^{52}Cr , (84% abundance), $^{40}\text{Ar}^{16}\text{O}$ on ^{56}Fe , (92% abundance), and $^{40}\text{Ar}^{40}\text{Ar}$ on ^{80}Se (50% abundance). Careful sample preparation and selection of instrumental parameters can minimise the interference problems caused by certain polyatomic ions. How this effects selenium determination in particular, will be discussed in the following chapter.

CHAPTER 3

SELENIUM DETERMINATION BY INDUCTIVELY COUPLED PLASMA MASS SPECTROMETRY

3.1. Introduction

Selenium has six isotopes, with the relative abundances as shown in Table 3.1. The distribution of the total intensity of signal at each m/z ratio and the low ionisation efficiency of 33%, contribute to the low sensitivity obtained for selenium determination by ICP-MS. Further problems are caused by spectroscopic interferences due to the formation of polyatomic ions in the plasma. Argon, oxygen, hydrogen and nitrogen and are the main constituents, in combination with additional elements from the sample matrix (OH⁻, Cl, Ca, S, and P). When these have the same nominal mass as the analyte, signal response is elevated due to the limited resolution of the quadrupole.

Table 3.1. Isobaric interferences on selenium determination by ICP-MS.

Isotope	% Abundance	Isobaric Interferent
⁷⁴ Se	0.9	³⁸ Ar ³⁶ Ar ⁷⁴ Ge ³⁷ Cl ₂
⁷⁶ Se	9.4	⁴⁰ Ar ³⁶ Ar ³⁸ Ar ₂ ⁷⁶ Ge
⁷⁷ Se	7.6	⁴⁰ Ar ³⁷ Cl ⁴⁰ Ar ³⁶ Ar ¹ H ⁴⁰ Ca ³⁷ Cl
⁷⁸ Se	23.8	⁴⁰ Ar ³⁸ Ar ⁷⁸ Kr
⁸⁰ Se	49.6	⁴⁰ Ar ₂
⁸² Se	8.7	⁴⁰ Ar ₂ H ₂ ⁸² Kr ⁴⁰ Ar ⁴² Ca ⁸¹ BrH

Isobaric argon-adduct ions, obscure any signal due to the most dominant selenium isotope at mass 80, and produce a significant background signal for ⁷⁶Se and ⁷⁸Se determination. With spectral overlap of the ⁴⁰Ca³⁷Cl signal on ⁷⁷Se, and ⁸¹Br¹H on ⁸²Se, measurement of ⁷⁴Se appears to be least affected by spectroscopic interferences, but with a natural abundance of less than 1%, cannot be used in quantitative analysis.

To avoid the formation of these argon-related interferences, nitrogen has been used as the support gas, but the addition of some argon gas was found to be necessary to maintain a stable plasma discharge, resulting in only a reduction in argon-adducts⁷⁵. For ICP sources that are maintained by argon, one approach used to overcome the impact of argon-adduct interferences, has been the application of mathematical corrections. Signal ratio measurements of ⁷⁸Ar₂⁺:⁷⁶Ar₂⁺ have been used to compensate for the interference experienced by the determined ⁷⁸Se⁺:⁷⁶Se⁺ ratio⁷⁶. Although successfully applied, a

disadvantage of the procedure is that any matrix-related interference affecting specifically $^{78}\text{Se}^+$ or $^{76}\text{Se}^+$ analysis, will not be adequately corrected for.

An alternate procedure is the use of organic solvents, such as propan-2-ol⁷⁷, ethanol⁷⁸, and methanol^{79,80} which on introduction into the nebuliser gas, have been shown to minimise the abundance of the interfering polyatomic ions and also enhance analyte response. A variety of mechanisms have been proposed to explain these effects, in which the large population of C^+ ions in the plasma plays a significant role. Competitive formation of carbon containing polyatomic species, such as argon carbides, shift the argon-related interferents from the region of interest, effectively reducing the level of spectroscopic interferents⁷⁷. The improved efficiency of nebulisation of the sample solution by the solvent, on creating a finer aerosol of the sample, would contribute to the increase in signal response. However, a more dominant effect in signal enhancement appears to be the increase in the degree of ionisation, facilitated by the concentration of carbon ions. This could be done by the transfer of electrons to the carbon ions⁸¹, or as the result of charge transfer mechanisms, with a charge exchange between C^+ ions and selenium atoms in the plasma made possible by the first ionisation energies of carbon being similar to that of selenium in its first excited state⁸².

In an effort to obtain a reliable analytical method for the determination of selenium in serum, the effect of butan-1-ol, an organic solvent which had not at that time been investigated, was examined as to the level of signal enhancement and background signal depression that could be achieved. In the developmental work described in this chapter, indium, an universally used internal standard, was employed to compensate for signal drift, instrument fluctuations and matrix effects. The procedures used to select the appropriate selenium isotope to monitor and to optimise both the concentration of solvent and instrumental parameters for maximum sensitivity, are outlined. This method was modified to allow the direct determination of whole blood and erythrocyte selenium. Further developments to the method involved the use of tellurium as an alternative internal standard. At a higher mass:charge ratio than indium, tellurium is further distanced from the selenium isotopes in the mass spectrum, but with its ionisation efficiency of 66%, being closer to that of the analyte, it would reflect any changes in signal enhancement more effectively. The method was validated by the participation in two External Quality Control Assessment schemes.

3.2. Instrumentation

A Perkin-Elmer SCIEX Elan 5000 ICP-MS (Perkin-Elmer, Beaconsfield) was used, with a Gilson 221 autosampler. The operating conditions are given in Table 3.2.

Table 3.2. Operating conditions for the ICP-MS.

Instrument	SCIEX Elan 5000
rf power	1.0 kW
Plasma gas flow rate	15.00 l min ⁻¹
Nebuliser gas flow rate	0.98 l min ⁻¹
Auxiliary gas flow rate	0.80 l min ⁻¹
Sampling /Skimmer cone	Nickel, 0.75 mm orifice diameter
Torch	Standard demountable quartz torch with 2.0 mm id alumina injector tube
Sample uptake rate	0.8ml min ⁻¹ (by peristaltic pump)
Neubuliser	Cross-flow
Data system	IBM Personal System/ 2 Model 70 386 computer
Measurements	80ms dwell time, 75 sweeps/reading, 1 reading/ replicate, 2 replicates
Masses	76, 77, 78, 82, 115, 128

The instrument was tuned for maximum sensitivity daily, by optimising the torch position and the settings of the ion-focusing using a tuning solution containing magnesium, rhodium, and lead at 10 µg l⁻¹ in 0.1% v/v nitric acid.

3.3. Reagents

Distilled, then de-ionised water (Milli-Q system, Millipore, Watford, Hertfordshire) and “Aristar” nitric acid (16M, Merck, Poole, Dorset) were used throughout.

Matrix-matched calibration standards were prepared using bovine serum and whole-blood (Selbourne Biological Services, Alton, Hampshire), with a stock selenium solution, at 1020 mg l⁻¹ (Sigma-Aldrich, Poole, Dorset). The samples were diluted with butan-1-ol, Triton-X-100, a blood diluent comprising of ammonia, (NH₄)₂H₂EDTA, and NH₄H₂PO₄, all of “Aristar” purity (Merck, Poole, Dorset). Internal standards employed were indium from a stock solution at 10,000 mg l⁻¹, and tellurium solution at 1 mg ml⁻¹, both of “Spectroscol” purity (Merck, Poole, Dorset).

Autosampler wash solution consisted of 0.05%v/v Triton-X-100.

Blood diluent: 0.14 M ammonia, 0.004 M ethylenediaminetetra aceytic acid diammonium salt, 0.029 M ammonium dihydrogen phosphate.

3.32 g $\text{NH}_4\text{H}_2\text{PO}_4$, and 1.16 g $(\text{NH}_4)_2\text{H}_2\text{EDTA}$ are dissolved in deionised water in a 1000 ml volumetric flask, 10.0ml ammonia solution is added and the solution is made up to volume.

Samples were directly dispensed into autosampler tubes. At 3 ml sample volume, these were 15 ml acid resistant polypropylene vials (Sarstedt), loaded on to autosampler tray coded: 22 (Gilson, Anachem, Luton, Bedfordshire), consisting of a maximum tube capacity of 44. On reduction of the sample to 1.5 ml, disposable test tubes RT25: 65x10 mm (Merck, Poole, Dorset), were used, loaded onto autosampler tray, coded: 28 (max. tube capacity of 108).

3.4. Quality control

Four internal quality control sera were prepared by adding selenium to pools of bovine serum to give increases of 0, 32, 79, 126 $\mu\text{g l}^{-1}$ (0, 0.40, 1.00, and 1.60 $\mu\text{mol l}^{-1}$). Target values of 23.7, 54.5, 102.7, 147.7 $\mu\text{g l}^{-1}$, were established by hydride generation atomic absorption spectroscopy, equivalent to 96.3, 100.0 and 98.4% recovery of the added selenium. These were referred to as Level 1, Level 2, Level 3 and Level 4.

A commercially available, lyophilised serum of human origin, Seronorm, (Nycomed Pharma Diagnostics, Oslo, Norway), was also used as an internal quality control. Batch number 311089 Seronorm, was used in the initial developmental work, which had an assigned selenium concentration of 84 $\mu\text{g l}^{-1}$ (1.06 $\mu\text{mol l}^{-1}$). Later work included the analysis of two certified reference materials, Seronorm 704121 and NIST 1598 (National Institute of Standards and Technology, USA). NIST 1598 quoted a certified value of $42.4 \pm 3.5 \mu\text{g l}^{-1}$ ($0.54 \pm 0.4 \mu\text{mol l}^{-1}$) selenium, and Seronorm 704121, listed $73 \mu\text{g l}^{-1}$ (0.92 $\mu\text{mol l}^{-1}$), measured by electrothermal atomic absorption spectrometry and 86 $\mu\text{g l}^{-1}$ (1.09 $\mu\text{mol l}^{-1}$) (by inductively coupled plasma atomic emission spectrometry) as the analytical values, which gave rise to the assigned value of $80 \mu\text{g l}^{-1}$ (1.01 $\mu\text{mol l}^{-1}$).

External quality assessment sera with established selenium concentrations, provided by two centres: UK-TEQAS (University of Surrey, Guildford) and Quebec National Institute of Public Health Laboratories, were used throughout the developmental work.

3.5. Standards

Working standards containing 0, 10, 20, 50, 100, 200 $\mu\text{g l}^{-1}$ selenium, in 0.1% v/v nitric acid, were prepared from 1020 mg l^{-1} selenium stock solution. Each standard, in turn, was diluted with the basal bovine serum in equal volume (200 μl) directly in the autosampler tube before the addition of the diluents, to obtain matrix-matched standards.

3.6. Sample preparation

200 μl serum samples were diluted with equal volumes of the “0” aqueous standard in the autosampler tubes. For both the serum samples and standards, 200 μl aliquots of 1% v/v Triton X-100, and blood diluent solution were added to aid sample nebulisation, with 200 μl indium at 20 $\mu\text{g l}^{-1}$ as an internal standard. The sample was further diluted to 3.0 ml with deionised water and 6% v/v butan-1-ol at the appropriate volume to give the specified solvent concentrations. Reagent blanks were prepared in the same way, with 200 μl of deionised water replacing the serum.

3.7. Establishing the optimum butan-1-ol concentration

Signals at masses 76, 77, 78 and 82 were monitored at different butan-1-ol concentrations. Background signals for aqueous solutions fell with increasing levels of the alcohol, with a 3-fold depression at 4% butan-1-ol (Figure 3.1).

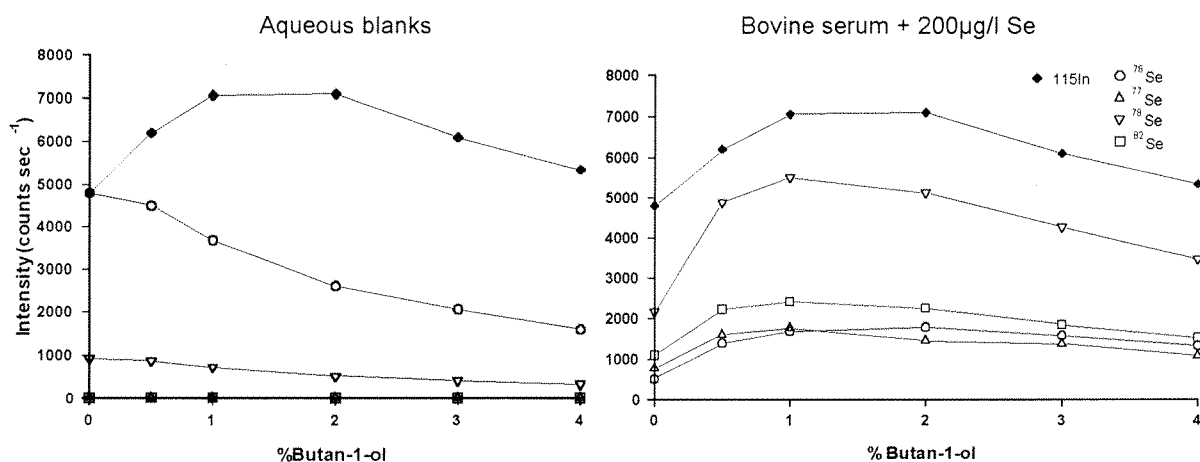


Figure 3.1. Change in signal intensities for selenium isotopes on increasing the butan-1-ol concentration, for aqueous blanks and a bovine serum sample.

On introduction of a serum sample, both with and without added selenium, the signals for all the isotopes were enhanced with increasing butan-1-ol concentration up to 1%, and thereafter decreased with higher solvent levels. The internal standard, ^{115}In , showed a similar pattern of signal enhancement.

The endogenous concentration of the bovine serum was calculated from the blank subtracted signals from selenium standard additions to the serum at each of the masses, and for each concentration of butan-1-ol. The target concentration was achieved at ^{78}Se in the presence of 0.5-4% v/v butan-1-ol, whereas higher concentrations of 2-4% v/v butan-1-ol were required at ^{77}Se (Table 3.3.). The enhanced signal and the accuracy of the observed results, indicated that a solvent concentration of 1.0% v/v butan-1-ol was appropriate for selenium analysis, with the signal at mass 78 being measured.

Table 3.3. Endogenous concentration of selenium found in serum.

Butan-1-ol %	[Se] $\mu\text{g l}^{-1}$					
	0	0.5	1.0	2.0	3.0	4.0
^{76}Se	339	57	58	54	54	56
^{77}Se	52	31	28	26	24	24
^{78}Se	34	24	24	24	24	24
^{82}Se	72	43	42	41	40	42

Acceptable data is shaded, target concentration of $24\pm3\mu\text{g l}^{-1}$ established by HG-AAS.

3.8. Effect of rf power on selenium analysis

Some of the common spectral interferences, such as ^{40}Ar on ^{40}Ca , $^{38}\text{Ar}^1\text{H}$ on ^{39}K , $^{40}\text{Ar}^{12}\text{C}$ on ^{52}Cr and $^{40}\text{Ar}^{16}\text{O}$ on ^{56}Fe can be reduced or even eliminated by applying reduced temperature (cool or cold) plasma techniques. Cool plasma conditions, produced by running the ICP-MS at low power and high central gas flow, suppress the ionisation of argon atoms⁸³. At reduced levels of the source ions (Ar^+), the plasma is dominated by NO^+ and O_2^+ , and the water derived ions, H_2O^+ and H_3O^+ . These conditions were effective in reducing background signals in the analysis of selenium, both in the presence and absence of butan-1-ol. At 750W rf power and a nebuliser gas flow rate of 1.10 l min^{-1} , the blank signals for ^{78}Se were reduced by 98%.

It has been observed that matrix effects under cold plasma conditions are more severe than those obtained under normal analytical conditions. This was the case with

respect to the introduction of a serum matrix, which was reflected by a drop in analyte signals of 95% and 65%, with and without butan-1-ol (Figure 3.2.).

When analysing serum samples, frequent blockage of the injector tube by the accumulation of sample deposits, gave rise to assay runs of less than an hour, indicating that sample vaporisation was incomplete. To prevent this, subsequent work was carried out at 1000W, which achieved a compromise between a reduction in background signal and a sensitivity of signal response that would enable accurate analysis of selenium.

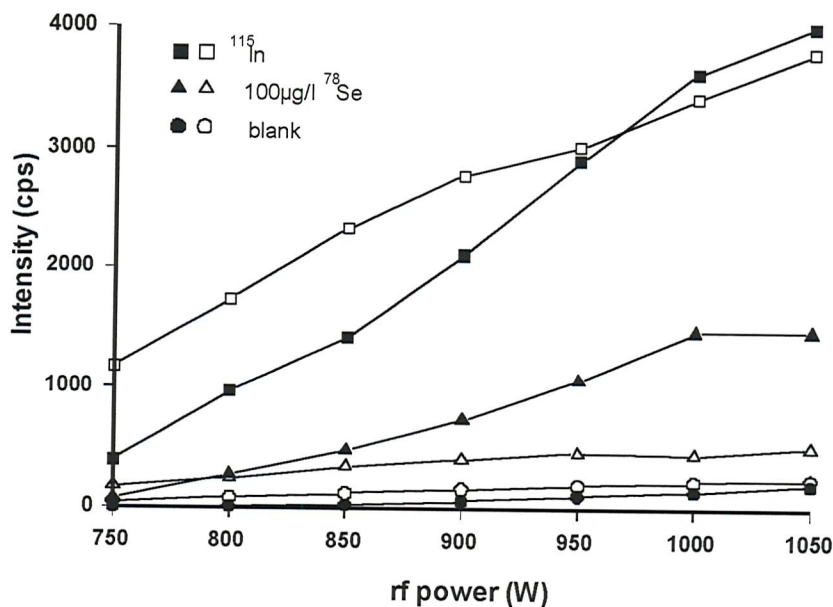


Figure 3.2. Effect of rf power and of 1% butan-1-ol on ⁷⁸Se (▲100 $\mu\text{g l}^{-1}$ Se, ●blank) and ¹¹⁵In (■) signals. Open symbols in absence of butan-1-ol.

3.9. Accuracy of analysis

Analysis of a certified quality control serum, Seronorm (311089) and external quality assessment (EQA) sera with established selenium concentrations, showed good agreement between the target concentrations and the observed results for the three isotopes (Figure 3.3). On monitoring isotopes ⁷⁷Se and ⁷⁸Se, analysis of internal quality control sera also matched target values. However, when determined by ⁸²Se, the observed values for the IQC samples were higher, indicating the presence of interferences. On scanning the two types of sera, it was seen that the bovine serum contained a considerably greater level of bromine compared to that of the human sera used in the EQA schemes, indicating that ⁸¹Br¹H was being formed, elevating the signal at mass 82.

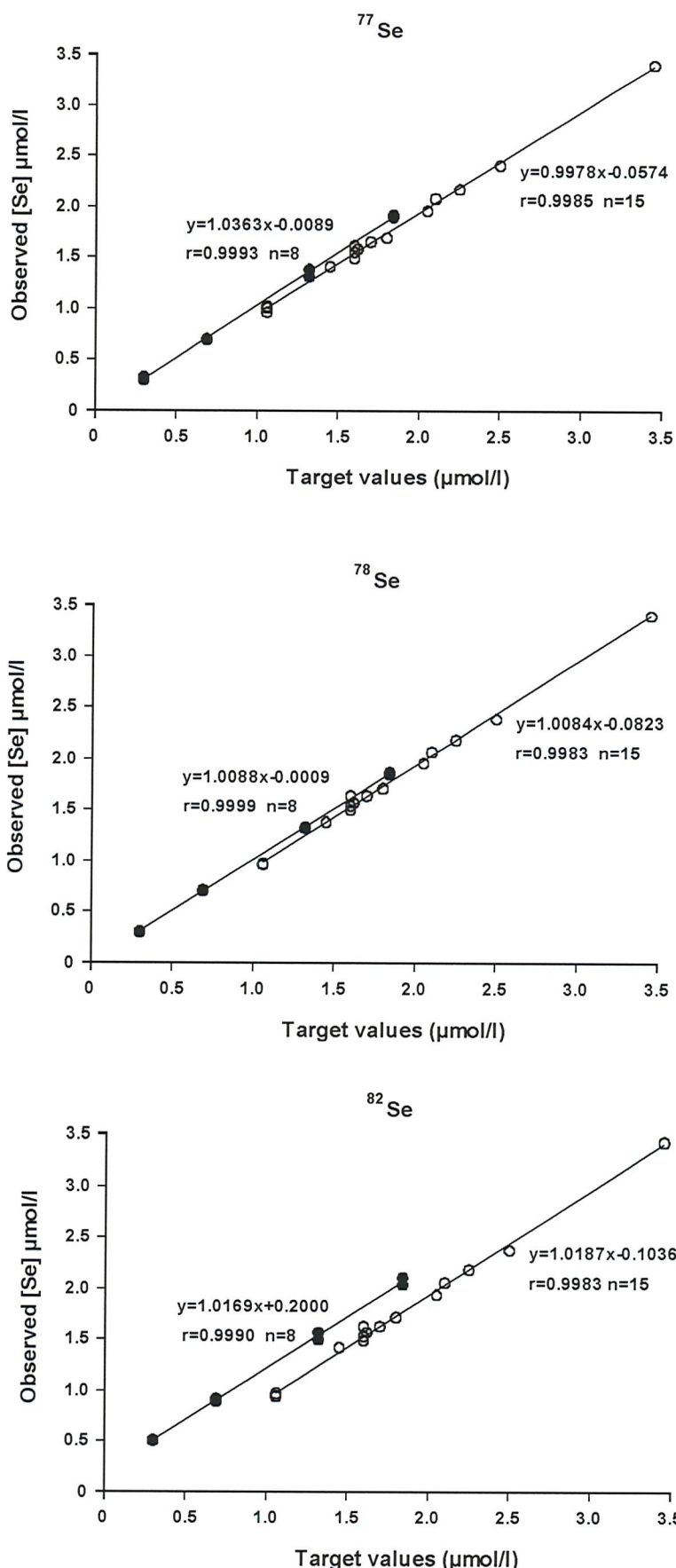


Figure 3.3. Comparison of serum selenium concentrations observed with the target values for the three isotopes: ^{77}Se , ^{78}Se and ^{82}Se (● bovine IQC serum, ○ human EQA serum).

3.10. Calibration Curves

Aqueous, bovine serum and bovine blood calibration curves can be seen in Figure 3.4. for the selenium isotopes at masses 77, 78 and 82, the matrix related suppression of the signals confirming the need to use matrix-matched standards in the analysis of serum and whole-blood specimens.

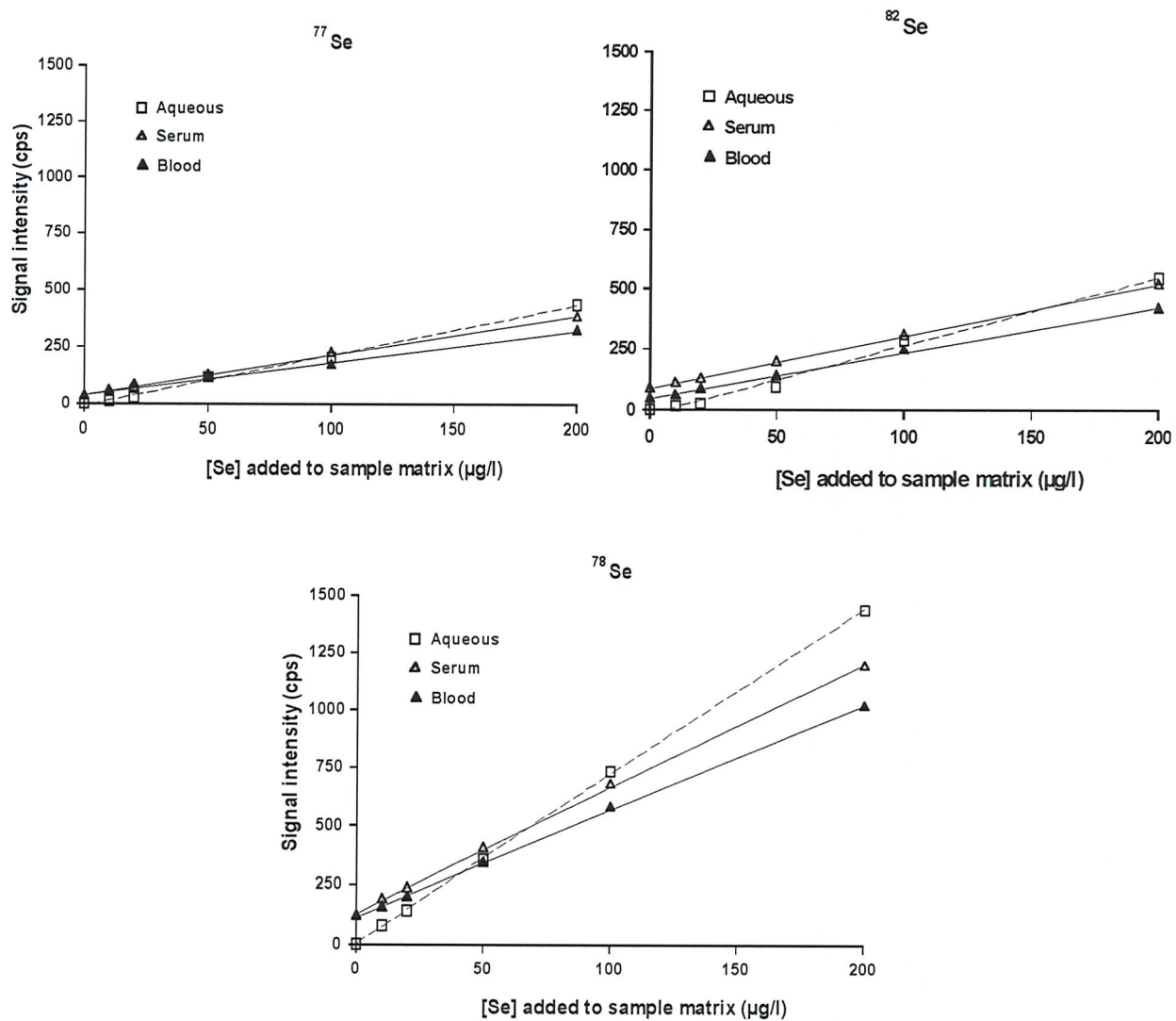


Figure 3.4. Aqueous, bovine serum and whole-blood calibration curves.

The display of a greater sensitivity by selenium measurement at mass 78, due to the relative abundances of the isotopes, and its capability of achieving good accuracy (demonstrated in section 3.9), determine the selection of ^{78}Se as the appropriate isotope to monitor.

3.11. Modification to sample preparation

For routine samples, the analysis had been scaled down so that 100 μl sample aliquots could be used per replicate, and by monitoring only ^{78}Se and ^{115}In , the analysis time was reduced to less than 2.5 minutes for each sample. The reagent volumes for sample preparation are listed in Table 3.4.

Table 3.4. Reagent volumes used for sample dilution.

Reagent	Concentration	Volume (μl)
Serum (Calibrating serum /QC/test serum)		100
Aqueous Standard	0 – 200 $\mu\text{g l}^{-1}$ for calibration 0 $\mu\text{g l}^{-1}$ for test + QC samples	100
Indium	20 $\mu\text{g l}^{-1}$ in 1%v/v HNO_3	100
Triton-X-100	1% v/v	100
Blood Diluent		100
Butan-1-ol	6% v/v	250
Deionised water		750

A 0.5% butan-1-ol/0.05% Triton-X-100 wash solution was aspirated for 10 minutes before the start of the assay to allow the background counts to stabilise, and was used throughout the assay as a rinse diluent between sample analysis. Diluted test samples were analysed in duplicate against a matrix-matched calibration curve, and reagent blanks were included between batches of forty samples. These were used in blank correction if a decrease in background signals was evident. Generally, despite the use of an internal standard, a small drift in selenium sensitivity during the day's run, necessitated a second calibration curve within the assay run.

Selenium analysis in plasma samples showed similar matrix effects to bovine serum (Figure 3.5), and therefore could be assayed against a bovine serum calibration curve. The detection limit, at three times the standard deviation of replicate blank measurements, was less than 2 $\mu\text{g l}^{-1}$ ($<0.03 \mu\text{mol l}^{-1}$).

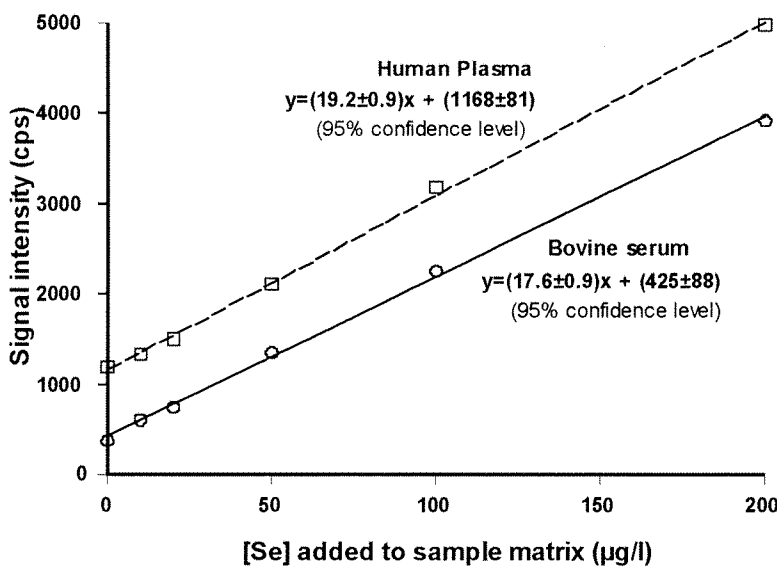


Figure 3.5. Regression lines for ^{78}Se measurement in bovine serum and plasma.

3.12. Tellurium as an internal standard

Initial studies were carried out using indium as an internal standard - although a good general purpose internal standard, it did not reflect the ionisation efficiency of selenium. Tellurium is in the same periodic group and has an ionisation potential similar to that of selenium of 9.0 eV (5.8 eV for indium), resulting in a more comparable ionisation efficiency of 66%. A plot of signal response with increasing levels of butan-1-ol (Figure 3.6.), illustrates how a closer response in signal enhancement is obtained by ^{125}Te (at 7% abundance), ^{126}Te (19%) or ^{128}Te (32%), then by using ^{115}In . All three isotopes appear to be suitable, and ^{128}Te , being the most abundant isotope, was used in the method described to obtain the maximum signal intensity. From Figure 3.6., it can be also seen, that a butan-1-ol concentration of 0.5-1.0% is necessary for maximum ^{78}Se signal enhancement.

In using ^{128}Te as the internal standard, one does need to be aware that post-surgical use of anti-microbial wash solutions that contain iodine, lead to the formation of $^{1}\text{H}^{127}\text{I}$, causing an elevation in the intensity at mass 128. For this to be significant, the iodine concentration would need to be greater than $80 \mu\text{mol l}^{-1}$ (reference range $<0.63 \mu\text{mol l}^{-1}$), and when such a serum is analysed, the iodine concentration has been found to be at a level at which the signal is so grossly elevated, that it gives rise to a depressed selenium:internal standard ratio concentration of $<1 \mu\text{g l}^{-1}$. A large iodine signal can also bring about problems when monitoring ^{126}Te , which would be subject to spectroscopic interference caused by the overlap of the broad iodine signal at mass 126.

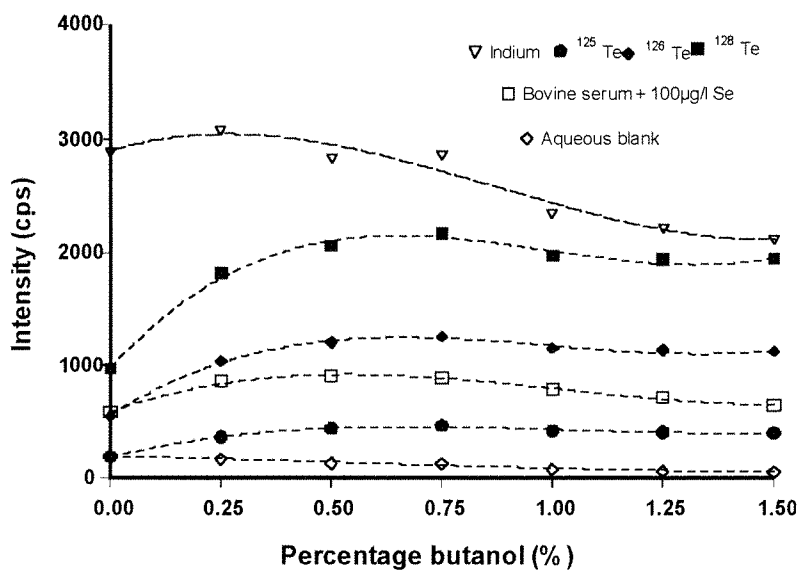


Figure 3.6. The change in signal intensity at m/z ratio 78, 115, 125, 126 and 128 with increasing concentration of butanol (at 1.0 l min^{-1} nebuliser gas flow).

3.12.1. Optimisation of nebuliser gas flow

The signal enhancement effect obtained in the presence of an organic solvent causes a shift of the maximum signal intensity to lower gas flow rates for both the tellurium and selenium signals. The optimal flow rate was established to be 0.1 ml min^{-1} lower than that used in the absence of an organic solvent. Both tellurium and indium showed a similar signal response with the change in gas flow (Figure 3.7).

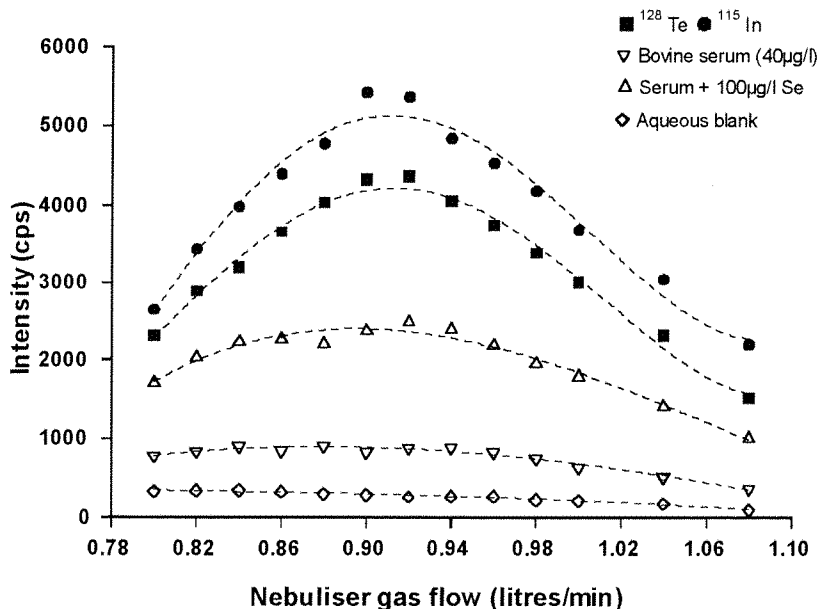


Figure 3.7. The effect of the intensity of signals at m/z ratio 78, 115 and 128, with increasing nebuliser flow rate, in the presence of 0.5% butan-1-ol.

3.12.1. Optimisation of scanning parameters

Using a wash solution containing 0.5% v/v butan-1-ol and 0.05% Triton-X-100, optimal scanning conditions were found to be 100 sweeps per reading at a dwell time of 80 ms. ^{78}Kr and ^{128}Xe , present as contaminants in the argon support gas, can be corrected for, by blank subtraction, and therefore their automatic correction equations were removed from the scanning parameters, reducing the overall time for selenium analysis on measurement of 3 replicates to less than 2 minutes.

3.12.3. Calibration curves

Aqueous, bovine serum and bovine blood calibration curves using tellurium (100 μl of 100 $\mu\text{g l}^{-1}$ Te in 0.1% v/v nitric acid) as the internal standard, can be seen in Figure 3.8. When compared with Figure 3.4., matrix-suppression of the tellurium-corrected selenium signal was less significant, indicating that tellurium would be the preferred internal standard in the analysis of urine, the matrix of which can vary considerably from sample to sample.

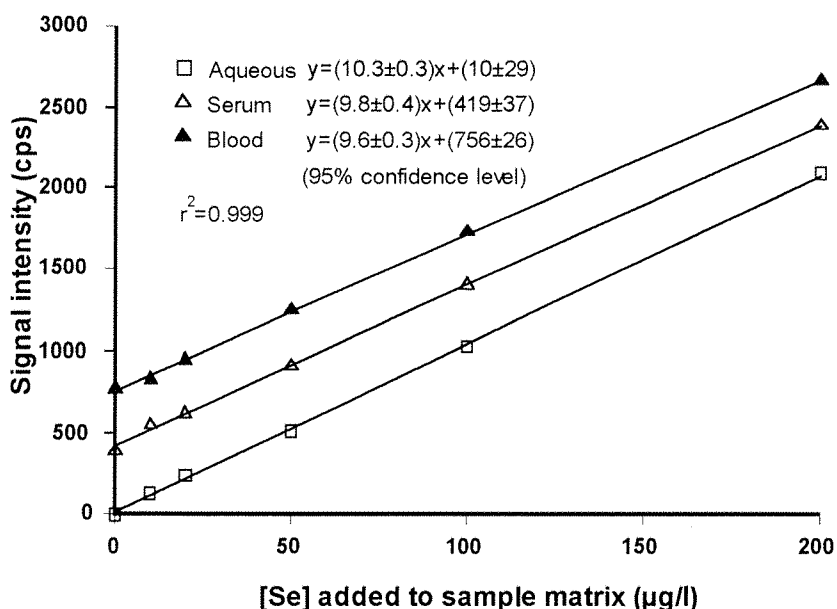


Figure 3.8. Aqueous, bovine serum and whole-blood calibration curves, using tellurium as the internal standard.

3.13. Accuracy and precision of analysis

3.13.1. Internal Quality Control

Analysis of certified quality control sera Seronorm and NIST 1598, and our own IQC material, showed a mean bias between observed and target values of $-1.4 \mu\text{g l}^{-1}$ ($-0.02 \mu\text{mol l}^{-1}$) using indium, and $+0.5 \mu\text{g l}^{-1}$ ($+0.01 \mu\text{mol l}^{-1}$) with tellurium. The between-day precision ranged from $\pm 9.3\%$ RSD at $20 \mu\text{g l}^{-1}$ ($0.25 \mu\text{mol l}^{-1}$) to $\pm 1.5\%$ at $150 \mu\text{g l}^{-1}$ ($1.90 \mu\text{mol l}^{-1}$) and the within-day precision ranged from $\pm 6.4\%$ at $20 \mu\text{g l}^{-1}$ to $\pm 1.2\%$ at $150 \mu\text{g l}^{-1}$, with analysis involving tellurium displaying a lower relative standard deviation at higher concentrations (Table 3.5 and Figure 3.9.).

Table 3.5. Internal quality control data for between assay serum analysis, using indium and tellurium as the internal standards.

IQC sample	Target value ($\mu\text{g l}^{-1}$)	Observed		Value ($\mu\text{g l}^{-1}$) $\pm\text{sd}$
		Mean	Indium	
Level 1	23.7	23.4 ± 2.2	22.4 ± 2.0	
Level 2	54.5	54.2 ± 4.1	54.7 ± 2.7	
Level 3	102.7	102.7 ± 4.6	103.4 ± 2.0	
Level 4	147.7	147.0 ± 6.2	149.9 ± 3.8	
Seronorm 311089	84	78.5 ± 3.7		
Seronorm 704121	73/86			74.7 ± 2.6
Nist 1598	42.4			42.5 ± 1.3

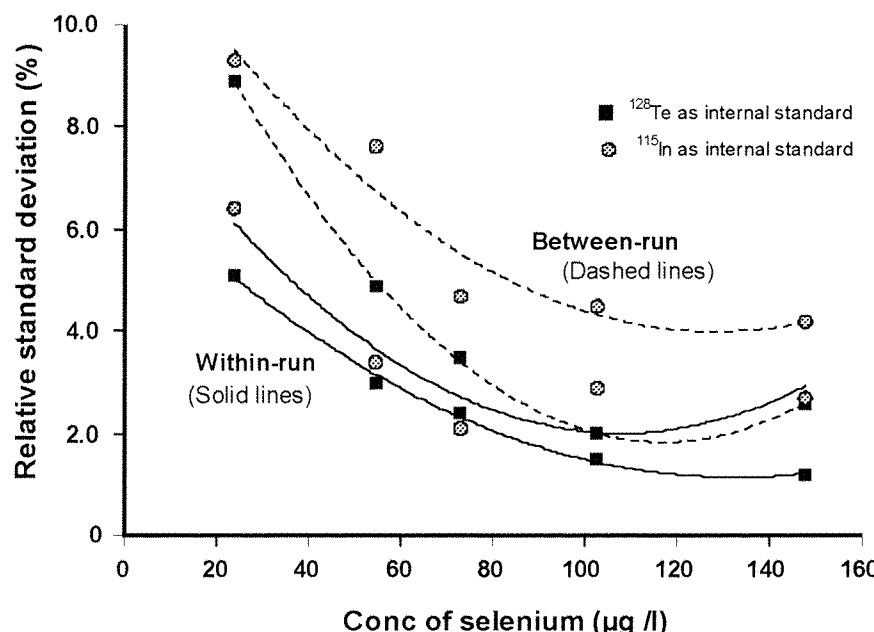


Figure 3.9. Comparison of within run (solid trend lines) and between run (dashed trend lines) precision for analysis employing indium (◎) and tellurium (■) as internal standards.

3.13.2. Intra-laboratory comparison

Twelve samples were provided by trace element quality assessment scheme UK-TEQAS, and twenty-five samples by Quebec laboratories, with the target values received after analysis. A Bland Altman plot of the bias of measured concentrations compared to the target values, for both analyses by HG-AAS and the presented method (using indium as the internal standard), is given in Figure 3.10. The variation in differences from target values is very similar for both techniques, with ICP-MS analysis displaying a small negative bias at higher concentration levels. A mean bias value of $-3.2 \pm 5.5 \mu\text{g l}^{-1}$ ($-0.04 \pm 0.07 \mu\text{mol l}^{-1}$) was obtained for the ICP-MS technique, compared with $-4.7 \pm 7.1 \mu\text{g l}^{-1}$ ($-0.06 \pm 0.09 \mu\text{mol l}^{-1}$) for HG-AAS, giving rise to 95% confidence intervals of (-5.0 to -1.4) and (-7.1 to -2.3) $\mu\text{g l}^{-1}$, respectively. The observed results are listed in Table 1 of Appendix I.

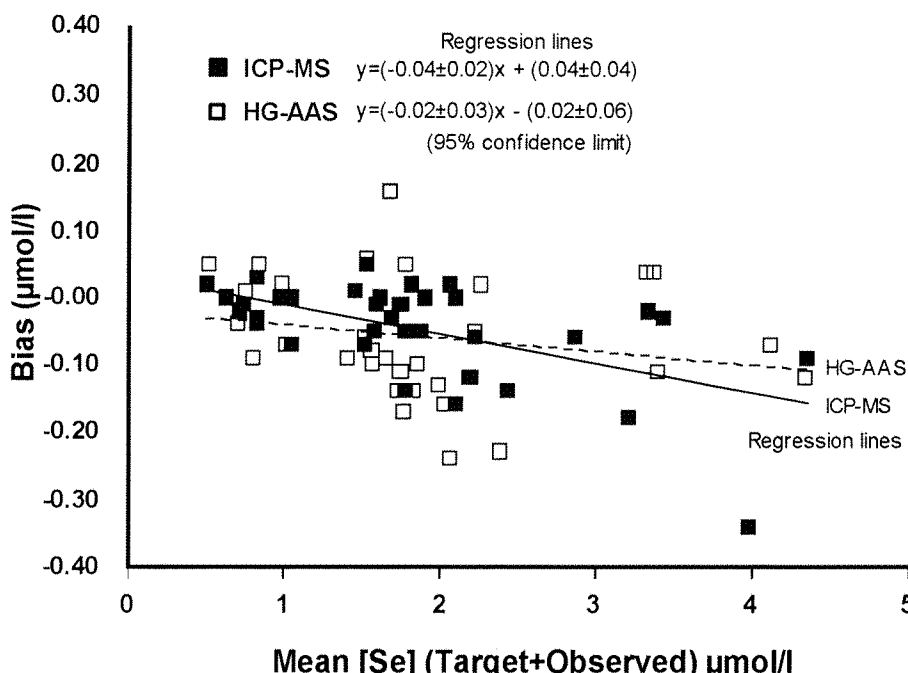


Figure 3.10. Bland Altman plot of the bias of measured serum samples determined by ICP-MS and HG-AAS, compared with target values.

3.13.3. External quality assessment (EQA)

The results for analysis of 108 samples of serum from two interlaboratory comparison programs run by UK-TEQAS and the Quebec National Institute of Public Health Laboratories, are shown in Figures 3.11. and 3.12. During this analysis period, the methodology employed involved indium as the internal standard.

The agreement between the reported result and the median/target value was excellent for 66 (61%) of samples and good for a further 33 (31%). There were, however, poor agreements for 9 specimens. Despite this, the regression equation from Figure 3.11. indicates biases of -0.7 to $-1.1 \mu\text{g l}^{-1}$ (-0.009 to $-0.013 \mu\text{mol l}^{-1}$) within the range of 50 - $95 \mu\text{g l}^{-1}$ (0.6 - $1.2 \mu\text{mol l}^{-1}$), which encompasses 95% of the range seen for UK subjects.

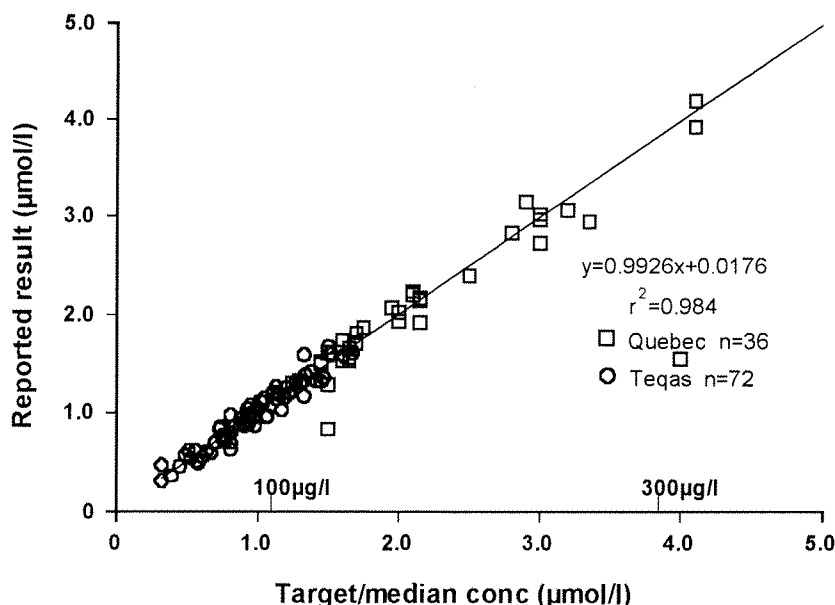


Figure 3.11. Performance in EQA schemes for selenium in serum - January 1997 to December 1998, showing proximity to target values.

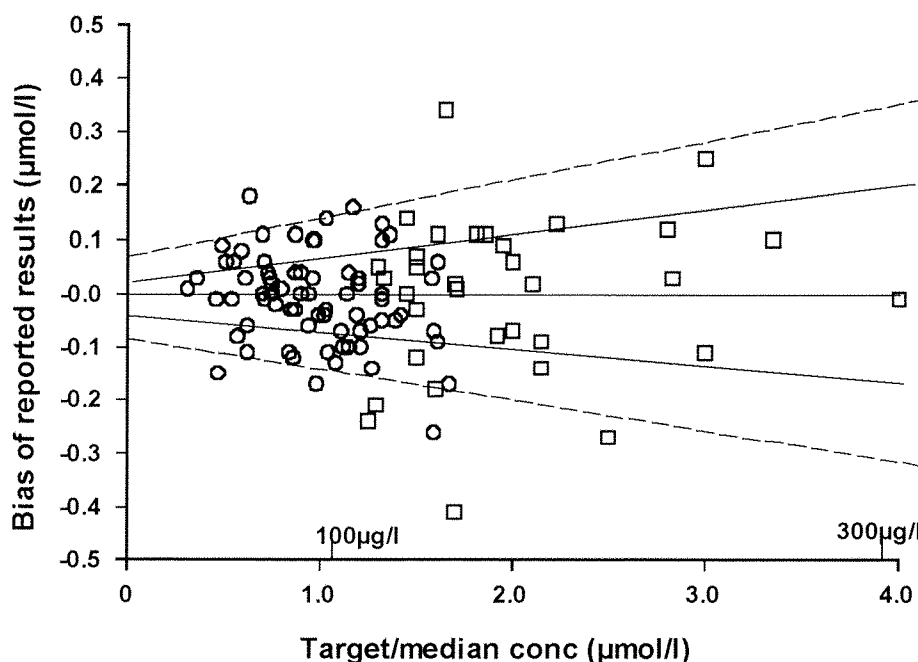


Figure 3.12. Differences between reported values and target values in the EQA schemes: Quebec and UK-TEQAS, from January 1997 to December 1998. Zone parameters defined by the EQA centres)

A better performance was observed using tellurium as the internal standard, as displayed in Figures 3.13. and 3.14., for which all but two of the results came within the zone parameters. The agreement to the target values was excellent for 72 (89%) of the reported results, although there does appear to be some problem with analysis at selenium concentrations greater than $250 \mu\text{g l}^{-1}$ ($3.5 \mu\text{mol l}^{-1}$).

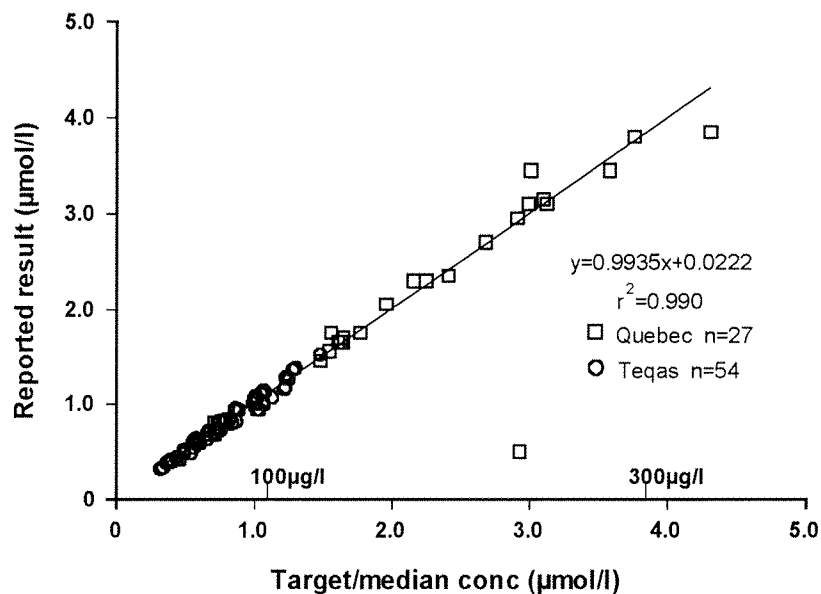


Figure 3.13. Performance in EQA schemes for selenium in serum- January 1999 to July 2000, showing proximity to target values.

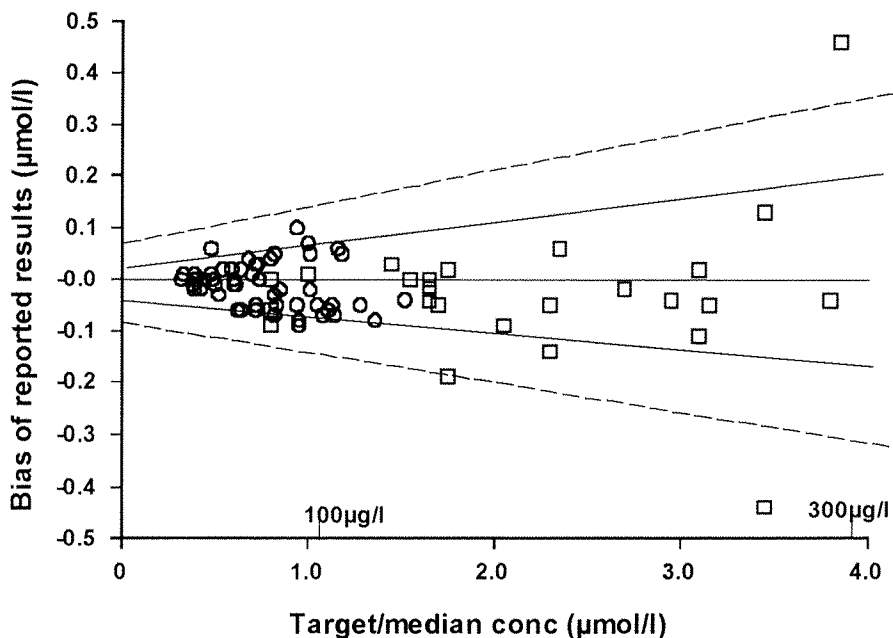


Figure 3.14. Differences between reported values and target values in the EQA schemes: Quebec and UK-TEQAS, from January 1999 to July 2000 (Zone parameters defined by the EQA centres).

3.14. Selenium determination in whole-blood and erythrocytes

Functional deficiency of selenium is defined by the activity of glutathione peroxidase (GSHPx), and the nominal requirement for selenium is an estimate of the dietary intake needed to achieve two-thirds of the maximum enzyme attainable activity¹⁹. Studies have shown that there is a positive correlation between GSHPx activity and selenium concentrations in blood from people with low selenium status^{84,85}. Although plasma also contains glutathione peroxidase, the protein is distinct from that present in erythrocytes and its contribution to the total enzyme activity found in whole-blood, is small.

Since selenium determination in whole-blood and red blood cells in particular, are generally accepted to reflect the levels of GSHPx, they are more of an effective indicator of long-term selenium status than the measurement of the metal in plasma. However, work carried out by Butler and Thompson et al.⁸⁶ has revealed a more complex situation. They found that the correlation to GSH-Px activity is dependent on the form of selenium present in the diet. Organic selenium (selenomethionine) raised the whole-blood selenium concentration to a greater extent than the inorganic form, but only 10% of which was found to be associated with GSH-Px. In contrast, selenate and selenite supplementation gave rise to a greater proportion of selenium being linked to the enzyme, with a positive correlation with GSH-Px activity exhibited at low levels.

Hydride generation coupled to atomic absorption spectroscopy^{87,88} is widely used for the measurement of selenium in whole-blood, but given the need to acid-digest the sample before analysis, the sample preparation is time consuming. Direct analysis by atomic absorption spectroscopy is possible, requiring chemical modifiers, such as palladium in combination with magnesium nitrate, to stabilise the selenium at the high temperature necessary for the removal of matrix components. However, problems are caused by the spectral interference due to the high concentration of iron in the blood^{89,90}. A modification of the developed ICP-MS method meets the need for a reliable method for selenium determination in erythrocytes, requiring very little sample preparation and a quick analysis time.

3.14.1. Modifications to the serum method

Measurement of whole-blood selenium was found to require a number of modifications to the serum/plasma method. As this work was carried out prior to the investigations with respect to tellurium, the internal standard used was indium, the concentration of which was increased 2.5 fold to compensate for the greater suppression of analyte sensitivity by the matrix. The rf power was increased to 1.05kW, in order to decompose effectively the greater solids content, of 220 g l⁻¹ protein in blood as opposed to 70 g l⁻¹ in plasma. Although this increased the ⁷⁸Se signal of aqueous blanks by 20%, the increase in sample: noise signal ratio was greater. This gave rise to the better within-run precision, as shown in the IQC data listed in Table 3.6., particularly at the lower concentrations.

3.14.2. Sample preparation of red blood cells

The sample blood red cells were initially diluted 1+1 with the blood diluent modifier solution (ammonia/phosphate/EDTA), and mixed thoroughly, prior to the 1+14 dilution required for sample preparation for selenium analysis (as described in Section 3.11.). The matrix effect of the 1in 2 diluted erythrocytes was similar to that of the bovine blood, as demonstrated by the parallel calibration curves in Figure 3.15., enabling the samples to be analysed against a bovine blood calibration curve.

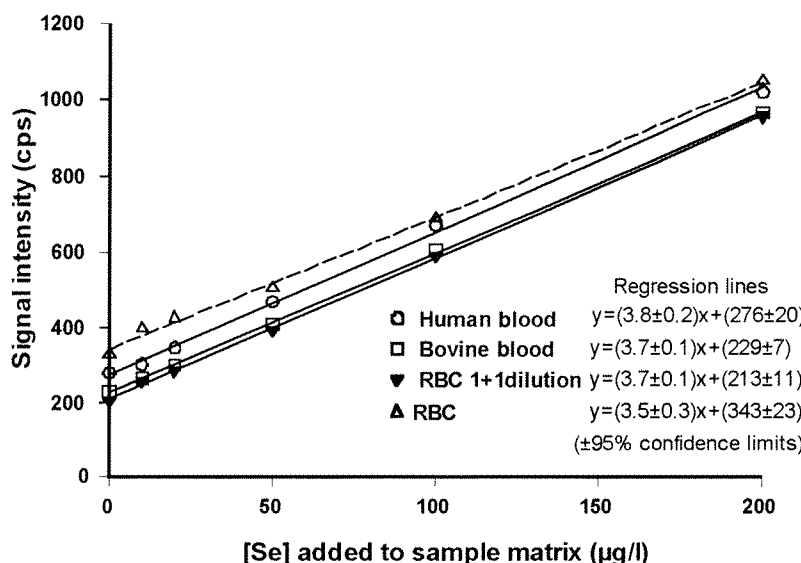


Figure 3.15. Standard addition calibration curves for ⁷⁸Se in whole-blood and red blood cells.

The measured erythrocyte selenium levels were expressed in terms of μmol per haemoglobin concentration for each sample, in order to compensate for any dilution caused by the presence of plasma in the specimen. The selenium levels in erythrocytes of healthy subjects was found to be, on average, 1.6 times that found in the plasma for each individual.

3.14.3. Internal quality control

Finding a pool of bovine whole-blood with a low selenium content for calibration purposes, had proved to be difficult. The endogenous selenium concentrations of the bloods analysed were of similar values, with the lowest level at $63 \mu\text{g l}^{-1}$ ($0.80 \mu\text{mol l}^{-1}$). This pool was divided for use as a calibration blood, an internal quality control (QcB), and diluted 1+1 with the blood diluent to give a second control sample (QcA).

Three Seronorm whole-blood reference samples were available, however, all of these had a similar assigned value of $81 \pm 2 \mu\text{g l}^{-1}$ ($1.03 \pm 0.03 \mu\text{mol l}^{-1}$) for selenium. Seronorm Level 1 (404107) and Seronorm Level 2 (404108) were used regularly, and the observed results compared to the target values are given in Table 3.6.

Table 3.6. Internal quality control data for selenium in whole-blood.

Quality Control Material	Target value ($\mu\text{g l}^{-1}$)	Observed Mean	% Relative		Standard	deviation
			Serum protocol	Within-run	Within-run	Between run
QcA Bovine bld (1+1)		30 \pm 2		5.8 (n=10)	3.4 (n=10)	7.4 (n=93)
QcB Bovine blood		63 \pm 3		2.9 (n=10)	2.9 (n=10)	4.7 (n=93)
Seronorm level1 (404107)	80 (80-91)	84 \pm 7		3.0 (n=10)	2.1 (n=10)	7.8 (n=91)
Seronorm level2 (404108)	82 (82-89)	84 \pm 7				7.4 (n=77)

The mean bias between observed and target values of the reference materials was $2.8 \mu\text{g l}^{-1}$ ($0.04 \mu\text{mol l}^{-1}$) 3.5%. The precision was similar to that obtained for serum analysis, ranging from $\pm 7\%$ at $30 - 90 \mu\text{g l}^{-1}$ ($0.38 - 1.14 \mu\text{mol l}^{-1}$) for between-run analysis, to $\pm 3\%$ RSD within-run measurements. In the absence of erythrocyte IQC

material, the RBCs were analysed alongside the whole-blood reference materials and IQC samples.

3.14.4. External quality assessment

At this present time, the only EQA scheme that includes whole-blood selenium determination is the ICP-MS interlaboratory comparison program, run by Quebec National Institute of Public Health Laboratories. Twice yearly, serum, urine, whole-blood and hair samples are analysed for 23 elements. Our whole-blood selenium measurements of 175, 170 and 250 $\mu\text{g l}^{-1}$, were at the lower end of the range of reported values, which had medians of 202 ± 28 , 188 ± 36 and $285 \pm 45 \mu\text{g l}^{-1}$, respectively. With such a large scatter of values for all specimens, very little can be read as to the accuracy of our performance in this particular scheme, and highlights the need of a specific interlaboratory comparison scheme for measurement of selenium in whole-blood.

3.15. Conclusion

Accurate determination of selenium in serum by the described method has been shown by the good agreement between the certified values of the reference materials and our performance in the external quality assessment schemes. The method has been successfully applied to the analysis of selenium in the more complex matrices of whole-blood and erythrocytes, giving good reproducibility and internal quality control data. It is in reference to this method that the performance of the other techniques is assessed.

CHAPTER 4

SERUM SELENIUM PROTEINS

The versatility of the developed ICP-MS method for selenium analysis, attained by minimal sample preparation, the accurate analysis of small sample volumes and short analysis time, enables its use in applications other than routine clinical analysis. One such application is in the measurement of the selenium associated with the separated fractions obtained through affinity chromatography used to quantify selenium carrier proteins.

Selenoprotein P, glutathione peroxidase and albumin can be isolated from human serum, using heparin-Sepharose and blue-Sepharose as the column packing materials⁹¹. The selenium content in the eluted fractions associated with these proteins, has been previously determined by spectrofluorimetry⁹¹, and GF-AAS⁹². Spectrofluorimetry, although a slow, indirect method of selenium analysis, has the advantage of a better sensitivity compared to GF-AAS, which required modification to the separation procedures to enable more concentrated sample fractions to be collected. The suitability of the adapted ICP-MS method to this application was demonstrated by the low detection limit ($0.6 \mu\text{g l}^{-1}$, $0.008 \mu\text{mol l}^{-1}$), a good precision of 5% RSD at low concentrations of $2 \mu\text{g l}^{-1}$ ($0.03 \mu\text{mol l}^{-1}$) and consistent recoveries of $101 \pm 4\%$ for the samples investigated.

4.1. Introduction

Selenium appears to exert its functions as a constituent of selenoproteins. Two selenoproteins have been identified in human plasma: glutathione peroxidase (GSHPx) and selenoprotein P, with the remaining selenium being incorporated into a variety of proteins, mainly albumin⁹³. The relative distribution of selenium between these proteins is influenced by dietary variables⁹⁴, such as the selenium species present, as illustrated by the preferential binding of selenomethionine to albumin⁹¹.

Purification and characterisation of plasma GSHPx, has shown that the protein is a tetramer, each sub-unit of apparent molecular weight of 19-23 kD, containing selenium in the form of a single selenocysteine residue⁹⁵. The plasma enzyme is distinct from the GSHPx present in red blood cells, exhibiting different structural and kinetic properties, such as its mobility on electrophoresis gels, elution pattern from ion-exchange chromatography columns, heat stability, and staining with a glycoprotein marker ^{125}I -concanavalin A⁹⁶.

Antibodies raised specifically for the erythrocyte GSHPx, failed to interact with the plasma enzyme, although cross-reaction with other tissue GSHPx's tested, did take place⁹⁷. In selenium deficiency, there is a decrease in GSHPx activity, with no inactive protein detected, suggesting a relationship between selenium status and the synthesis of the GSHPx protein⁹⁸.

Selenoprotein P, with a molecular weight of 57 kD, contains at least seven⁹⁹, and possibly ten⁹³ selenocysteines in it's polypeptide chain. It's name stems from ⁷⁵Se-P, so called because the protein was identified solely through its incorporation of ⁷⁵Se¹⁰⁰. Selenoprotein P is rich in histidine and cysteine - normally associated with metal binding, they can provide redox active sites, enabling free-radical scavenging to take place¹⁰¹. Selenoprotein P is secreted into the plasma by the liver, although its messenger ribonucleic acid has also been detected in other organs¹⁰², indicating that it is also secreted by other tissues. There appears to be a stronger correlation between selenium status and selenoprotein P, than that with GSHPx¹⁰³, with a preferential biosynthesis of selenoprotein P over GSHPx at low selenium levels¹⁰⁴.

4.2. Separation procedure

The distribution of selenium among the main three selenoprotein groups has been successfully carried out by using affinity chromatography. In rat serum, Deagen et al.⁹¹ employed a sequential procedure, whereby Sepharose bound heparin was used to retain selenoprotein P, blue-Sepharose retained albumin, and GSHPx passed through both resins. Selenoprotein P's interaction with heparin was noted during the initial studies to characterise the protein¹⁰⁵, and its separation by heparin-Sepharose was confirmed using an antibody developed against it⁹¹. Albumin does not bind to heparin-Sepharose¹⁰⁶, and is retained by the blue reactive resin¹⁰⁷, as was demonstrated by quantitative colorimetric determination of the eluted fraction^{91,92}. The efficiency of the elution of GSHPx through both columns, was assessed by measuring the protein activity.

The procedure used in the present study, is the method described by Harrison et al⁹². The columns were used independently, with serum applied to each column. This was made possible by the retention of selenoprotein P with the albumin by the blue-Sepharose¹⁰⁰, allowing the separation of GSHPx.

4.2.1 Materials and reagents

Columns were packed with 2.25 g of heparin-Sepharose CL-6B and 2.75 g blue-Sepharose CL-6B (Biorad, Richmond) into glass analytical columns (25 x 1 cm, Whatman, Maidstone), with 25 μ m Teflon frits. LKB bromma 2120 varioperfex II peristaltic pumps, with 1mm id tubing, maintained the appropriate flow rate of buffers through the columns. The eluted sub-fractions were collected into 2.5 ml polycarbonate tubes (Teklab).

Buffer solutions were prepared daily.

Equilibrium buffer: 0.02 mol l⁻¹ ammonium acetate (pH 6.8).

1.54 g Ammonium acetate (Merck, Poole, Dorset) dissolved in 1000 ml deionised water.

Elution buffer 1: 2.0 ml sodium heparin at 5000 U ml⁻¹ (Leo Laboratories) diluted to 20.0 ml in 0.02 mol l⁻¹ ammonium acetate.

Elution buffer 2: 0.6 mol l⁻¹ sodium chloride in 0.02 mol l⁻¹ ammonium acetate.

3.5 g NaCl (Merck, Poole, Dorset), dissolved in 100 ml equilibrium buffer.

Regeneration buffer 1a: 0.02 mol l⁻¹ ammonium acetate with 0.5 mol l⁻¹ sodium chloride, and 20 μ l Nitric acid “Aristar” (Merck, Poole, Dorset), to obtain pH5.

Regeneration buffer 1b: 0.02 mol l⁻¹ ammonium acetate with 0.5 mol l⁻¹ sodium chloride, and 150 μ l Ammonia solution at 30% (Merck, Poole, Dorset), to obtain pH10.

4.2.2. Column separation procedure (using columns of 2 ml bed volume)

Both affinity columns were equilibrated with 20 ml of equilibrium buffer. 500 μ l serum was applied on each column, with a 0.2 ml min⁻¹ flow rate of equilibration buffer through the columns. Eight 1.0 ml fractions of eluant were collected in preweighed polycarbonate tubes for each column. The heparin-Sepharose column was eluted with a heparin solution (Elution buffer 1), and up to ten sub-fractions were collected. The column was regenerated by alternate use of the salt solutions at pH5 and pH10, at three times the bed volume being passed through twice, followed by 10 ml of equilibrium buffer. Elution buffer 2 was passed through the blue-Sepharose column to produce eight 1 ml sub-

fractions. Alternate washing through of equilibrium and elution buffer 2, followed by 10 ml of the equilibrium buffer, regenerated the column. Each sub-fraction was weighed after collection.

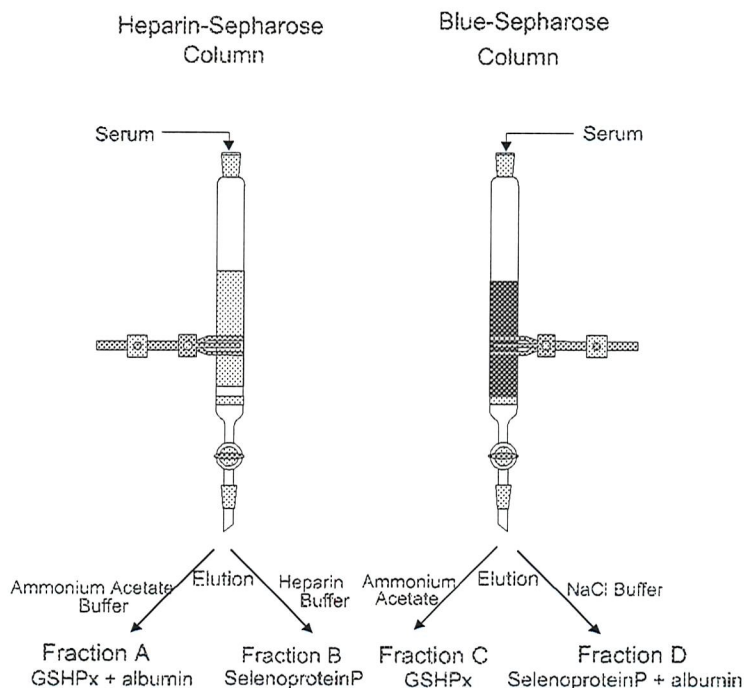


Figure 4.1. A schematic diagram showing the separation procedure for the heparin-Sepharose and the blue-Sepharose columns.

Four fractions, A,B,C and D were obtained from each sample (Figure 4.1.).

Fraction A which contained GSHPx plus albumin, was the eluate obtained from loading the heparin-Sepharose column with equilibrium buffer. Subsequent elution of this column with heparin solution yielded fraction B that contained selenoprotein P. On introduction of serum to the blue-Sepharose column, GSHPx was washed through with the equilibrium buffer to provide fraction 'C', and the bound albumin plus selenoprotein P, were co-eluted with a salt solution to yield fraction 'D'.

The selenium contained in each sub-fraction was quantified by ICP-MS detection. The selenium associated with selenoprotein P and GSHPx was measured in fractions B and C, respectively. The rest of the analyte present in the serum sample, assumed to be bound with albumin, was calculated from fractions: A minus C, and D minus B.

4.2.3. Selenium determination in sub-fractions

4.2.3.1. Instrumentation and reagents

Selenium analysis was carried out on the Perkin-Elmer SCIEX Elan 5000. The operating conditions are summarised in Table 4.1.

Table 4.1. Operating conditions for the ICP-MS.

rf power	1.0 kW
Plasma gas flow rate	15.00 l min ⁻¹
Nebuliser gas flow rate	0.92 l min ⁻¹
Intermediate gas flow rate	0.8 l min ⁻¹
Sampling/skimmer cone	Platinum, 0.75 mm orifice diameter
Torch	Standard demountable quartz torch with 2.0 mm id alumina injector tube
Sample uptake rate	0.8ml min ⁻¹ (by peristaltic pump)
Neubuliser	Cross-flow
Masses measured	78 and 128 (⁷⁸ Kr and ¹²⁸ Xe correction removed)
Parameters	80 ms dwell time, 100 sweeps/reading, 1 reading/replicate, 2 replicates.
Wash solution	0.5%Butan-1-ol, 0.05% Triton-X100

The instrument was tuned for maximum sensitivity, by optimising the settings of the ion-focusing and nebuliser gas flow, using a tuning solution containing 1+14 dilution of selenium and tellurium at 100 µg l⁻¹ in 0.5% v/v butan-1-ol.

Reagents are listed in Section 3.3 of Chapter 3.

4.2.3.2. Method

Buffer matrix-matched standards were prepared, to give a selenium calibration of 0, 1, 2, 5, 10, 20 µg l⁻¹. 200 µl sample/buffer with 200 µl of aqueous standard, 100 µl tellurium standard (at 100 µg l⁻¹), 100 µl Triton solution at 1%, 100 µl modifier solution and 125 µl 6% v/v butan-1-ol, were pipetted directly in the autosampler tubes. The volume was made up to 1.5 ml by the addition of 875 µl deionised water, and the solutions were mixed before the autosampler tubes were loaded on to the autosampler. The selenium concentration determined in each fraction was corrected for solution weight.

The detection limit was found to be $0.6 \mu\text{g l}^{-1}$, based on 3 standard deviation's on the analysis of 10 blank solutions ($0.2 \pm 0.2 \mu\text{g l}^{-1}$). However, due to the low selenium concentrations being determined in the subfractions, levels of greater than $0.2 \mu\text{g l}^{-1}$, were included in the calculation of the total selenium present in the fractions collected.

4.3. Reducing the volume of serum applied to the column

Preliminary work carried out by our laboratory using the methodology of Harrison et al⁹², found comparable selenium distributions associated with the protein fractions of samples provided by the research group (Table 4.2)¹⁰⁸. The separation was performed by applying 2.0 ml serum volumes on both columns, each with a bed volume of 8 ml, and eluting with a buffer flow rate of 1ml min^{-1} , with fifteen 2 ml sub-fractions collected. The method outlined in Section 4.2.3.2. requiring the application of only $500 \mu\text{l}$ serum on each column (established by the reducing the bed volume from 8 to 2 ml), was a development of this protocol, and was verified by the comparison of the protein separation of Seronorm serum by the two procedures.

Table 4.2. Interlaboratory comparison of the selenium distribution associated with protein fractions of two serum samples*.

Sample	Total Se($\mu\text{g/l}$)	% Recovery	%Se as .. Se P	GSHPx	Albumin
Harrison et al.					
S259-210 H6 (High)	90	93	60	23	18
S257-210 H4 (Low)	54	97	56	35	9
Southampton					
S259-210 H6 (High)	79	101	53	21	27
S257-210 H4 (Low)	54	96	54	29	13

(*Reproduced from the unpublished research report: L. Schuitemaker, Southampton General Hospital, 1998¹⁰⁸)

Initial attempts to reduce the volume of serum applied to the columns to $500 \mu\text{l}$, gave poor recoveries (58-60%), due to the difficulties of measuring such low levels of selenium in each sub-fraction. Columns of 0.5 ml capacity were assessed and found to be prone to blockage and air locks, on introduction of the serum. Using the original column,

but scaling down the bed volume of resin in the original columns to 2 ml, and reducing the buffer flow rate to 0.2 ml min⁻¹, restricted the spread of serum flow sufficiently to confine the selenium eluent to less than ten, 1ml sub-fractions.

Bovine serum (Sigma, Lot no: 77H3357) at 38.5 ± 1.4 µg l⁻¹ selenium, was characterised by the original methodology (Figure 4.2) using 2.0 ml serum for each column. The separation of the serum proteins by the scaled down method, gave a similar protein distribution profile, as can be seen in Figure 4.3., with a comparison of data for two separations by each procedure given in Table 4.3. Each separation was carried out in duplicate.

Table 4.3. Comparison of the protein distribution found for the Sigma serum at 38.5 µg l⁻¹ total selenium, when separated on columns with 8 ml and 2 ml bed volumes.

%Se associated with:	8 cm column 2.0 ml serum	2 cm column 0.5 ml serum
Selenoprotein P	36.4 ± 1.1	32.6 ± 0.0
GSHPx	43.3 ± 0.5	45.9 ± 1.1
Albumin	23.5 ± 0.1	25.9 ± 0.0
%Recovery	103.1 ± 1.4	104.4 ± 1.1

Figure 4.2. Profile of eluted sub-fractions of 8 ml columns, for 2.0 ml bovine serum.
(Two separations were carried out, denoted by solid and open symbols.)

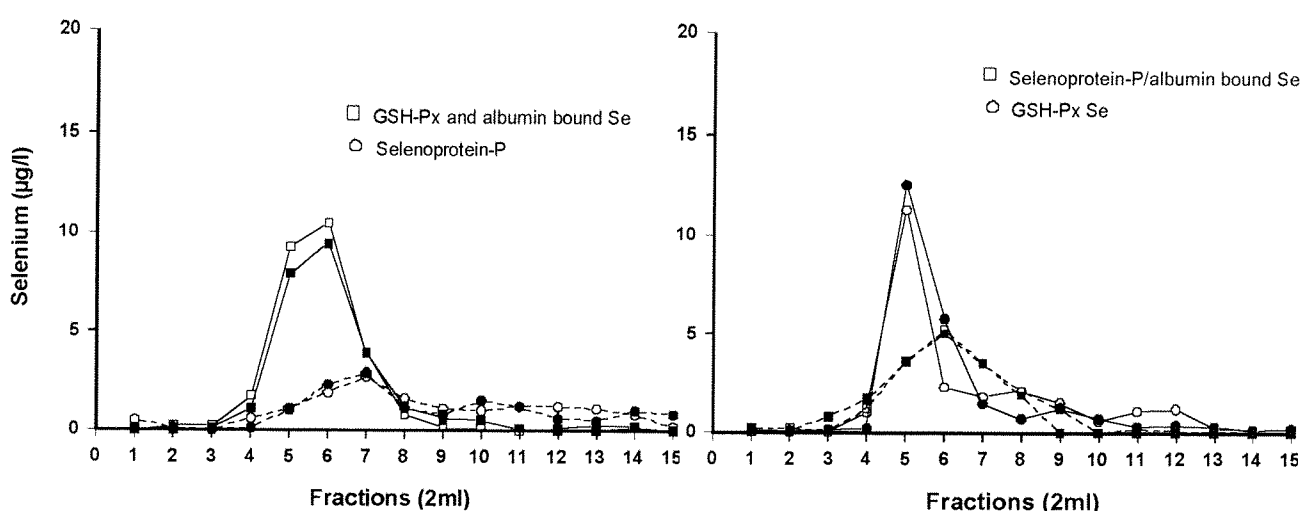


Figure 4.2.a: Heparin-Sepharose column

Fraction A: Se associated with GSHPx and albumin
Fraction B: Se associated with SeP

Figure 4.2.b: Blue Sepharose column

Fraction C: Se associated with GSHPx
Fraction D: Se associated with SeP and albumin

Figure 4.3. Profile of eluted sub-fractions of 2 ml columns, for 500 μ l bovine serum.
(Two separations were carried out, denoted by solid and open symbols.)

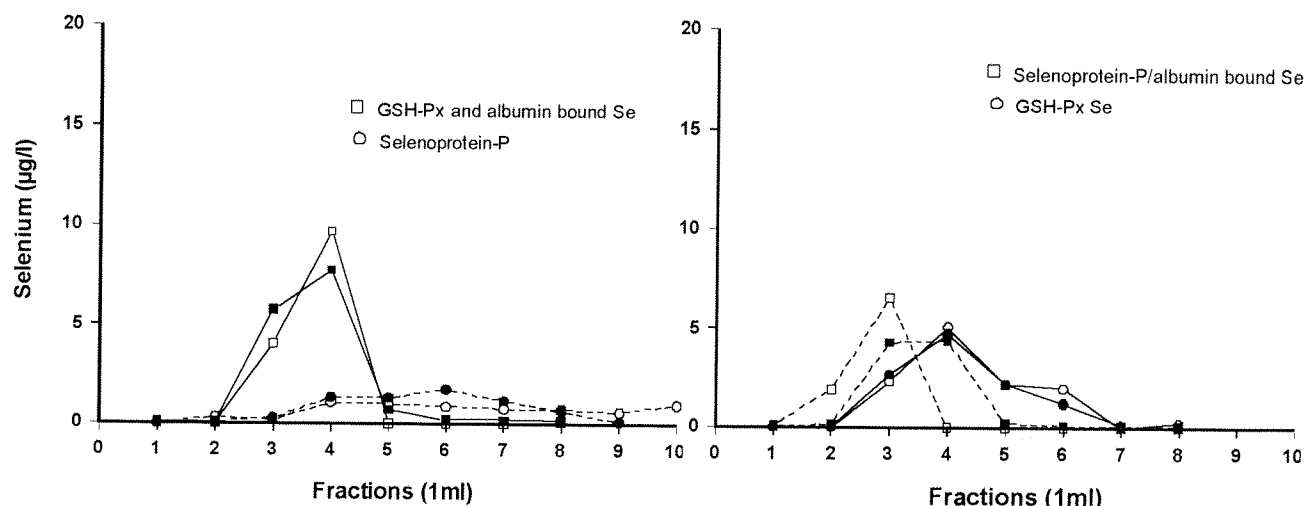


Figure 4.3.a: Heparin-Sepharose column

Fraction A: Se associated with GSHPx and albumin
Fraction B: Se associated with SeP

Figure 4.3.b: Blue Sepharose column

Fraction C: Se associated with GSHPx
Fraction D: Se associated with SeP and albumin

Separation of the serum proteins of the reconstituted lyophilised serum of human origin, Seronorm (Lot: 704121), produced a percentage distribution of 38 % (SD=0 for $n=2$) for selenoprotein P, $50 \pm 0.7\%$ for glutathione peroxidase, and $8\% \pm 1.4\%$ for albumin. This was consistent with the distribution obtained for previous determinations of reconstituted Seronorm serum (Lot 009024), at 34%, 54%, 12% respectively⁹². The measured percentage selenium associated with selenoprotein P was similar to that obtained for the commercially available bovine serum, which would suggest that the values obtained were altered by the processing of the sera rather than reflecting the protein distribution of untreated sera.

4.4. Selenium measurement in Fraction D

Selenium measurement of Fraction D obtained using the recommended sodium chloride levels of Elution buffer 2 (1.4 mol l^{-1} NaCl in 0.02 mol l^{-1} ammonium acetate)⁹², proved to be problematic. The high salt content of the buffer solution lowered the sensitivity of analysis of ^{78}Se , as is illustrated by the calibration curve shown in Figure 4.4.

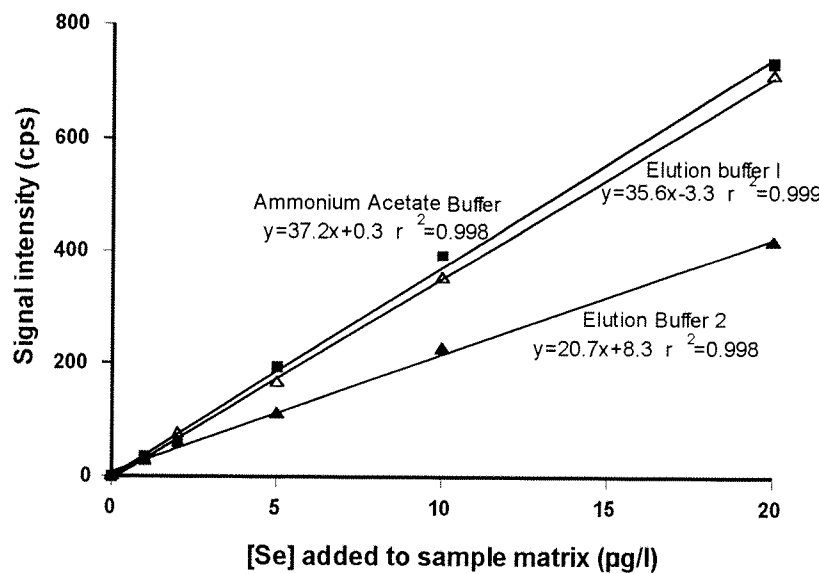


Figure 4.4. Selenium standard additions to ammonium acetate buffer, elution buffers 1 and 2.

Separation of the serum proteins for the reconstituted lyophilised serum, Seronorm (Lot: 704121), produced a fraction D, in which the NaCl buffer sub-fractions contained a substance which caused spectral overlap at masses 78 and 82 (Figure 4.5).

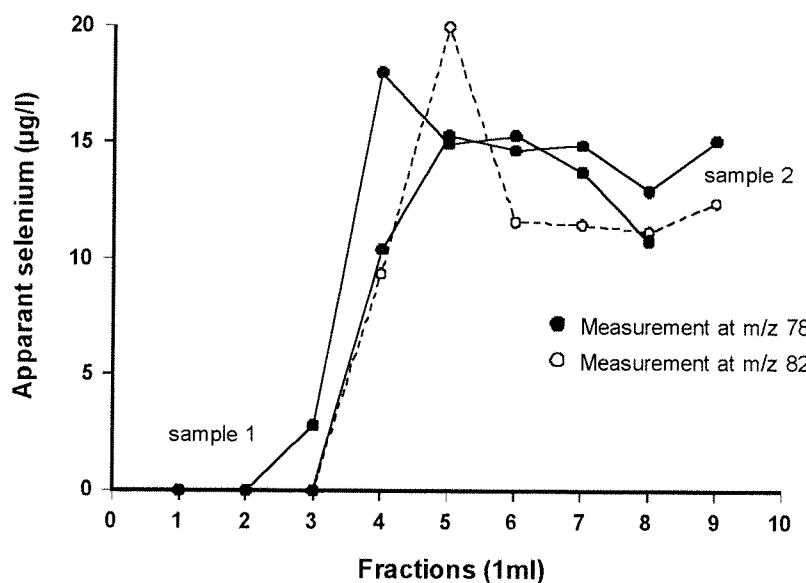


Figure 4.5. Signal intensity at m/z 78 for two Seronorm serum aliquots (●), and at 82 m/z for sample 2 (○).

In an attempt to find the lowest salt concentration at which complete elution of proteins from the blue-Sepharose column was achieved, buffers containing increasing levels of NaCl (0.1 - 0.6 mol l⁻¹) were passed through the column pre-loaded with serum, and washed through with equilibrium buffer. A NaCl concentration of 0.6 mol l⁻¹ was found to be necessary in the elution buffer, for complete recovery of the serum proteins bound to the column (Figure 4.6). The amount of selenium associated with the eluted serum protein, on using 0.6 mol l⁻¹ NaCl was 15.0 µg l⁻¹, which compared well with that obtained with 1.4 mol l⁻¹ NaCl at 14.7 µg l⁻¹.

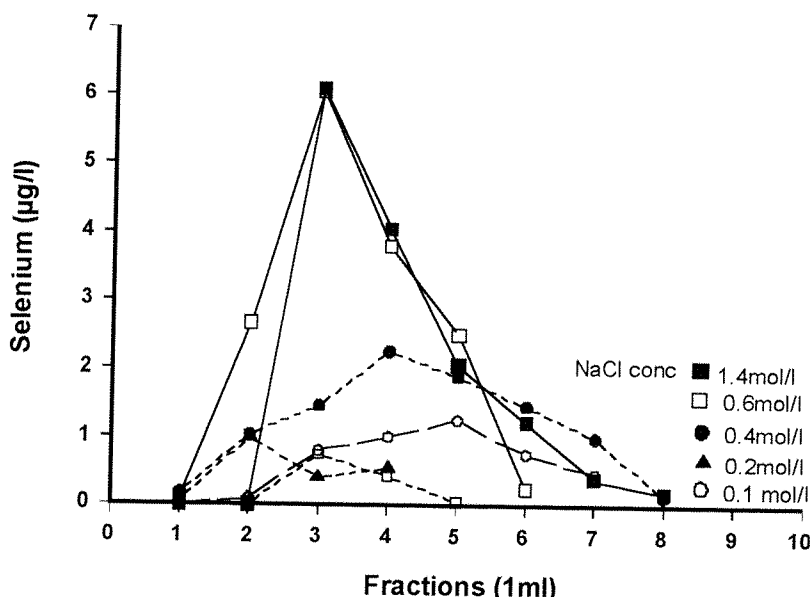


Figure 4.6. Selenium elution profiles of serum proteins, obtained using buffers containing increasing concentrations of NaCl from the blue-Sepharose column.
(Dashed lines: sequential elution with buffer containing increasing NaCl concentration.)

However, problems were still encountered with a few samples, with selenium concentrations obtained for fraction D being less than that determined for fraction B. To be consistent, the estimated percentage selenium associated with albumin was calculated solely from fraction A minus C, for all samples separated.

4.5. Selenium distribution in healthy adults

Plasma/serum samples of healthy adults were separated by the columns, and the percentage selenium distributions associated with selenoprotein-P, GSH-Px and albumin were determined. The presence of an anticoagulant in the sample produces no appreciable differences in the distribution of selenium⁹². The results are given in Table 4.4.

Table 4.4. Selenium distribution in a healthy population, expressed as a percentage of total selenium and as a selenium concentration.

Sex	Age (yrs)	Specimen Type	Total Se ($\mu\text{g l}^{-1}$)	%Se Recovery	%Se As			Se as ($\mu\text{g l}^{-1}$)			
					Se P	GSH-Px	Albumin	Se P	GSH-Px	Albumin	
1	F	23	Serum	88.7	103	50	42	11	44	37	10
2	M	28	Serum	76.5	108	52	39	17	39	30	11
3	M	28	Serum	109.8	94	42	50	2	46	55	2
4	M	30	Serum	98.4	99	52	42	5	51	41	10
5	M	33	Serum	91.2	102	54	44	4	49	40	2
6	F	36	Plasma	90.3	103	48	54	1	43	49	1
7	M	47	Serum	88.0	102	48	38	16	42	34	14
8	F	63	Plasma	65.9	97	53	35	9	35	23	6
9	M	68	Plasma	56.6	105	50	34	21	28	19	12
23-68		Range	54-110	94-106	42-54	34-54	1-21	28-49	19-55	1-14	
		Mean \pm sd	85 \pm 16	101 \pm 4	50 \pm 4	42 \pm 7	10 \pm 7	42 \pm 7	36 \pm 12	8 \pm 5	

In healthy subjects, selenium was found to be distributed between the three main plasma proteins at $50 \pm 4\%$ for selenoprotein P, $42 \pm 7\%$ for glutathione peroxidase and $10 \pm 7\%$ for albumin. These results are consistent with those observed by Harrison, at $53 \pm 6\%$ for selenoprotein P, $39 \pm 6\%$ for glutathione peroxidase and $9 \pm 4\%$ for albumin, obtained using a larger sample population of twenty-one adults. Two samples included in this study were taken from adults over 60 years of age, these showed lower total selenium concentrations, although the percentage selenium associated with the proteins remained of the same order as that found with the other samples.

4.6. Selenium distribution in TPN patients

Patients on Total Parenteral Nutrition (TPN), are administered selenium to maintain normal concentrations of the element in plasma. To investigate whether the selenium distribution was different in these patients, samples from nine patients on TPN were assessed. The percentage selenium distributions associated with the proteins were determined to be $53 \pm 3\%$ for selenoprotein P, $45 \pm 7\%$ for glutathione peroxidase and $3 \pm 2\%$ for albumin. Table 4.5. lists the individual results.

Table 4.5. Selenium distribution in TPN samples, expressed a percentage of total selenium and as a selenium concentration.

	Sex	Age (yrs)	Specimen type	Total Se ($\mu\text{g l}^{-1}$)	%Se Recovery	%Se As			Se as ($\mu\text{g l}^{-1}$)		
						Se P	GSH-Px	Albumin	Se P	GSH-Px	Albumin
1	M	33	Plasma	64.4	102	46	55	1	30	36	1
2	F	54	Plasma	60.1	101	54	40	7	33	24	4
3	M	57	Plasma	66.7	109	52	52	5	34	35	3
4	M	59	Serum	32.7	101	52	44	5	17	14	2
5	F	62	Plasma	44.5	106	56	48	2	25	22	1
6	M	63	Serum	85.2	102	53	47	2	45	40	2
7	F	72	Plasma	65.4	106	52	50	4	34	33	3
8	M	77	Plasma	49.4	91	54	36	1	29	19	1
9	M	79	Plasma	53.6	94	56	37	1	30	20	1
33-79 Range				33 - 85	9 - 109	46-56	36-55	1 - 7	17-45	14 - 40	1 - 4
Mean \pm sd				58 \pm 15	101 \pm 6	53 \pm 3	45 \pm 7	3 \pm 2	31 \pm 8	27 \pm 9	2 \pm 1

4.7. Conclusion

The majority of selenium was found to be associated with selenoprotein P, with more variation in the proportion of selenium measured in the glutathione peroxidase fraction, than that for selenoprotein P. The group sizes used were small, and further work needs to be carried on a larger number of samples in order to determine whether there are any statistically significant differences between TPN patients and healthy subjects. However, the distribution of the percentage of selenium associated with the proteins in the group receiving TPN does appear to be similar to that of the healthy subjects, with less being bound to albumin when selenium status is low.

CHAPTER 5

SELENIUM DETERMINATION BY ISOTOPE DILUTION

5.1. Introduction

Isotope dilution (ID) mass spectrometry is a technique of quantitative analysis capable of achieving high precision and accuracy in the determination of elements that have more than one stable isotope¹⁰⁹⁻¹¹². It can also be applied using radioactive isotopes under suitable conditions. Analysis by isotope dilution depends upon measuring the change in a specific endogenous isotopic ratio in a given sample following the addition of a known amount of the element artificially enriched in one of its isotopes. The altered isotopic ratio (R) is a measure of the proportion of one isotope present in both the natural sample and spike with respect to the enriched isotope, and is defined by equation [1]^{109,110}.

$$\text{Isotopic ratio, } R = \frac{X}{Y} = \frac{\text{moles } X_n + \text{moles } X_s}{\text{moles } Y_n + \text{moles } Y_s} \quad [1]$$

X_n and Y_n are the isotopes X and Y in the natural sample, X_s and Y_s are the isotopes in the spike. Since atoms are detected, the concentration of the isotopic species must also be in terms of number of moles of atoms rather than abundances.

If the total number of moles of natural and spike selenium are represented by M_n and M_s , and the percentages indicate the isotopic abundances, the ratio can be calculated as follows:

$$R = \frac{M_n * \%X_n + M_s * \%X_s}{M_n * \%Y_n + M_s * \%Y_s} \quad [2]$$

The following rearrangement of this equation gives rise to [3]:

$$\begin{aligned} R (M_n * \%Y_n + M_s * \%Y_s) &= M_n * \%X_n + M_s * \%X_s \\ (R * M_n * \%Y_n) - (M_n * \%X_n) &= (M_s * \%X_s) - (R * M_s * \%Y_s) \\ M_n (R * \%Y_n - \%X_n) &= M_s (\%X_s - R * \%Y_s) \end{aligned}$$

$$M_n = M_s * \frac{(\%X_s - R * \%Y_s)}{(R * \%Y_n - \%X_n)} \quad [3]$$

As the number of moles equates to mass / relative molecular weight, this equation when expressed in terms of concentration, gives rise to the following:

$$\frac{C_n * wt_n}{A_n^r} = \left(\frac{C_s * wt_s}{A_s^r} \right) * \frac{(\%X_s - R * \%Y_s)}{(R * \%Y_n - \%X_n)} \quad [4]$$

Concentrations of the solutions are denoted by C_n and C_s , with wt_n and wt_s being the weights (or volumes) of the sample and spike, relative to the total atomic weight of the sample (A_n^r) and spike (A_s^r).

The sample concentration of the analyte can be calculated from a rearrangement of equation [4]:

$$\text{Concentration, } C_n = \frac{C_s A_n^r wt_s * (\%X_s - R * \%Y_s)}{A_s^r wt_n * (R * \%Y_n - \%X_n)} \quad [5]$$

The enriched isotope represents the ideal internal standard, compensating for many sources of error, since any losses of the element in subsequent steps of analysis should effect both isotopes equally. Recommendations for the application of this technique, specify that the detection of the selected isotopes needs to be free of any spectral interference, which would otherwise affect the observed ratio for this technique^{112,113}. Nevertheless, it has been shown that ID analysis can be successfully applied for the accurate determination of certain elements, provided isobaric interferences are reduced to sufficiently low levels¹¹⁴⁻¹¹⁶. Lam et al.¹¹⁴ studied the possibility of using ID-MS in the determination of chromium in biological samples, for which conventional analysis is hampered by isobaric interferences on the major isotope at mass 52. It was found that the interfering polyatomic species could be reduced sufficiently to allow accurate measurement of the ^{52}Cr : ^{53}Cr ratio, by the introduction of air-argon mixture into the ICP-MS plasma to destabilise the isobaric ^{40}Ar : ^{12}C ions. Gregoire¹¹⁶ used measured ^{10}B : ^{11}B ratios (determined with a background level of 150 counts s^{-1}), in obtaining boron concentrations that agreed well with results generated by conventional analysis.

Evaluation of the possible matrix-related interferences on the individual isotope determinations, would be necessary. Published ID-ICP-MS methods employed hydride

generation or electrothermal vaporisation (ETV-ICP-MS), as the modes of sample introduction to separate the analyte from the matrix interferences¹¹⁸⁻¹²¹. Selenium isotope determination by the developed direct ICP-MS method, utilises butan-1-ol to reduce the level of spectroscopic overlap on masses 76, 77 and 78, but the extent to which the interferences still exist, vary for each isotope. The aim of the following investigations is to determine the effect that this and that of the signal enhancement, will have on the measured isotope abundance ratio and the overall precision of the analysis.

5.2. Isotope ratio measurement

5.2.1. Mass bias correction

Observed isotopic ratios can differ from the calculated “true” isotope abundance ratio, because of changes induced from the differential efficiency of transmission and detection by the mass spectrometer, as a function of the difference in mass between the two isotopes. The “true” ratio can be related to the measured ratio by the equation:

$$\text{Measured ratio} = \text{True ratio} (1 + \alpha n)$$

Where α is the bias per mass unit, and n is the mass difference between the isotopes⁶⁴.

These instrumental discrimination effects can be compensated for, by means of a standard solution of known isotopic composition, analysed under the same conditions. The observed ratio is then used to normalise the measured ratio of the unknown sample¹¹⁷. Ideally, the mass bias solution should also match the spiked sample in count rate obtained by the ICP-MS^{109,113} but this would be impractical when measuring selenium in clinical matrices that could vary within the range of 15 to 160 $\mu\text{g l}^{-1}$. It would therefore be appropriate to assess whether a single concentration solution would be adequate in producing a corrected isotope ratio across a range of concentrations without significantly altering the accuracy of the analytical results.

5.2.2. Dead time correction

Another consideration in accurate isotope ratio determination, is how the measured count rate for each isotope relates to the true count rate, which for large analyte signals, is

dependent on the dead time correction set for the analysis. At higher count rates, pulse counting systems register fewer events than actually occur, with the “dead time” being the interval during which the detector is unable to resolve successive pulses. As a consequence, the instrument signal response becomes non-linear at count rates higher than 10^6 cps, requiring the application of a dead time correction to compensate for this. However, the relatively low count rates normally encountered in the measurement of selenium in clinical matrices avoid the need to assess the dead time corrections applied to the individual isotope signal responses.

5.2.3. Optimal blend

The optimum mixture of the spike and the natural solution is such that the uncertainty in concentration ($\Delta C/C$) versus the uncertainty in ratio measurement ($\Delta R/R$) is at a minimum^{111,122}. Error propagation varies as a function of the isotope ratios in the spiked sample, and can be calculated for each specific combination of sample and spike isotope abundances. Referred to as the error magnification factor (F), it can be calculated theoretically with equation [7], derived from equation [6], where X is the natural sample isotope and Y is the enriched spike isotope.

$$\frac{\Delta C}{C} = F \times \frac{\Delta R}{R} \quad [6]$$

$$\text{Error magnification factor, } F = \frac{X}{Y} = \frac{(X_n Y_s - X_s Y_n)R}{(Y_n R - X_n)(X_s - Y_s R)} \quad [7]$$

The theoretical optimal isotopic ratio, which provides the minimum error magnification factor, can be derived from equation [7], and specifically calculated when this equation is simplified to the following formula, [8]^{109, 111, 123, 124}.

$$\text{Optimum ratio} = \sqrt{\left(\frac{X \text{ abundance in spike}}{Y \text{ abundance in spike}} \right) \times \left(\frac{X \text{ abundance in sample}}{Y \text{ abundance in sample}} \right)} \quad [8]$$

The sample:spike isotope mixture calculated to give the minimum error propagation may not necessarily be the appropriate blend to provide the best analytical precision. In

practice, instrumental detection precision has been found to be at its best for the measurement of equimolar amounts of spike and sample¹⁰⁹. In cases where this differs from the “optimal” blend, only a comparison of RSDs of repeated measurements would ascertain the appropriate ratio to use.

5.3. Isotopically enriched selenium elements

Two stable isotope enriched standards were used in the following investigation: ⁷⁴Se (Stock reference number: 4) and ⁷⁷Se (Stock reference number: 3) purchased from AEA Technology, (Nuclear Science, Didcot). The isotopic abundances for these materials are given in Table 5.1.

Table 5.1. Isotopic abundances for the ⁷⁴Se and ⁷⁷Se enriched selenium standards.

Isotope	Mass	%Natural Abundance ¹²⁵	Enriched ⁷⁴ Se %abundance (⁷⁴ Se/4)	Enriched ⁷⁷ Se % abundance (⁷⁷ Se/3)
⁷⁴ Se	73.92	0.89	31.83	0.27
⁷⁶ Se	75.92	9.36	15.27	2.6
⁷⁷ Se	76.92	7.63	6.21	68.69
⁷⁸ Se	77.97	23.78	14.26	17.51
⁸⁰ Se	79.92	49.61	27.73	9.28
⁸² Se	81.92	8.73	4.71	1.65
Atomic Weight		78.96	77.03	77.42

The ratio of the natural abundances of the isotopes in the selenium stock solution was confirmed by comparison with a solution of selenium metal digest (Digest solution prepared at the Laboratory of the Government Chemist (LGC) from selenium metal pellets, Aldrich).

A selenium stock solution of 20 µg ml⁻¹ Se in 0.2% HNO₃ was obtained for each enriched isotope standard by digesting 2.0 mg of the metal in 200 µl concentrated nitric acid, and diluting the solution to 100 ml with deionised water. The mean selenium concentration in a 1:200 dilution, measured by conventional ICP-MS and by reverse ID analysis, showed that total selenium levels corresponded to 100% and 97% total selenium

for ^{74}Se and ^{77}Se enriched standards, respectively.

Figure 5.1. shows how the predicted error magnification factor (F) calculated from equation [7], changes as a function of the selenium isotope ratios for the standards employed.

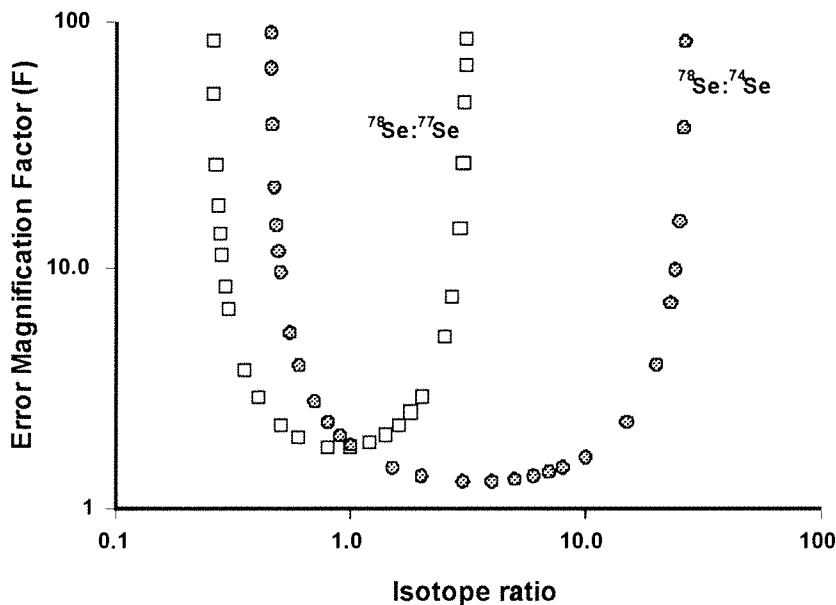


Figure 5.1. Log-log plot of the error magnification factor as a function of natural: spike selenium isotopic ratios ($^{78}\text{Se}:\text{Se}^{74}$ and $^{78}\text{Se}:\text{Se}^{77}$).

F is at a minimum when the ratios are 3.46 for the ^{74}Se spiked samples and 0.89 for those spiked with ^{77}Se . Therefore, for a $80 \mu\text{g l}^{-1}$ selenium reference solution, the optimal blend would require concentrations of $17 \mu\text{g l}^{-1}$ ^{74}Se -enriched standard ($^{78}\text{Se}:\text{Se}^{74}$ ratio=3.437) and $30 \mu\text{g l}^{-1}$ ^{77}Se -enriched standard ($^{78}\text{Se}:\text{Se}^{74}$ ratio=0.899).

5.4. IDMS equations employed

The “true” abundance ratio for a given pair of isotopes on mixing two solutions with different isotopic compositions, can be calculated using equation [9].

$$\text{Isotopic ratio} = \frac{X}{Y} = \frac{X * \% \text{ }^{78}\text{Se in natural}/A^r_n + Y * \% \text{ }^{78}\text{Se in spike}/A^r_s}{X * \% \text{ }^{78}\text{Se in natural}/A^r_n + Y * \% \text{ }^{78}\text{Se in spike}/A^r_s} \quad [9]$$

Where: X = Volume x concentration of natural solution,

Y = Volume x concentration of spike solution

A^r_s = Relative Atomic weight of spike selenium standard

A^r_n = Relative Atomic weight of natural selenium

$$\text{ie. } {}^{78}\text{Se:}^{74}\text{Se ratio} = \frac{X*23.78/78.96+Y*14.26/77.03}{X*0.89/78.96+Y*31.83/77.03} \quad {}^{78}\text{Se:}^{77}\text{Se ratio} = \frac{X*23.78/78.96+Y*17.51/77.42}{X*7.63/78.96+Y*68.69/77.42}$$

The measured ${}^{78}\text{Se:}^{\text{spike}}\text{Se}$ ratio (R), is normalised to the reference solution to correct for mass bias, by multiplying it by the true / measured isotope abundance ratio of the reference solution. This normalised value of R, can be used in equation [5] to calculate the concentration of the sample.

Therefore,

$$\text{Concentration} = \frac{X * A^r n * (\% {}^{78}\text{Se in spike} - (R * \% {}^{\text{spike}}\text{Se in spike solution}))}{\text{Volume of natural} * A^r s * ((R * \% {}^{\text{spike}}\text{Se in natural}) - \% {}^{78}\text{Se in natural})}$$

ie. for ${}^{78}\text{Se:}^{74}\text{Se}$ ratio,

$$\text{Conc} = \frac{X*78.96*(14.26-(R*31.83))}{\text{vol of natural} * 77.03 * ((R*0.89)-23.78)}$$

and for ${}^{78}\text{Se:}^{77}\text{Se}$ ratio

$$\text{Conc} = \frac{X*78.96*(17.51-(R*68.69))}{\text{vol of natural} * 77.42 * ((R*7.63)-23.78)}$$

5.5. Method

A Perkin-Elmer Elan 6100 DRC ICP-MS (Perkin-Elmer, SCIEX, Canada) was used. Instrumental conditions are summarised in Table 5.2., and reagents were as described in Section 3.3., with “Aristar” selenium solution, at $1001 \mu\text{g ml}^{-1}$ (BDH, Poole, Dorset) used to prepare the calibrating solutions.

Table 5.2. Operating conditions for the Elan 6100 ICP-MS.

rf power	1.2 kW
Plasma gas flow rate	15.00 l min^{-1}
Auxiliary gas flow rate	1.0 l min^{-1}
Sampling /skimmer cones	Platinum
Lens voltage	8-11 V (Optimised daily)
Quadrupole rod offset	0.5 V
Cell rod offset	-18 V
Cell path voltage	-18 V
Nebuliser flow rate	$0.8-0.9 \text{ l min}^{-1}$ (Optimised daily)
Sample uptake rate	Setting of -18 for the peristaltic pump
Neubuliser	Cross-flow
Wash solution	0.5% butan-1-ol, 0.05% Triton-X100, 6.7% blood diluent.

100 μl serum/aqueous samples were diluted with equal volumes of 1% v/v Triton X-100 and the blood diluent solution (ammonia/EDTA/phosphate), 125 μl 6% v/v butanol,

and 875 µl deionised water, directly into the autosampler tubes. Matrix-matched reference solutions were prepared by diluting serum samples containing 40, 80, 160 µg l⁻¹ selenium (bovine serum + aqueous spike), in the same way as the samples. The reference and the sample solutions were all spiked with 100 µl enriched isotope ⁷⁴Se standards at the optimum concentration calculated for a solution containing 80 µg l⁻¹. The aqueous blanks (containing all the diluents except for the spike) and reference solutions were analysed at the start of each run, and at intervals of ten test samples. The samples were blank-subtracted and the average of the ratio correction factor was applied to the bracketed measured ratios.

IQCs and certified reference sera: Seronorm and NIST 1598, were used to validate the method. A new set of four sera internal quality control material (series B) was required, these were prepared to contain the equivalent selenium content of the previous series, by spiking pools of bovine sera (Lot no. 78H3355, Sigma-Aldrich, Poole, Dorset) with aqueous selenium. 40, 120, 240 and 340 µl aliquots of selenium at 100 µg ml⁻¹ were added to 250 ml volumes of serum (endogenous concentration of 10 µg l⁻¹), to give increases of 16, 48, 96 and 136 µg l⁻¹. The target values were established by intra-laboratory comparisons and were analysed by The Laboratory of the Government Chemist, using ETV-ICP-MS.

5.6. Optimisation of the mass scanning conditions

The overall precision of the ID analysis is mainly determined by the reproducibility that can be achieved in measuring the isotopic ratio itself. A short dwell time is required in the scanning parameters, in order to monitor the isotopes in rapid succession^{120,122,126}.

In routine analysis of clinical samples, the volume of sample is a major consideration. A 100 µl aliquot diluted 1+14, with a sample uptake rate of 0.8 ml min⁻¹, enables an analysis time of 2 minutes. Within this constraint, the dwell time was increased, with a change in the number of sweeps per reading to restrict the analysis time. Figure 5.2. shows the observed RSD values derived from the analysis of five replicates of the aqueous reference solution (80 µg l⁻¹ natural solution + 30 µg l⁻¹ ⁷⁷Se-enriched standard).

At dwell times greater than 5ms, the observed ⁷⁸Se:⁷⁷Se ratio deviated by only ±4% from the expected ratio and a precision of less than 0.75% RSD was achieved. A dwell time of 20 ms (450sweeps per reading) was selected for subsequent analysis.

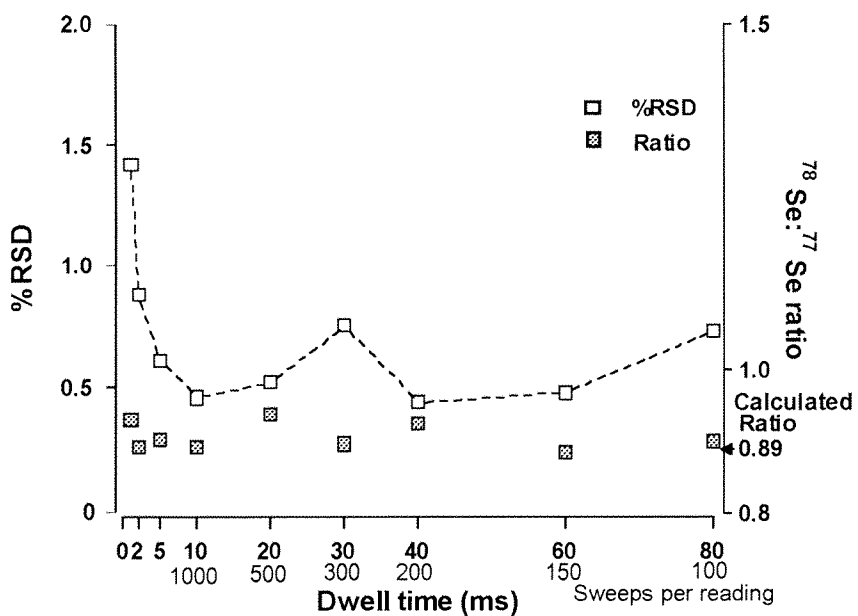


Figure 5.2. Percent relative standard deviation and the observed isotopic ratio ($^{78}\text{Se} : ^{77}\text{Se}$) as a function of dwell time.

5.7. Aqueous analysis

A series of aqueous solutions were prepared using the natural selenium digest standard solution to give concentrations of 10, 20, 50, 100, 150 and 200 $\mu\text{g l}^{-1}$ selenium in 0.1% nitric acid. These solutions were used to compare the analysis by conventional ICP-MS analysis, with that of IDMS. Table 5.3. shows the variation obtained on correction of the ratio using reference solutions at 80 $\mu\text{g l}^{-1}$ natural selenium, 40, 80, 160 $\mu\text{g l}^{-1}$ and at the specific concentration of test solution.

Table 5.3. Measurement of selenium in aqueous solutions by conventional and IDMS analysis using ^{77}Se and ^{74}Se -enriched isotope standards, with and without reference solution correction.

Solutions $\mu\text{g l}^{-1}$ Se	Conventional ICP-MS	No correction $\mu\text{g l}^{-1}$		80 corrected $\mu\text{g l}^{-1}$		40, 80, 160 corrected		Individual conc corrected	
	$\mu\text{g/l}$	^{77}Se	^{74}Se	^{77}Se	^{74}Se	^{77}Se	^{74}Se	^{77}Se	^{74}Se
10	11.3	11.7	13.4	10.0	10.0	10.7	10.0	9.9	9.9
20	20.6	22.4	26.9	20.1	21.5	21.0	21.5	20.1	20.0
50	53.0	54.1	58.0	49.8	47.8	51.4	47.8	50.3	48.3
100	102.0	106.6	107.2	98.3	88.7	98.3	88.7	101.3	99.3
150	150.9	156.4	180.2	143.4	147.8	144.5	146.3	147.6	150.1
200	208.0	218.0	258.3	198.3	209.0	199.9	206.9	202.0	200.0
Mean Bias $\mu\text{g/l}$ (%)	2.6 (2.9)	6.5 (7.4)	19.0 (21.5)	-1.7 (-1.9)	-0.9 (-1.0)	-0.7 (-0.8)	-1.5 (-1.7)	0.5 (0.6)	-0.4 (-0.45)

A comparison of the mean bias illustrates how correction of the measured ratio with reference solutions is essential for accurate IDMS analysis. The ideal situation would be to prepare mixtures of spike with natural standard, which closely match the test sample in isotopic ratio and in count rate, to run alongside the sample as recommended Catterick¹¹³ and Henrion¹¹⁷. This would be impractical for large numbers of clinical samples. A compromise of just analysing three reference solutions containing 40, 80 and 160 µg l⁻¹ natural selenium, at frequent intervals throughout the assay run, gave similar or better bias values when compared with conventional ICP analysis.

5.8. Serum analysis

Serum matrix-matched solutions were prepared by using a bovine serum spiked with a selenium standard solution, to give working values of 80 and 160 µg l⁻¹ selenium. The endogenous selenium concentration of the serum, measured by conventional ICP-MS, was 40 ± 2 µg l⁻¹ and was used in preparation of the 40-reference solution.

The need for matrix-matched reference solutions was demonstrated by the lower ⁷⁸Se:⁷⁷Se ratios observed in the reference solutions when serum was used (Table 5.4.). Similar ratio values were obtained for both matrices on ⁷⁸Se:⁷⁴Se analysis - higher than the calculated values, the difference increased with concentration.

Table 5.4. Comparison of measured aqueous and serum reference solution ratio values, obtained on spiking with 30 µg l⁻¹ ⁷⁷Se, and 17 µg l⁻¹ ⁷⁴Se standard.

Reference Solution	⁷⁸ Se: ⁷⁷ Se			⁷⁸ Se: ⁷⁴ Se		
	Aqueous	Serum	Calculated value	Aqueous	Serum	Calculated value
40	0.635	0.523	0.618	2.353	2.177	2.033
80	0.940	0.811	0.899	3.975	3.867	3.437
160	1.361	1.212	1.306	6.772	6.786	5.185

Samples initially measured to assess the accuracy of the developed conventional method (Section 3.11.2.) were reanalysed by IDMS and the results corrected using a single reference solution at 80 µg l⁻¹, and three solutions at 40, 80 and 160 µg l⁻¹, in both aqueous and serum matrix.

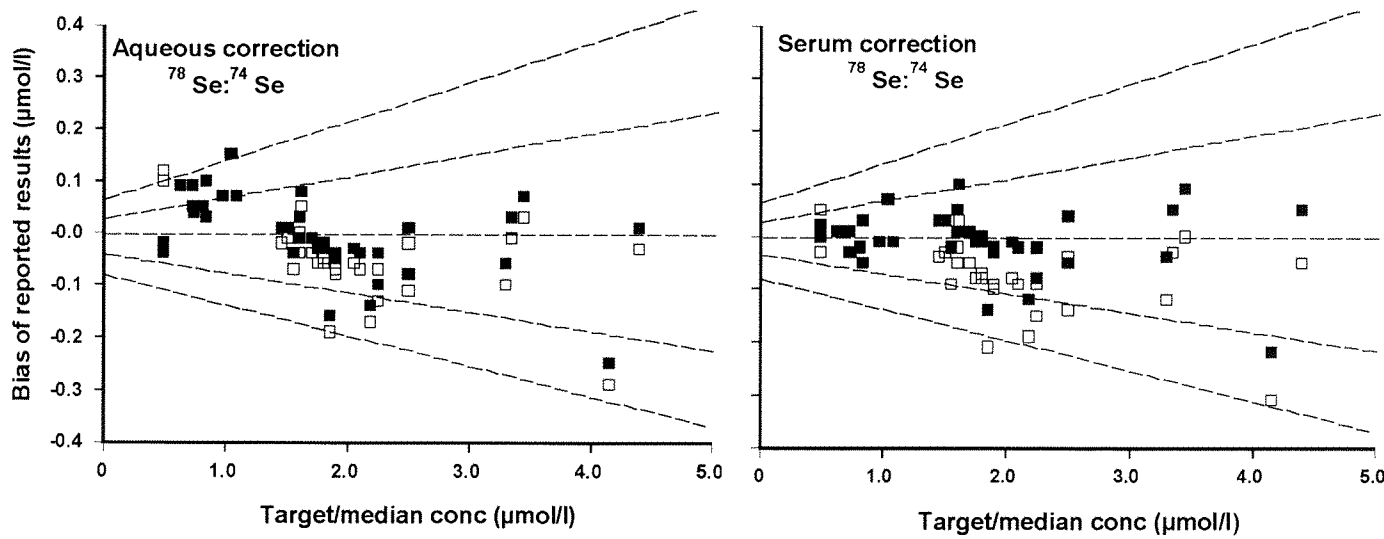


Figure 5.3. Comparison of the bias from target values of serum samples analysed by IDMS, using ^{74}Se -enriched standard of 80-corrected (open symbols), and 40/80/160 corrected results (closed symbols), with aqueous and serum reference solution calibration.

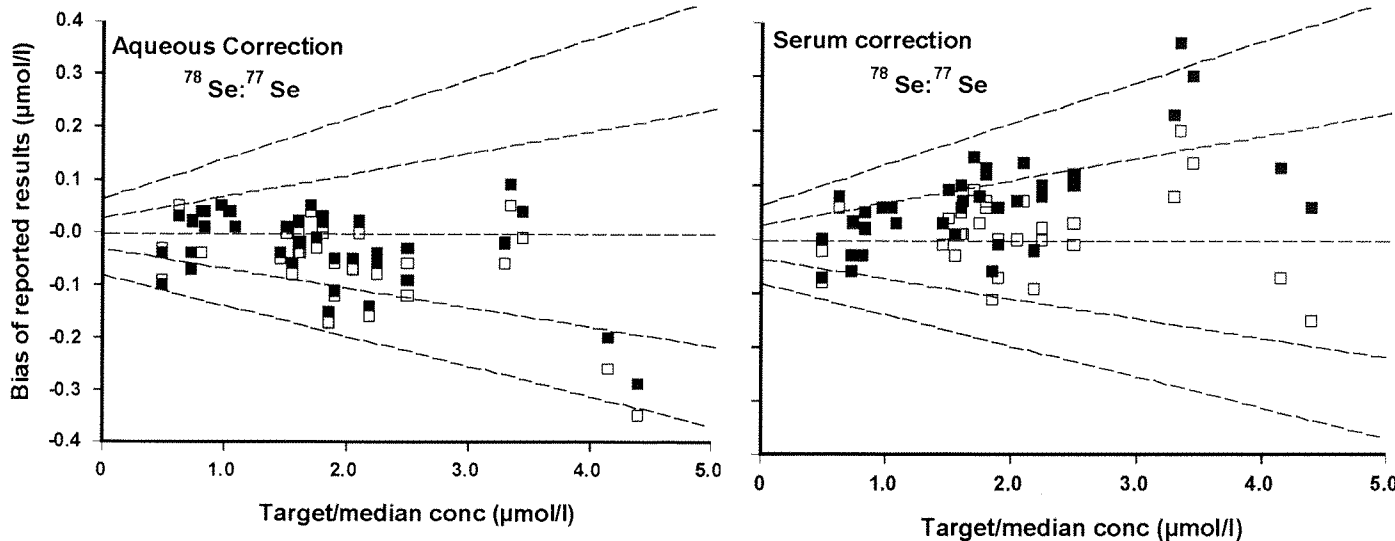


Figure 5.4. Comparison of the bias from target values of serum samples analysed by IDMS, using ^{77}Se -enriched standard of 80-corrected (open symbols), and 40/80/160 corrected results (closed symbols), with aqueous and serum reference solution calibration.

The best accuracy was achieved by normalising the measured $^{78}\text{Se} : {^{74}\text{Se}}$ ratio to the three serum reference solutions, which produced a mean bias of $-0.8 \mu\text{g l}^{-1}$ ($-0.01 \mu\text{mol l}^{-1}$) (Figure 5.3.). The 40-reference solution was applied to concentrations of less than $60 \mu\text{g l}^{-1}$ the 80-reference solution for concentrations between 60 and $120 \mu\text{g l}^{-1}$, and 160-reference

solution for levels greater than $120 \mu\text{g l}^{-1}$. A listing of the individual results obtained and their percentage bias from target values is given in Tables 2A and 2B of the Appendix.

The variation in bias shown in Figure 5.4. for ^{78}Se : ^{77}Se indicates a problem with respect to utilising sera correction solutions. Concentrations obtained by spiking with the ^{77}Se -enriched isotope approached the target values when corrected by just the serum 80 reference solution. The use of matrix-matched 40 and 160 reference solutions to correct for concentrations below 60 and above $120 \mu\text{g l}^{-1}$, produced a large positive bias of $5.5 \mu\text{g l}^{-1}$ ($0.07 \mu\text{mol l}^{-1}$). Chloride in the form of $^{40}\text{Ar}^{37}\text{Cl}$ or $^{40}\text{Ca}^{37}\text{Cl}$ can give rise to enhanced signals at mass 77, and the susceptibility of ^{77}Se measurement to matrix-related interferences would explain the low ^{78}Se : ^{77}Se ratios found in sera (Table 5.4.). Because of this, ^{77}Se was found to be an unsuitable isotope for ID measurement, and further investigations were limited to the use of the ^{74}Se -enriched standard.

5.9. Optimal blend for ^{78}Se : ^{74}Se analysis

Accurate analysis has been shown to be dependent on the normalisation of the measured ^{78}Se : ^{74}Se ratio to reference solutions. Graphical treatment of the ratios, permits this correction to be incorporated more easily into routine analysis. The addition of the ^{74}Se -enriched standard at a specific concentration to three calibrating solutions at 40, 80, $160 \mu\text{g l}^{-1}$ enables the isotopic ratio to be plotted as a function of concentration. The analyte selenium content can be calculated by employing the equation of the regression line to convert the measured isotopic ratios of the spiked sera, to concentrations.

A plot of the calculated ratios at the optimal blend concentration of ^{74}Se ($17 \mu\text{g l}^{-1}$) for $80 \mu\text{g l}^{-1}$ natural selenium, shows that the regression curve is not linear (Figure 5.5.). A better approximation to linearity is observed, using ratios calculated for the addition of $100 \mu\text{g l}^{-1}$ ^{74}Se /4. At this concentration, equimolar levels of the sample and spike isotope abundances are present, providing the conditions for the best mass spectrometric precision to be achieved. A 0.6% relative standard deviation was obtained for five dilutions of $80 \mu\text{g l}^{-1}$ natural selenium.

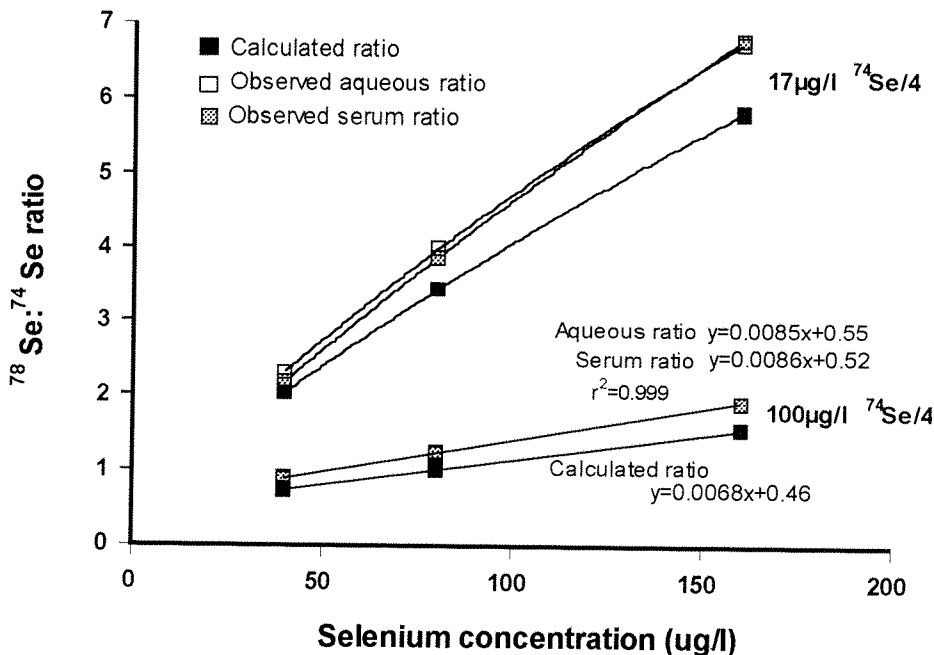


Figure 5.5. Calculated and measured ^{78}Se : ^{74}Se ratios as a function of increasing levels of selenium, on addition of ^{74}Se -enriched standard at 17 and 100 $\mu\text{g l}^{-1}$.

5.10. Optimisation of scanning parameters

It was evident during these studies that the precision found in aqueous solutions (<0.5%), could not be achieved for serum analysis because of the influence of a more complex matrix on the counting statistics. The removal of the automatic correction for the presence of ^{74}Ge and ^{78}Kr from the scanning parameters on the Elan 6100, effectively halves the time for data acquisition for the specific selenium isotopes. Any krypton present would originate from the argon gas flow and would therefore be compensated by blank subtraction. Scanning the bovine serum, IQC, external quality assessment material and various human sera/plasma samples, showed that the count rates for germanium were at blank levels. Should the sample contain germanium, the resultant elevation of the ^{74}Se signal would be uncharacteristic and therefore noticeable.

Under these conditions, the optimal scanning parameters for the Elan 6100 were evaluated by averaging the relative standard deviation of five dilutions of the reference solution at 80 $\mu\text{g l}^{-1}$ natural selenium (Figure 5.6.). The influence of dwell time and sweeps per reading within sample determination, were assessed and optimised with respect to each other to obtain the lowest %RSD, keeping the analysis time constant at around 1 min

(+ 60 seconds read delay), with a rinse time of 60 seconds between sampling. A minimum of 0.2% RSD was reached at 10 msec dwell time with 1000 sweeps per reading (the maximum number of sweeps which can be selected in the scanning parameters for the Elan 6100) with three replicates per sample analysis.

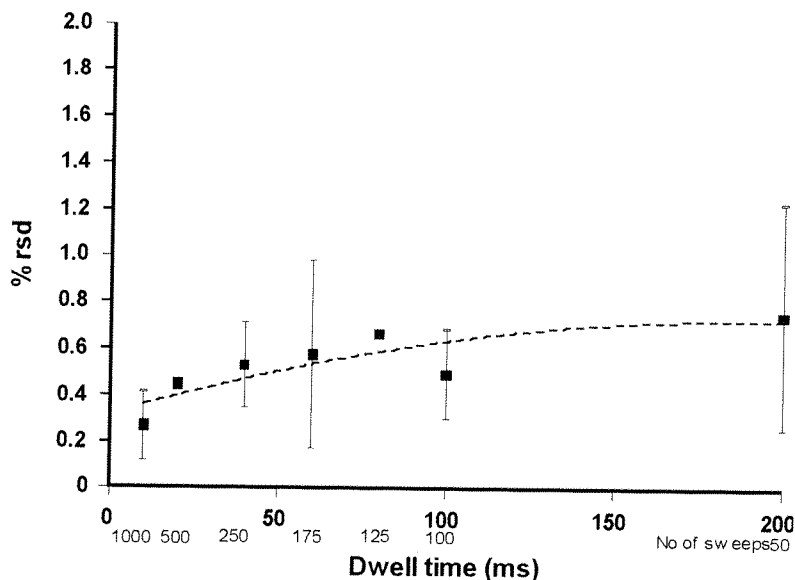


Figure 5.6. Percent relative standard deviation of $^{78}\text{Se} / ^{74}\text{Se}$ ratio measurement as a function of the dwell time, $n=2$: with the error bars representing the SDs. (Dashed line shows general trend.)

A further reduction of 0.1% RSD was achieved by doubling the sample and spike volumes, and increasing the butanol concentration to 1%. This combination effected a 9% rise in signal sensitivity and a drop of 20% in count rate for ^{78}Se blank signals. The blank count rate was still significantly higher than that obtained by the Elan 5000, at typically 4000 cps (equivalent to $20 \mu\text{g l}^{-1}$ selenium).

Nebuliser gas flow and lens voltage were optimised daily for maximum sensitivity for a spiked $100 \mu\text{g l}^{-1}$ selenium solution containing serum with butanol at 1%. This was carried out at mass 74, to avoid any changes in optimal values due to the influence of the argon interference on signal response at mass 78.

5.11. Artificial matrix for calibrating reference solutions

Under the conditions stated, ^{78}Se : ^{74}Se isotopic ratios determined in diluted sera and aqueous solutions were found to be comparable. However, matrix-related changes of signal intensities with sera, warrants the use of matrix-matched calibrating solutions to accurately correct for variation in instrumental detection of the two isotopes. One approach would be to analyse standard additions to a bovine serum of low endogenous selenium, with the count rate of the unspiked serum subtracted from each signal response of the ^{74}Se -spiked calibrating solution. Alternatively, an artificial matrix inducing equivalent changes in signal sensitivity, could replace the serum in the calibrating reference solutions.

Of the major constituents of serum, listed in Table 5.5., protein and sodium chloride are the most likely components to have a significant effect on the measured isotopic ratio.

Table 5.5. Major constituents of serum.

	Concentration (g l^{-1})
Sodium	3.2
Potassium	0.2
Magnesium	0.02
Calcium	0.1
Chloride	3.6
Phosphate	0.1
Carbonate	1.8
Total protein	70
Albumin	40
Amino-acids	0.5
Triglycerides	1.0

Albumin, present in serum at a concentration of 40 g l^{-1} , makes up almost half of the total protein content, and its effect on signal sensitivity at this level in aqueous calibration solutions was investigated.

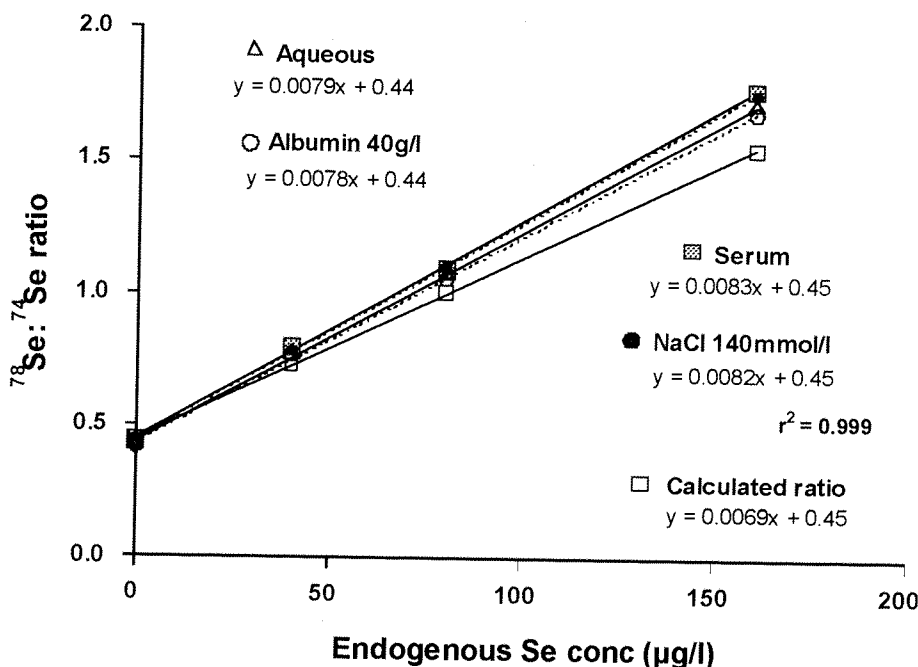


Figure 5.7. Effect of albumin and NaCl on the observed ^{78}Se : ^{74}Se isotopic ratio, for reference solutions at 0, 40, 80, 160 $\mu\text{g l}^{-1}$ selenium.

The small differences between regression line gradients for sodium chloride, albumin, sera and aqueous dilutions, were due to the varying degrees of matrix-related signal enhancement. Sodium chloride had the effect of increasing the count rate of both isotopes (by 10%), nearer to that measured in serum. Selenium signals in the presence of albumin were at the levels obtained for the aqueous solutions.

A comparison of the deviation of measured ratios from the calculated values (Figure 5.7.), shows only a small mass bias, which does however, vary with concentration. Differences of -2% at $50 \mu\text{g l}^{-1}$ to $+2\%$ at $150 \mu\text{g l}^{-1}$ are displayed, which prevent adequate compensation across a range of concentrations by a single concentration reference solution. Employing calibrating solutions at $40, 80, 160 \mu\text{g l}^{-1}$, lead to a negative bias which varied from 4% RSD at $100 \mu\text{g l}^{-1}$ to as high as 40% at $20 \mu\text{g l}^{-1}$ selenium. To obtain the correct regression line slope, it was necessary to include a calibrating solution containing no added natural selenium.

The regression line equation calculated from the three aqueous calibrating solutions at $0, 80, 160 \mu\text{g l}^{-1}$ containing NaCl at 140 mmol l^{-1} , was found to change slowly as an assay-run progressed. Typically, $y = (0.0076 \pm 0.0001) + (0.43 \pm 0.004)$, $n=9$, a variation

of less than 2% for a run of 8 hours. The calibrating solutions were analysed at the beginning of the assay, and at a frequency of one set per ten samples throughout the analytical run. Count rates were blank subtracted by the average of the enclosing NaCl reagent blanks. The regression line equations obtained from meaned ratios of the two sets of calibrating solutions, were used to convert the measured ^{78}Se : ^{74}Se isotopic ratios of the enclosed test samples to concentrations. Analysis of ten serum samples at the beginning of the day's run was found to be necessary, before accurate determinations were possible.

Intra-laboratory assays showed that using sodium chloride in the calibrating solutions gave a level of accuracy for IQC and EQA samples, similar to that obtained by serum correction (Figure 5.8.). Application of the 3 level correction as described in Section 5.8., using serum reference solutions, produced a more variable bias from target values.

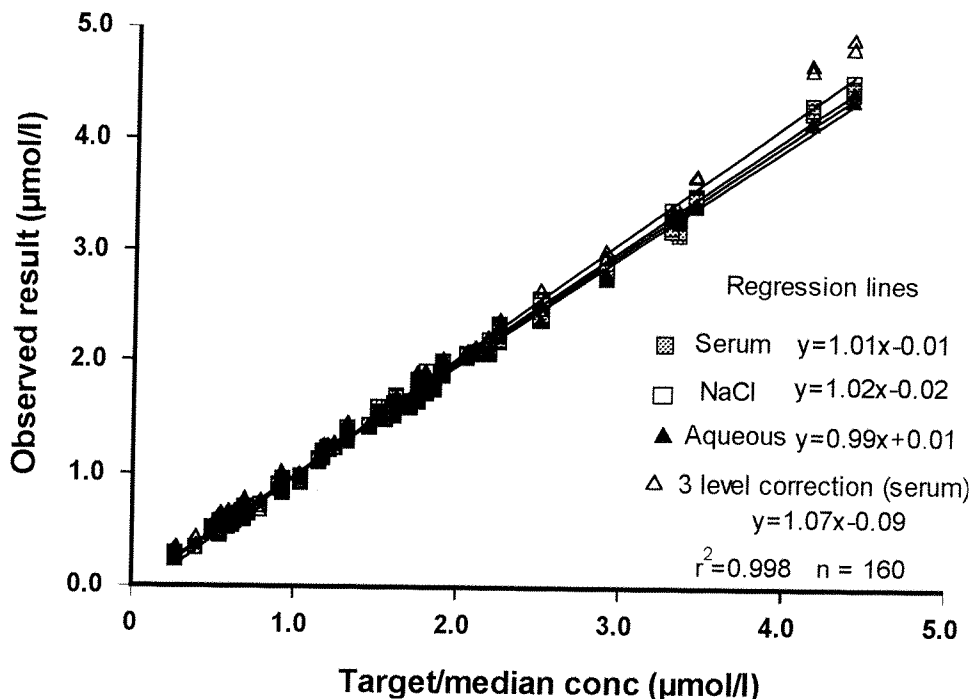


Figure 5.8. Serum selenium concentrations determined using serum (graphical method and by 3 level correction), NaCl and aqueous reference solutions at 0, 80, 160 $\mu\text{g l}^{-1}$, plotted against target values.

5.12. Accuracy and precision of IDMS using NaCl calibrating solutions

Reanalysis of forty EQA samples (provided by Quebec National Institute of Public Health Laboratories and UK-TEQAS), gave excellent agreement between the target values and the measured concentrations, as shown by the plot of the bias against sample concentration (Figure 5.9.). The EQA organisers regard an acceptable analytical performance as 60% of the results within the inner limits and 80% within outer limits, 98% of results derived by IDMS were within the inner limits. The individual results obtained are listed in Table 3 of Appendix I.

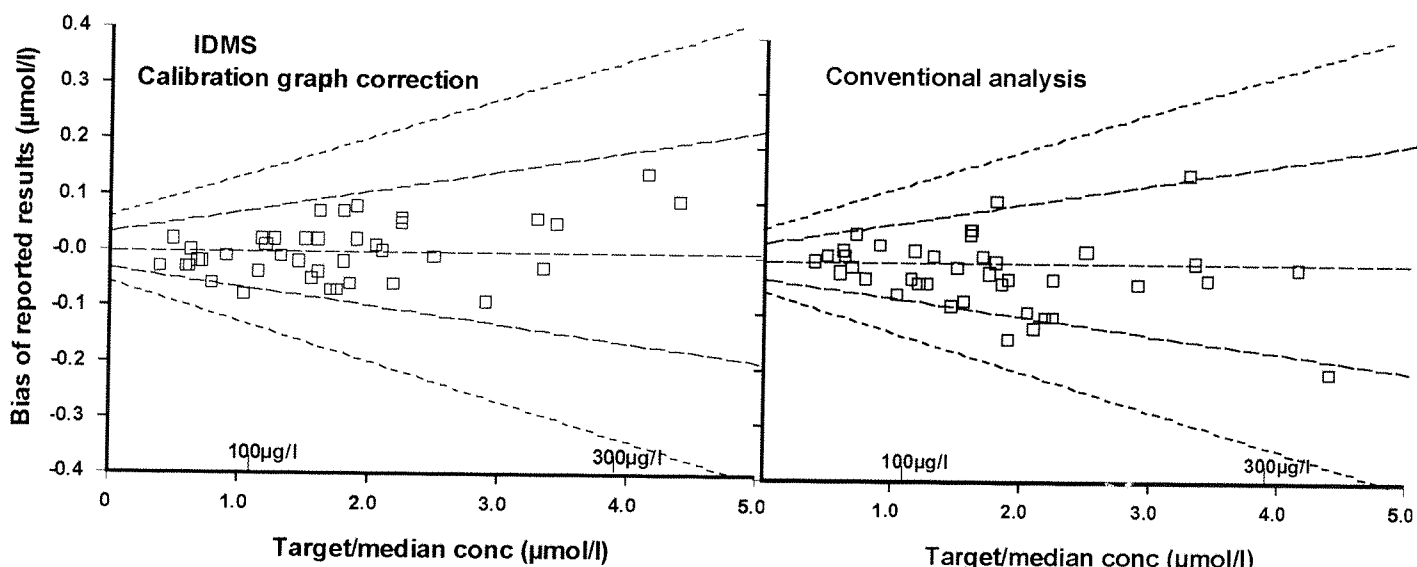


Figure 5.9. Comparison of the bias from target values, of serum samples determined by IDMS (NaCl calibration) with conventional quantitative analysis.

There was a reduction in the variation of the differences of concentrations from target values for IDMS analysis, which achieved a mean bias of $0.0 \pm 4.0 \mu\text{g l}^{-1}$ ($0.0 \pm 0.05 \mu\text{mol l}^{-1}$), compared with $-0.8 \pm 5.5 \mu\text{g l}^{-1}$ ($-0.01 \pm 0.07 \mu\text{mol l}^{-1}$) for conventional analysis. A higher level of accuracy was achieved by this technique, as demonstrated by the narrower 95% confidence intervals of this data. These were: (-1.3 to 1.3) for IDMS, and (-2.6 to 0.96) for the conventional analysis, given in $\mu\text{g l}^{-1}$. Since the confidence intervals included zero, there is no evidence of any bias.

Analysis of certified quality control sera Seronorm (704121) and NIST 1598, and our own IQC material, showed a mean bias between observed and target values of $-0.2 \mu\text{g l}^{-1}$ ($0.002 \mu\text{mol l}^{-1}$), -0.4% for IDMS. The between-run precision ranged from $\pm 6\%$ at $20 \mu\text{g l}^{-1}$ ($0.25 \mu\text{mol l}^{-1}$), to $\pm 2\%$ at $150 \mu\text{g l}^{-1}$ ($1.90 \mu\text{mol l}^{-1}$) and the within-run precision was consistent at $\pm 2\%$ across the concentration range (Table 5.6). This demonstrates the improvement in between-run precision with this technique on conventional analysis (Figure 5.10.), for which the data approached values obtained for within-run determination by standard addition analysis.

Table 5.6. Internal quality control data for serum analysis by IDMS (NaCl calibration).

IQC sample	Target Value ($\mu\text{g l}^{-1}$)	Within Run		Between Run		N
		Observed Value Mean \pm sd	Bias $\mu\text{g l}^{-1}$ (%)	Observed Value Mean \pm sd	Bias $\mu\text{g l}^{-1}$ (%)	
Level 1B	21.5	22.0 ± 0.4	0.5 (2.3)	21.1 ± 1.2	-0.4 (-1.9)	10
Level 2B	54.6	51.7 ± 0.9	-2.9 (-5.3)	53.4 ± 1.2	-1.2 (-2.2)	10
Level 3B	104.0	103.5 ± 2.0	-0.5 (-0.5)	105.3 ± 2.2	1.3 (1.3)	10
Level 4B	138.2	142.0 ± 2.7	3.8 (2.7)	137.5 ± 2.4	-0.7 (-0.5)	10
Seronorm	73 / 86	72.6 ± 1.3	-0.4 (-0.5)	72.0 ± 1.9	-1.0 (-1.4)	10
NIST1598	42.4			43.3 ± 1.9	0.9 (2.1)	10

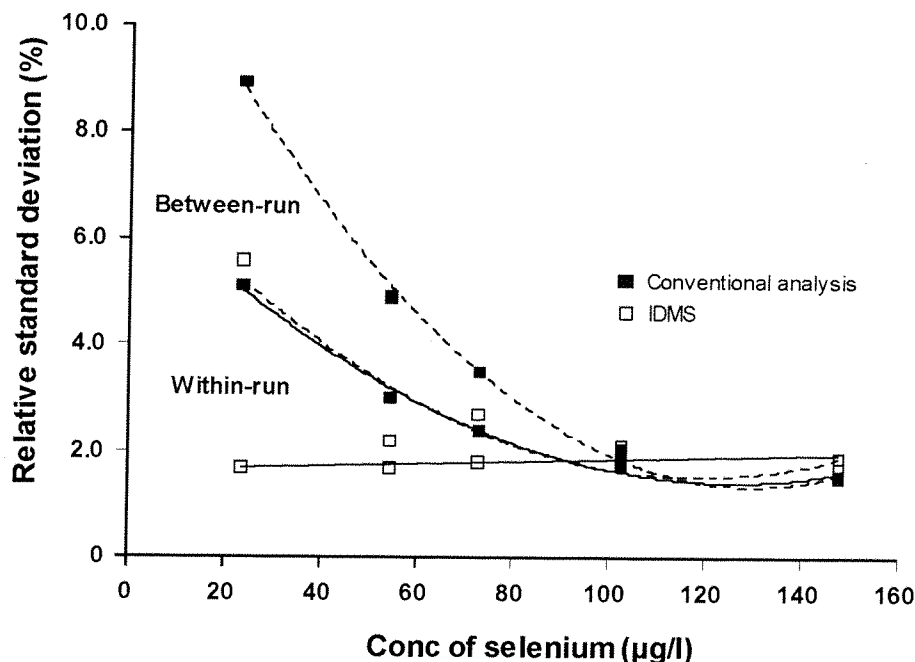


Figure 5.10. Comparison of within (solid trend lines) and between run (dashed trend lines) precision data for IDMS with conventional ICP-MS analysis of IQC material.

5.13. Conclusion

The high precision and accuracy which can be attained with IDMS, gives the technique its reputation as a definitive reference method, and as such, is associated with complex data processing and lengthy analysis times. In the method described, a protocol has been developed to enable the use of this technique for clinical analysis, consisting of a simple sample preparation and a relatively short analysis time. A sample volume of 200 μ l per replicate enables accurate analysis over a wide range of selenium concentrations within a single assay run.

Both ^{74}Se and ^{77}Se -enriched standards were assessed, and only ^{74}Se was found to be a suitable choice of isotope for this technique. As the signal at mass 77 was affected by matrix-related spectral interferences, determination of $^{78}\text{Se}:\text{Se}^{77}$ ratios could not consistently achieve the high accuracy which was found to be possible with $^{78}\text{Se}:\text{Se}^{74}$ measurement.

The procedure consisted of isotopic abundance ratio analysis of the changed $^{78}\text{Se}:\text{Se}^{74}$ ratio on the addition of a fixed amount of isotopically enriched standard to the samples and three calibrating solutions containing increasing amounts of the analyte. The isotopic composition of the ^{74}Se -enriched standard, was such, that the amount of spike calculated to achieve an equimolar mixture of ^{78}Se to ^{74}Se at 80 $\mu\text{g l}^{-1}$ analyte concentration (ie 100 $\mu\text{g l}^{-1}$), produced a calibration curve that fitted a linear regression ($r^2 > 0.998$). The regression equation obtained on plotting the calibration solution ratios with analyte concentration, can be used to convert the measured isotope ratio of spiked samples into concentrations. Referencing the measured ratios to calibrating solutions has the added advantage of compensating for any errors in spike standard concentrations or relative isotope composition that may occur, as well as for analytical differences due to instrumental detection of the isotopes.

Matching the salt content of aqueous reference solutions to that of serum using sodium chloride, was found to produce calibrating solutions which displayed equivalent signal intensities for both ^{78}Se and ^{74}Se isotopes, as that found in serum. Optimisation of scanning parameters, enabled $^{78}\text{Se}:\text{Se}^{74}$ determination to produce data of a precision of less than 0.2% relative standard deviation and of a high accuracy, shown by the analysis of certified material and intra-laboratory comparison.

The data processing, which is required by IDMS, had been simplified by the employment of calibrating reference solutions, to provide an equation from which the concentration can be predicted. As a result, the presented procedure is as straightforward as conventional quantitative analysis, but offering a better reproducibility and accuracy for selenium determination by low resolution ICP-MS.

CHAPTER 6

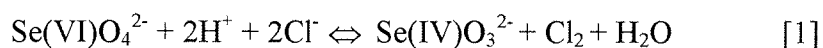
SELENIUM DETERMINATION BY FLOW-INJECTION HG-ICP-MS

6.1. Introduction

Coupling the ICP-MS to a hydride generation (HG) system has been successfully used to determine selenium levels in serum^{57,58,127}. The isotope monitored has generally been ⁸²Se, as it does not suffer from argon-adduct interferences, and by the formation of the hydride, allows its separation from other matrix components. This technique has been shown to be particularly sensitive, resulting from the formation of the hydride gas, which effectively concentrates the sample.

The hydride-generation method is based on the reduction of the element from one higher oxidation state to the gaseous hydride, by a strong reductant. As selenium can exist in several oxidation states: Se(II), Se(IV) and Se(VI), each with a different rate of reduction, sample preparation involves all the analyte being brought into the tetravalent state, before the reduction by sodium borohydride.

The initial decomposition of the sample by acid-digestion is carried out to enable the selenium to be disassociated from the organic material, effectively oxidising the selenium to the tetravalent and hexavalent forms¹²⁸. Conversion to Se(IV) is achieved using hydrochloric acid¹²⁹, the chloride ions being the reducing species, according to the following equilibrium [1].



The high concentration of H^+ and Cl^- ions present, forces the reaction to the right and back-oxidation is prevented by the use of an open-topped vessel that allows the generated chlorine gas to escape.

6.2. Instrumentation

A Perkin-Elmer SCIEX Elan 5000 ICP-MS (Perkin-Elmer, Beaconsfield) was used, coupled with a FIAS-200. The operating conditions are given in Table 6.1.

Table 6.1. Operating conditions for the ICP-MS and the parameter file for the analysis of serum digests.

rf power	1.25 kW
Plasma gas flow rate	15.00 l min ⁻¹
Nebuliser gas flow rate	0.95 l min ⁻¹
Intermediate gas flow rate	0.80 l min ⁻¹
Sampling/skimmer cone	Platinum, 0.8 mm orifice diameter
Torch	Standard demountable quartz torch with 2.0 mm id alumina injector tube
Between sample wash-out time	10 sec
Sweeps per reading	1
Dwell time	200
Readings per replicate	54
Number of replicates	2
Points across peak	1
Scanning mode	Peak Hop Transient
Baseline time (ms)	500

A schematic diagram for the FIAS-200 Flow Injection HG System (Perkin-Elmer, Beaconsfield, UK.) is given in Figure 6.1. The FIAS programme for the ICP-MS is listed in Table 6.2.

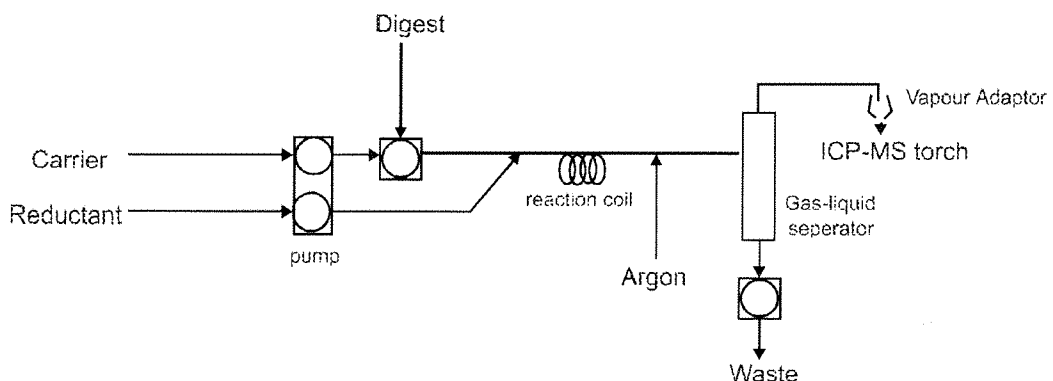


Figure 6.1. Schematic diagram of FIAS-200.

Silicone pump tubes with the following colour codes and inner diameter were used: red-red (1.14 mm) for the reductant, yellow-blue (1.52 mm) for the carrier and sample

loading, and violet-violet (2.06mm) for the waste. All other tubing was 1 mm polytetrafluoroethylene (PTFE) tubing.

Table 6.2. FIAS programme.

Program step	Start Read	Time (sec)	Speed(rpm) Pump 1	Speed(rpm) Pump 2	Valve Position
Pre-sample		10	100	0	1
1		5	100	0	1
2		3	0	0	1
3		1	0	70	2
4	X	11	0	70	2
5		1	0	0	1
6		0	0	0	1
7		0	0	0	1
8		0	0	0	1
Post-run		10	100	0	1

The nebuliser and FIAS carrier gas were introduced into the torch of the ICP-MS via a “vapour adapter” piece. The hydride, generated by mixing the acidic analyte solution and the alkaline solution of the sodium tetrahydroborate, was stripped from the aqueous solution of the reaction products by the argon gas and swept into the ICP-MS for quantification. The FIAS argon carrier gas flow was set at 200 ml min^{-1} .

6.3. Reagents and equipment

Matrix-matched calibration standards were prepared using bovine serum (Lot no: 78H3355), with a stock selenium solution (1020 mg l^{-1}), both from Sigma-Aldrich, Poole, Dorset. Distilled, then de-ionised water (Milli-Q system, Millipore, Watford, Hertfordshire) was used throughout.

The samples were decomposed using nitric acid “Aristar” 16 mol l^{-1} , (Merck, Poole, Dorset), sulphuric (18 mol l^{-1}) and hydrochloric acids (11 mol l^{-1}), both “Primar” quality (Fisons, Loughborough, Leicestershire). Digestions were carried out in borosilicate test tubes (16 x 110 mm) on a Grant QBT block heater (Grant Instruments, Cambridge), and transferred to plastic tubes, 10 ml (Teklab, Sacriston, Durham) for analysis.

The selenium reductant was made up by dissolving 1 pellet (0.9-1.2 g) of sodium borohydride (“Spectrosol”, Merck, Poole, Dorset), to give 0.2% m/v in a solution made alkaline by the addition of sodium hydroxide at 0.05% m/v (Fisons, Loughborough, Leicestershire). This was made up on the day of analysis.

Stable isotopes: Enriched $^{74}\text{Se}/4$ and $^{77}\text{Se}/3$ isotope standards (AEA Technology, Nuclear Science, Didcot) were employed in the ID procedure, prepared as described in Section 5.3.

6.4. Procedure for sample digestion

The mineralisation method employed was based on the protocol published by Lloyd et al.¹³⁰. This was the established method of digestion used at our laboratory, to prepare samples for routine serum selenium analysis by HG-AAS.

A series of aqueous selenium standards containing 0, 10, 20, 50, 100, and 200 $\mu\text{g l}^{-1}$ of selenium were made up in 0.1% v/v nitric acid. Matrix matched standards were prepared by pipetting an equal volume (100 μl) of the appropriate aqueous standard with bovine serum, and 100 μl serum test samples were aliquoted into the borosilicate tubes, in duplicate, with water replacing the serum in the reagent blanks. Aliquots of 250 μl of nitric acid and 200 μl 25% v/v sulphuric acid were added to each tube, before being placed in the heating-block set at 130°C for 1 hour. On the addition of 300 μl hydrochloric acid (30% v/v), the solutions were heated for a further 15 minutes. When cool, the digests were quantitatively transferred into preweighed 10ml plastic tubes and the volume of which was made up by weight, to 6.0 ml with deionised water.

6.5. Method for selenium analysis

A method used by LGC for the determination of selenium in aqueous samples¹³¹, provided the basis for the instrumental conditions and the FIAS programme described in Section 6.2. The power, sampling parameters, nebuliser and FIAS carrier gas flow, were optimised in turn, to maximise the analytical sensitivity and produce good peak profiles for the serum digests, an example of which can be seen in Figure 6.2. The signals for ^{77}Se , ^{78}Se and ^{82}Se were monitored.

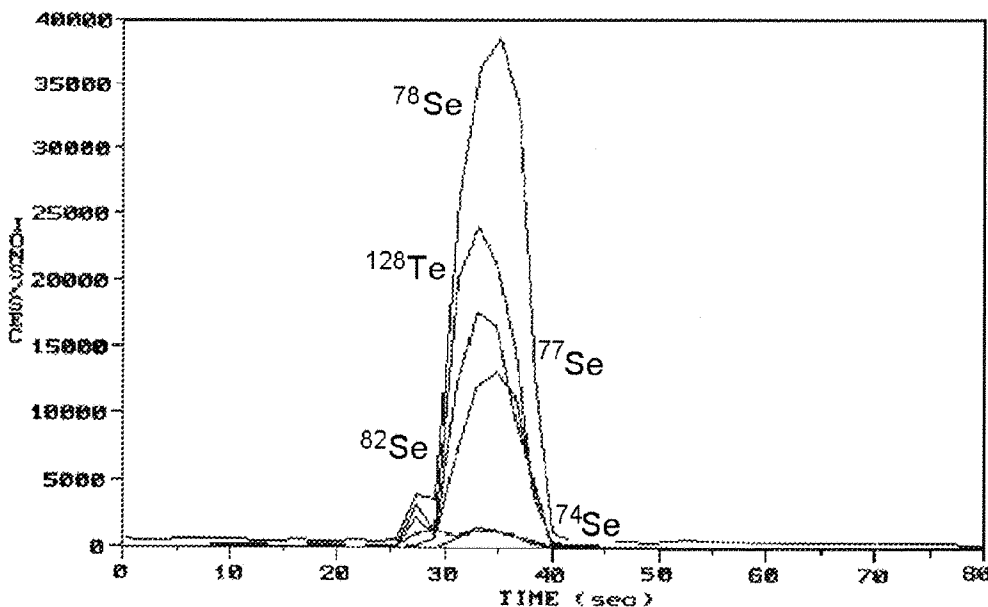


Figure 6.2. The signal response of the ICP-MS, showing the peak profile obtained under optimised conditions for serum digest containing $150 \mu\text{g l}^{-1}$ selenium ($+100 \mu\text{l}$ tellurium at $100 \mu\text{g l}^{-1}$).

The introduction of an organic solvent to the sample, which enhanced sensitivity in pneumatic nebulisation, was found to have a less significant effect on the isotope signals for hydride generation. The addition of butan-1-ol to the serum digests to give a working concentration of 0.5%, only increased the isotope signals by an average of 9%, compared with 50% for pneumatic nebulisation, and with no noticeable improvement in the precision of analysis evident - this was not further investigated.

6.6. Use of internal standard

Determination of selenium by HG-ICP-MS has been successfully achieved without normalising to any internal standard, the bulk of this work being carried out in the aqueous matrix^{127,132,133}. The use of an internal standard to compensate for potential changes in instrumental sensitivity of the ICP-MS has been investigated by Ek et al.⁵⁷, and Rayman et al.⁵⁸. Because of the poor hydride forming properties of indium, its introduction into the plasma as an aqueous solution was by continuous pneumatic nebulisation. The presence of water in the plasma potentially increases the formation of interfering polyatomic ions, and decreases the available energy for analyte ionisation. Since this procedure effectively removes the benefits derived from using a dry plasma to transport the analyte, it is highly

likely to be responsible for the short-term instability observed by Rayman, despite adequate compensation for overall drift in instrumental stability by changes in indium signal.

Three approaches were evaluated: the introduction of tellurium (a hydride forming element) that was added to the serum prior to digestion, tellurium added to the serum digest itself, and utilising the continuous background ^{131}Xe signal¹³⁴ to correct for changes in signal drift. Adding tellurium directly to the serum digest was found not to be possible, as in this form, the element was not being converted to the hydride. Introduction of the tellurium pre-digestion, produced tellurium hydride, which could be detected. Normalising the selenium isotope count sec^{-1} to the ^{128}Te signal, and to that produced by ^{131}Xe , was found to introduce imprecision, as can be seen in both Table 6.3. and Figure 6.3. No internal standard was therefore applied to subsequent measurements.

Table 6.3. Comparison of the RSDs obtained for five measurements of serum digest containing selenium at $80 \mu\text{g l}^{-1}$, for ^{77}Se , ^{78}Se , ^{82}Se signals, on normalisation to ^{128}Te and ^{131}Xe .

Normalisation	% Relative Standard Deviation	77Se	78Se	82Se
Without internal std		1.1	1.7	1.9
^{128}Te		6.3	6.4	8.1
^{131}Xe		3.5	2.5	5.0

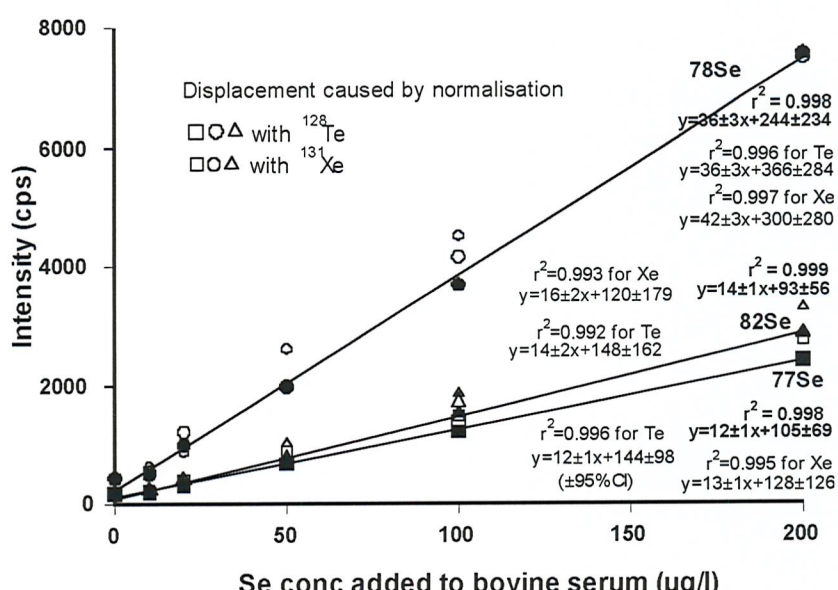


Figure 6.3. Comparison of standard additions for ^{77}Se , ^{78}Se , ^{82}Se signals, without any normalisation, and on normalisation to ^{128}Te and ^{131}Xe .

6.7. Internal quality control

Analysis of certified quality control sera Seronorm (704121), NIST 1598, and IQC material (Series B), show a mean bias between observed and target values of $-0.1 \mu\text{g l}^{-1}$ (-0.1%) for the ^{77}Se determination, $-0.6 \mu\text{g l}^{-1}$ (-0.8%) for both ^{78}Se and ^{82}Se isotopes. The between-run precision ranged from $\pm 14\%$ at $20 \mu\text{g l}^{-1}$, to $\pm 3\%$ at $150 \mu\text{g l}^{-1}$ and the within-run precision ranged from $\pm 9\%$ at $20 \mu\text{g l}^{-1}$ to $\pm 3\%$ at $150 \mu\text{g l}^{-1}$ (Table 6.4.).

Table 6.4. Internal quality control data for serum analysis by measurement of ^{77}Se , ^{78}Se , ^{82}Se , for ten determinations.

IQC	Target	Observed Value $(\mu\text{g l}^{-1} \pm \text{sd})$			Between run		
		With-in Run			^{77}Se	^{78}Se	^{82}Se
		^{77}Se	^{78}Se	^{82}Se			
Level 1B	21.5	21.1 ± 1.9	21.2 ± 1.0	20.6 ± 2.0	22.8 ± 3.3	22.4 ± 3.3	22.2 ± 2.9
Level 2B	54.6	50.4 ± 2.4	49.4 ± 2.1	50.3 ± 3.4	51.7 ± 4.8	51.9 ± 2.8	52.0 ± 2.5
Level 3B	104.0	102.5 ± 4.3	102.1 ± 4.7	103.3 ± 4.5	99.9 ± 2.4	100.0 ± 3.5	98.8 ± 3.5
Level 4B	138.2	137.3 ± 5.6	135.0 ± 3.8	138.0 ± 3.9	143.4 ± 4.4	142.6 ± 5.0	141.4 ± 3.9
Seronorm	73 / 86	73.8 ± 3.5	72.7 ± 3.1	73.9 ± 3.2	74.0 ± 3.2	73.3 ± 3.7	74.2 ± 4.9
Nist 1598	42.4				41.3 ± 4.4	40.7 ± 3.9	41.5 ± 4.1

The data obtained by HG (averaging the observed values for the 3 isotopes) could not match the precision obtained by conventional nebulisation analysis by ICP-MS (Figure 6.4.).

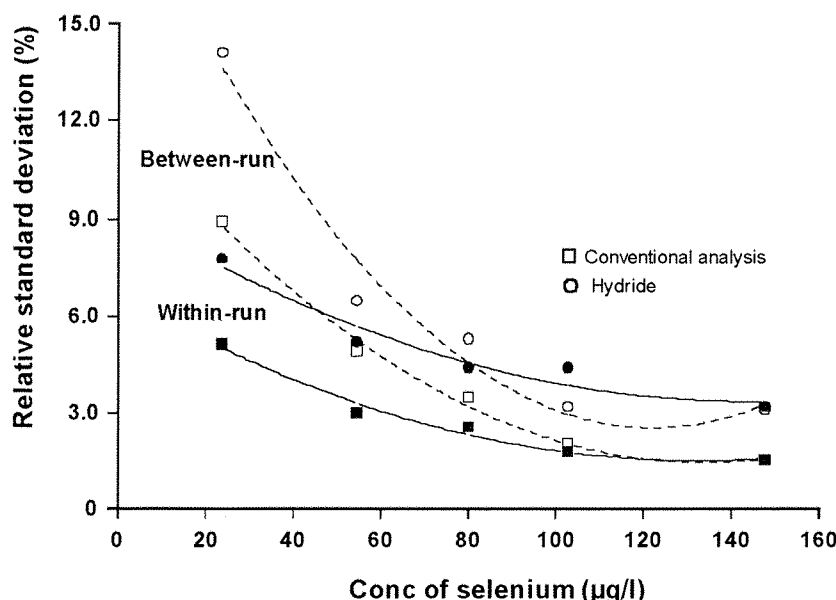


Figure 6.4. Comparison of within (continuous line) and between run precision data (dashed line) for HG-ICP-MS with conventional pneumatic ICP-MS analysis of IQC material.

6.8. Intra-laboratory comparison

The greater imprecision shown by the IQC data, is reflected in the poor accuracy achieved on the analysis of the twenty-five samples provided Quebec National Institute of Public Health Laboratories and fifteen by UK-TEQAS (Figure 6.5), when compared with IDMS, the plot of which can be found in Section 5.12. The individual results obtained and their percentage bias from the target values is listed in Table 4 in Appendix I. 65% of the values are within the inner zone, which denotes a good performance, and 84% are within the outer ‘acceptable’ zone, for both ^{77}Se and ^{78}Se isotopes. The accuracy of ^{82}Se measurement appeared to be slightly worse, with only 55% of the values within the inner zone, while maintaining the same percentage of values in the outer zone.

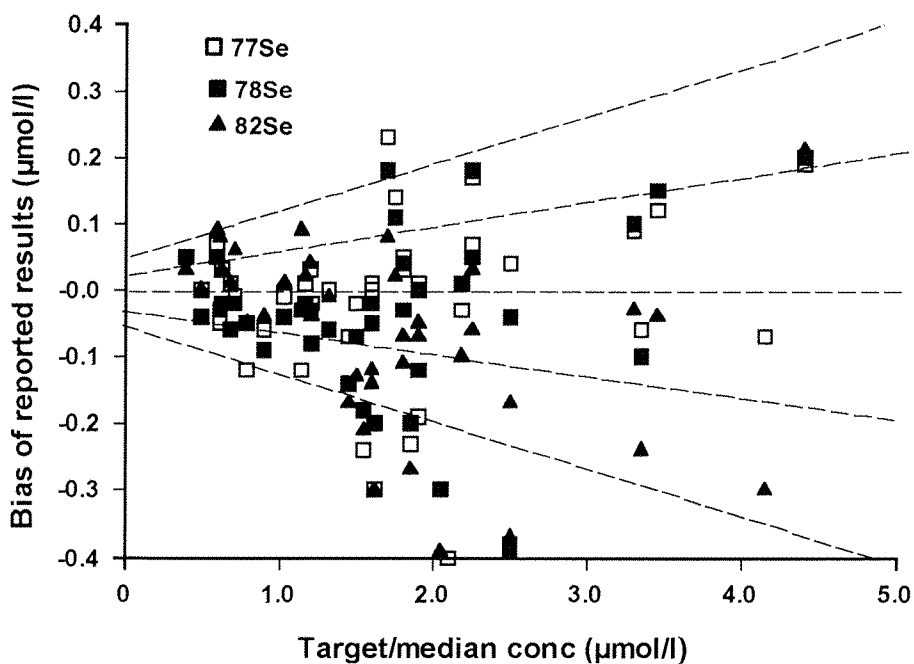


Figure 6.5. Comparison of the bias from target values, of serum samples analysed by HG-ICP-MS using ^{77}Se , ^{78}Se , ^{82}Se isotopes. Zone parameters are defined by the EQA schemes.

6.9. IDMS by hydride generation

Significant memory effects were evident on use of the ^{74}Se -enriched standard for isotopic analysis by hydride generation. Janghorbani et al.¹³⁵ had also observed memory effects for both ^{82}Se and ^{74}Se isotopes, for which signals decreased to 1% of the analytical level only after a 10 minute monitoring of intensities on analysis of a $1\mu\text{g l}^{-1}$ selenium solution. The significance of these effects were investigated by spiking each serum aliquot with an equal volume of ^{74}Se standard prior to digestion and employing instrumental parameters which desensitised the isotopic signals (ie. power at 1000 W, nebuliser gas flow at 0.85 ml min^{-1} and carrier gas flow at 100 ml min^{-1}). Following a test sample, blank signals did not return to base line values, even after the third analysis, as can be seen in Figure 6.6. Because of the impact of this memory effect on the reproducibility and accuracy of analysis, further work involving the ^{74}Se -enriched isotope was abandoned.

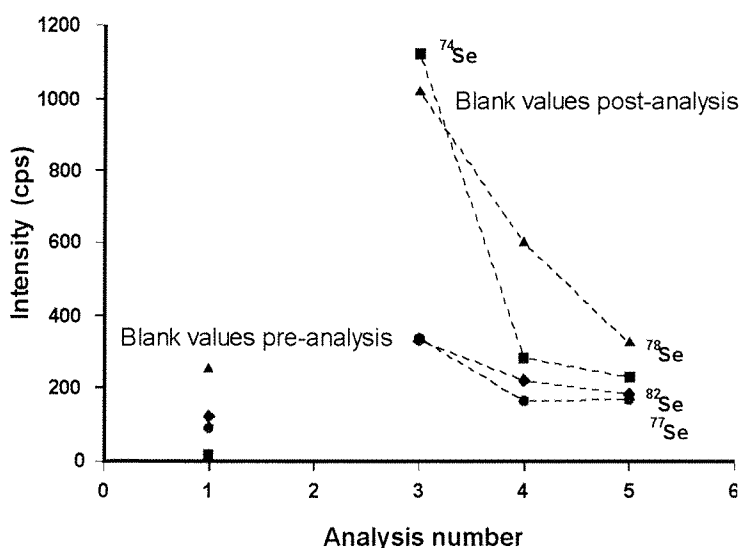


Figure 6.6. Blank signals observed for ^{74}Se , ^{77}Se , ^{78}Se and ^{82}Se , pre and post analysis of spiked sample at $140\text{ }\mu\text{g l}^{-1}$ natural selenium, giving 58000, 13500, 34800, 12250 cps, respectively.

On spiking with ^{77}Se -enriched standard, analysis was not subject to any noticeable memory effects, owing to the measurement of lower isotopic concentrations of selenium. However, use of the ^{77}Se spike did introduce instability to the analysis, as can be seen in Table 6.5. A similar imprecision was obtained regardless of whether the correction factors for ^{78}Kr and ^{82}Kr were included or removed from the scanning parameters.

Table 6.5. Comparison of the RSDs obtained for five measurements of serum digest containing selenium at $80 \mu\text{g l}^{-1}$, for ^{77}Se , ^{78}Se , ^{82}Se signals, spiked with ^{77}Se -enriched standard at $20 \mu\text{g l}^{-1}$.

	% Relative standard	Deviation	
	^{77}Se	^{78}Se	^{82}Se
Without spike	1.1	1.7	1.9
Spike with Kr correction	3.4	4.3	3.4
Spike without Kr correction	3.2	2.5	2.5

The $^{78}\text{Se} : {}^{77}\text{Se}$ ratio measured for five replicates of a serum digest containing $80 \mu\text{g l}^{-1}$ natural selenium with $20 \mu\text{g l}^{-1}$ ^{77}Se spike, gave a value of 3.229 ± 0.047 (1.5% RSD) employing the Kr correction, and 3.197 ± 0.053 (1.7% RSD) with the correction equation removed, equivalent to a factor of 3 difference from the expected ratio of 1.14. A large positive bias was observed when the measured isotopic ratios of serum IQC material were converted to concentration values, varying from up to 50% at $50 \mu\text{g l}^{-1}$ to 10% at $150 \mu\text{g l}^{-1}$.

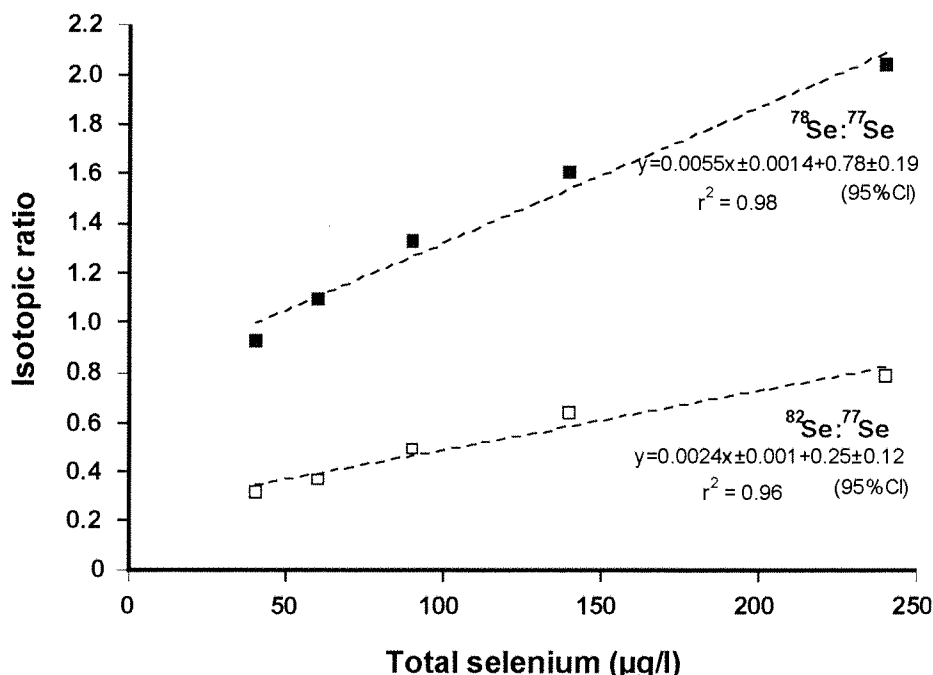


Figure 6.7. Measured $^{78}\text{Se} : {}^{77}\text{Se}$ and $^{82}\text{Se} : {}^{77}\text{Se}$ isotopic ratios as a function of increasing levels of selenium in the test sera, on addition of ^{77}Se -enriched standard at $20 \mu\text{g l}^{-1}$.

The isotopic ratios determined on addition of the ^{77}Se spike to sera with increasing concentrations of selenium, could only produce linear regressions with correlation coefficient squared of less than 0.98 (Figure 6.7.) and sodium chloride mass bias solutions showed similar unacceptable precision. The large 95% confidence limits for the regression lines, confirm the unsuitability of this approach being the basis for a routine clinical method.

6.10. Conclusion

In comparison with pneumatic nebulisation, the use of HG provided a substantial enhancement in signal intensity. The background count rates for the three isotopes, and the detection limit at $2 \mu\text{g l}^{-1}$ ($0.03 \mu\text{mol l}^{-1}$) were equivalent to that found by nebulisation. The reproducibility and accuracy of the data produced by all three isotopes were very similar, although the ^{78}Se determinations would be preferred due to the greater isotope abundance. Working without an internal standard to compensate for instrumental fluctuations, has meant that precision and accuracy of HG cannot match that obtained by pneumatic nebulisation, despite close monitoring of internal quality control data to identify signal changes due to instrumental drift.

The application of ID to HG methodology, proved to be problematic. Memory effects evident on use of the ^{74}Se enriched standard, and converted concentrations that deviated greatly from the target values when spiking with ^{77}Se enriched standard, prevented further work being carried out.

CHAPTER 7

SELENIUM DETERMINATION BY

COLLISION AND REACTION CELL ICP-MS INSTRUMENTATION

Recent developments in ICP-MS technology have introduced ‘collision’ or ‘reaction’ cells for ion focusing and filtering of selected ions out of the plasma prior to the measurement of the analyte. The greater detection power and the potential of interference free measurement of the selenium isotopes are expected to give further improvements in precision for both conventional and isotope dilution analysis.

7.1. MULTICOLLECTOR MAGNETIC SECTOR MASS SPECTROMETER

Multicollector magnetic field instrumentation is ideally suited to the measurement of isotopic composition of samples at high precision, with relative standard deviations of <0.05% being reported for isotope abundance ratios^{61,136,137}. It offers simultaneous detection of analytes within the sample and the capability of extremely high ionisation efficiency for almost all elements. This, together with the ability to destabilise interfering polyatomic ions, makes ICP-MC-MS a particularly attractive technique for selenium determination.

7.1.1. Instrumentation

The Micromass Isoprobe (Micromass, Manchester) was used in this study, located at the Southampton Oceanography Centre. A schematic diagram of the instrument is shown in Figure 7.1.

The Inductively coupled plasma Multicollector mass spectrometer (ICP-MC-MS), consists of a hexapole collision cell, located behind the sampler and skimmer cones, which is used to control the energy spread of the ions. The addition of a small amount of argon (1 ml min⁻¹ flow rate) into the cell at relatively high operating pressures enables focusing of ions through the loss of axial kinetic energy. Initially, at levels of 20 - 30 eV, the ions collide with the argon in the cell, reducing their energy to that of the thermal motion of gas molecules, at 1 eV. This collisional focusing effectively increases the signal intensity. The presence of electrons produced on the ion collision with argon atoms, neutralises ions of

very high ionisation potential, such as the argon ions, and dissociates polyatomic species. This process can be accelerated by the addition of hydrogen at a flow rate of 0.2 ml min^{-1} into the collision cell. Subsequently, the argon ion signal is substantially reduced and polyatomic ions, such as ArN , ArO , and ArCl are not formed to any significant level.

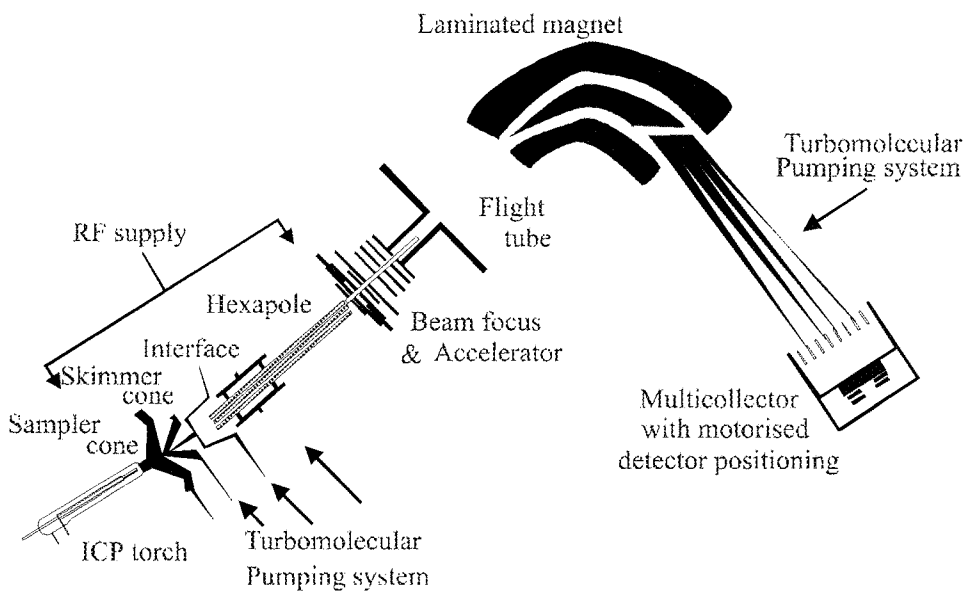


Figure 7.1. Schematic representation of the Micromass Isoprobe.

The ions are accelerated around a curved laminated magnet, towards an array of ion collectors, which allow simultaneous measurement of ions, minimising the influence of plasma noise on the analytical precision. Resolution of the ions is determined by the mass, with the heavier elements being deflected less by the magnet. On the instrument used, nine Faraday collectors (analogue mode detector) are aligned with a Daly detector situated behind the middle Faraday, which comes into use on the measurement of low levels.

Operational conditions are listed in Table 7.1.

Table 7.1. Operating conditions for the ICP-MC-MS.

Instrument	Isoprobe
rf power	1.35 kW forward,
Cool gas flow rate	14.00 l min ⁻¹
Intermediate gas flow rate	1.00 l min ⁻¹
Nebuliser gas flow rate	0.75 l min ⁻¹
Sampling /Skimmer cones	Nickel
Torch	Standard quartz
Sample uptake rate	0.5 ml min ⁻¹ (by peristaltic pump)
Nebuliser	Meinhardt
Wash solution	2.0% HNO ₃
Ion detection	9 Faraday detectors ± Channeltrons ± Daly detector

Operational parameters such as torch positions, argon gas flow rates, ion energy and extraction voltage, lens settings were tuned to maximise the transmission of analyte signals using strontium at 1 µg l⁻¹. Each sample analysis consisted of twenty measurements of 5 seconds integration time.

Reagents were as described in Section 3.3.

7.2.2. Conventional analysis

The capability of the instrument to monitor different ions simultaneously, contributes to the high precision attainable. Internal standards suitable for selenium determination, such as indium (¹¹⁵In) and tellurium (¹²⁸Te), are beyond the appropriate mass unit spread, for the measurement of the selenium isotopes. Therefore, ⁷⁷Se was also measured alongside ⁷⁸Se

- the analyte isotope, in order to correct for instrumental fluctuations. The determined ⁷⁷Se:⁷⁸Se ratio was corrected for any mass bias, using the measured value of a calibrating solution, before being converted to a concentration.

The detector linearity for signal response with concentration is such, that a one-point calibration of the top working standard could be used. This contained a 1 + 14 dilution of bovine serum with endogenous concentration of 10 µg l⁻¹, spiked with 200 µg l⁻¹ selenium (the signal obtained from 1% nitric acid established a base line). Only a small mass discrimination effect was observed for the measured ⁷⁷Se:⁷⁸Se ratio of 0.317 for the standard, compared with the true value of 0.321. This ratio was used to normalise the measured ⁷⁷Se:⁷⁸Se voltage, for the four IQCs (Table 7.2.).

Table 7.2. Observed concentrations obtained for IQCs, by ICP-MC-MS detection.

IQC sample	Target value	Accepted Range	Observed		Value		$\mu\text{g l}^{-1}$
			^{78}Se Normalised	^{78}Se not normalised	^{77}Se Normalised	^{77}Se not normalised	
Level 1B	21.5	17.5 – 25.5	43.6	18.3	18.2	7.6	
Level 2B	54.6	50.6 – 58.6	53.1	52.4	52.4	51.7	
Level 3B	104.0	99.5 – 108.3	106.0	103.7	103.7	101.4	
Level 4B	138.2	134.0-142.4	135.4	135.9	135.9	136.4	

A one-point calibration was adequate for the accurate determination of the serum concentration across the range of 20 to 200 $\mu\text{g l}^{-1}$ selenium. The measurement of ^{78}Se appears to be the more reliable determination, as errors were introduced on normalisation to the ^{77}Se : ^{78}Se value, as demonstrated by the odd results obtained for level 1 analysis (Table 7.2.). The detection system of the Isoprobe is such that with the signal response given in mV, preventing direct comparison of sensitivity with the Elan 5000, for signal and blank measurements.

The presence of butan-1-ol at 0.5% v/v, increased sensitivity by 150% for ^{78}Se analysis, 200% for ^{77}Se . Selenium values for IQC samples determined against a one-point calibration of 210 $\mu\text{g l}^{-1}$ serum working standard, were within the acceptable range. During this analysis, with a throughput of only ten samples, it became evident that the sample flow-through into the nebuliser was being hampered. A brown crystalline precipitate had formed in the torch injector tube, preventing further analysis. Pre-analysis sample treatment appears to be necessary. This could be by a column separation procedure (eg. anion exchange) to isolate the selenium from the sample matrix, by dissolution using tetramethylammonium hydroxide, or by acid-digestion of the samples.

7.2.3. Isotope dilution

The potential for high sensitivity (further enhanced by the use of an organic solvent), and good reproducibility demonstrated by the Isoprobe, suggests that the application of isotope dilution does warrant further investigation. However, the additional sample preparation found to be necessary, may compromise the precision and accuracy of selenium determination. As a result, the scope is limited for a significant improvement in the level of precision and accuracy by the employment of ICP-MC-MS, on that attained by quadrupole instrumentation.

7.2. DYNAMIC REACTION CELL ICP-MS

Located between the ion optics and the mass analyser quadrupole of a standard ICP-MS, the Dynamic Reaction Cell (DRC) is a quadrupole mass filter enclosed within a cell device. Pressurised with a reactive gas, the DRC enables improved specificity and detection power on measurements, which normally suffer from polyatomic interferences. A schematic diagram of the instrument is shown in Figure 7.2. Various papers on the theory, operation and analytical performance of the DRC-ICP-MS have been published 62,138-141.

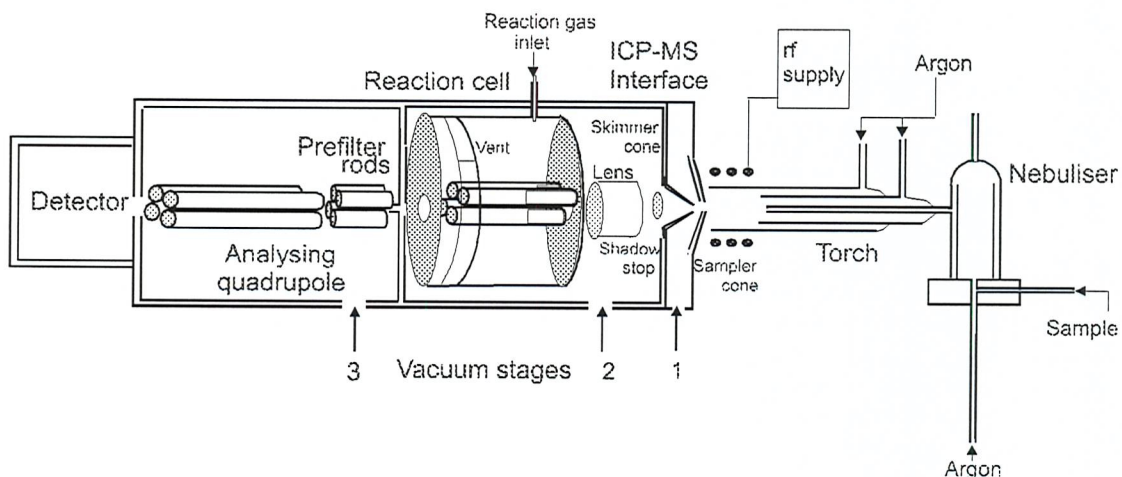
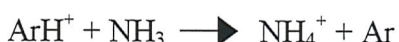


Figure 7.2. Layout of the PerkinElmer Elan 6100DRC ICP-MS.

The Dynamic Reaction Cell selectively removes isobaric species from the ICP-MS ion beam using controlled ion-molecule chemistry⁶². This ‘chemical resolution’ is achieved by the introduction of a reactive gas into an enclosed cell placed in the ion path, which reacts selectively with the polyatomic ions through charge, electron or hydrogen ion transfer, converting them into neutral species or ions of a different mass. Examples of these using ammonia as the reaction gas, are given below.



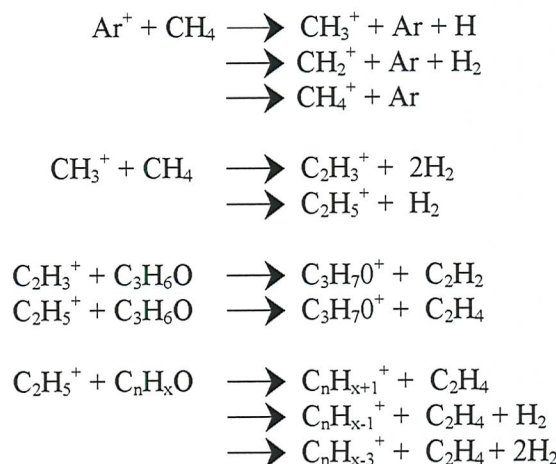
Charge transfer



Proton transfer

The specific chemistry in the cell is dependent on the nature and the density of the reactive gas and the electrical field within the cell. Gases that have been successfully used are: ammonia, methane and hydrogen in a 40:60 mixture with argon (to enable better management of such a low-density gas). The selection of the gas is based on the difference in ionisation potential of reactions with the interfering species, to produce non-isobaric species, compared to those involving the analyte. Ammonia is very effective for removing most argides, but it is methane that has been particularly efficient at removing the argon dimers isobaric associated with the selenium isotopes¹⁴⁰.

Both rf and dc voltages are applied to the quadrupole in the cell device which allows a bandpass of masses to be transmitted to the mass spectrometer quadrupole. The electrical parameters of the DRC quadrupole define the low and high mass characteristics of the cell. The selected values for the Mathieu parameters, q and α , (functions of the rf frequency and the dc voltage applied to the quadrupole rods) control the bandpass low mass and the high mass cut-offs, respectively. The default value is $\alpha=0$ and $q=0.45$, setting up a moving bandpass when scanning through the spectrum, equivalent of a low mass cut-off of 19-60 amu (atomic mass unit). This ensures that by-products of the reaction gas, such as the ionised species of the gas, are filtered away preventing their transmission to the mass spectrometer quadrupole. The sequential ion chemistry of methane is given below, showing the potential by-products that can be formed. The reactions take place virtually simultaneously and continuously while intermediate ions and neutrals are present within the cell⁶².



The neutral molecules of the reactive gas remain within the cell device, and continue to react with the interfering species by collisional dissociation and gas phase chemical reactions. The position of the bandpass window is adjusted in concert with the analysis mass, which provides for high transmission of the analyte ions while permitting reactive isobars to be converted to other masses and simultaneously suppressing the formation of new interferences. The operating settings for a and q , can be varied from analyte to analyte. They can be selected to maintain a more or less constant ion population within the cell device throughout the analysis, or to produce a bandpass with both a high and low mass cut-off, that is shifted with the analytical mass. The optimal q value for ^{78}Se monitoring is 0.70, which determines a lower mass cut-off of 60 amu, preventing a large proportion of potentially interfering matrix-related ions from being stable in the cell. The same lower mass cut-off is attained for tellurium, used as an internal standard for the measurement of selenium, when the q value is set at 0.44. Under these conditions, with an effectively constant population of stable ions in the cell, the settling time (the time required for the analyte signal to stabilise) for ^{78}Se and ^{128}Te detection, can be set to a relatively low value for DRC operation of 3 msec.

The reaction cell can be vented, to operate as a conventional ICP-MS instrument (default $q=0.25$). The change over to DRC mode is made by the introduction of the reaction gas into the cell, regulated by a gas flow controller. Two flow controllers can be connected to the cell device to enable the use of two gases in turn within a single analysis of a sample. The reaction gas is passed over a “getter” - a device that removes water from the gas, to prevent additional oxide formation.

7.2.1. Instrumentation and reagents

A Perkin-Elmer Elan 6100 DRC ICP-MS (Perkin-Elmer, SCIEX, Canada) was used, with a Gilson 221 autosampler. Instrumental conditions are summarised in Table 7.3. Reagents were as described in Section 3.3.

Table 7.3. Operating conditions for the DRC-ICP-MS.

rf power	1.20 kW
Plasma gas flow rate	15.00 l min ⁻¹
Auxiliary gas flow rate	1.0 l min ⁻¹
Sampling /skimmer cones	Platinum
Lens voltage	8-11 V (Optimised daily)

DRC parameters:	Methane gas flow rate	0.5 ml min ⁻¹
	Cell nebuliser flow rate	0.8-0.9 l min ⁻¹ (Optimised daily)
	Cell rod offset	0 V
	Quadrupole rods offset	-16 V
	Cell potential voltage	-20 V
	<i>q</i> parameter	0.7
	<i>a</i> parameter	0.0
	Sample uptake rate	Setting of -18 for the peristaltic pump
	Neubuliser	Cross-flow
	Wash solution	0.5% butan-1-ol, 0.05% Triton-X-100 6.7% blood diluent
Analyser parameters:	Scan mode	Peak hopping
	Detector mode	Pulse counting
	Settling time	3 ms
	Isotopes measured	⁷⁴ Se (⁷⁴ Ge correction removed) ⁷⁶ Se, ⁷⁷ Se ⁷⁸ Se (⁷⁸ K correction removed) ⁸⁰ Se, ⁸² Se (with ⁷⁹ Br correction)
	Measurements	500 ms dwell time, 5 sweeps/reading, 1 reading/ replicate, 3 replicates
	Calibration type	Standard additions

Internal standard solutions used for conventional analysis were rhodium and indium solution from a stock solution at 10,000 mg l⁻¹, of "Spectroscol" purity (Merck, Poole, Dorset), tellurium at 1 mg ml⁻¹ (Merck, Poole, Dorset), and germanium, gallium, niobium, and yttrium at 1 mg ml⁻¹ (Perkin-Elmer, Buckinghamshire).

7.2.2. DRC optimisation

The reaction cell was pressurised with methane (Ultra High Purity Grade, BOC gases, Guildford). The flow rate of the gas was optimised to maximise the removal of the interfering species while maintaining the sensitivity for the analyte. The appropriate cell pressure was determined by measuring the signal response for the selenium isotopes while aspirating a blank solution and a 10 µg l⁻¹ selenium solution, in turn, while the gas flow was ramped in small steps from 0 to 2 ml min⁻¹. The two plots of the change of intensity with the cell gas flow for each isotope, were overlaid by the computer software. The initial fall in counts sec⁻¹ reflects the rate of loss of the interferent until the transmitted signal is dominated by the analyte. This signal also decays at higher cell gas pressure, corresponding to either the scattering of the analyte ion or a reaction with the cell gas. Figures 7.3 and 7.4. show the resultant plots for ⁷⁸Se and ⁸⁰Se as a function of cell gas flow.

The pulse intensity at mass 80, illustrates the differences in the rate of the decay of the signal as shown by the change in slope, when dominated by the argon dimer compared to when influenced by selenium. The difference in reaction profiles between the blank and sample solutions yields the net signal for the analyte ion as a function of reaction gas flow and an estimation to the achievable detection limit is calculated by the Elan software:

$$\text{Estimated detection limit (ppt)} = \frac{3 \sqrt{\text{background signal}}}{\text{signal intensity}}$$

The cell gas flow is at the optimum at the minimum value of the estimated detection limit, being the compromise between the reactive conversion of the interferent and the reaction/scattering loss of the analyte ion. At a cell gas rate of 0.5 ml min^{-1} , the background for the selenium isotopes 78 and 80 was less than 50 cps. As the cell pressure increased, the signal intensity fell as the collision of the analyte ions with the gas molecules became increasingly frequent, and at 2 ml min^{-1} methane flow, all signals were lost.

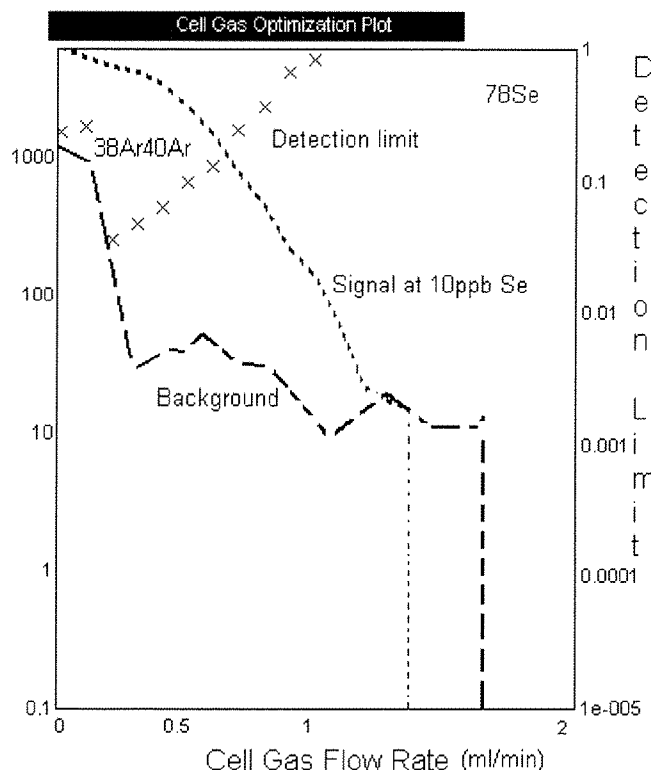


Figure 7.3. Methane gas flow optimisation plot (log scale), showing signal profiles for background and $10 \mu\text{g l}^{-1}$ Se as the gas flow is increased, for ^{78}Se .

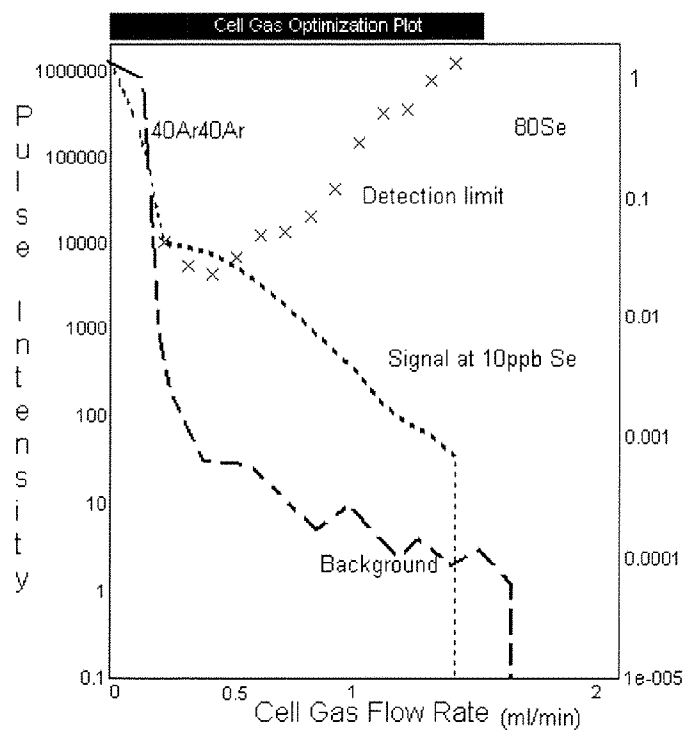


Figure 7.4. Methane gas flow optimisation plot (log scale), showing signal profiles for background and $10 \mu\text{g l}^{-1}$ Se as the gas flow is increased, for ^{80}Se .

At mass 77, while argon-based interferences are reduced, there is a focusing of $^{40}\text{Ca}^{37}\text{Cl}$, which can be seen particularly in the background signal intensity (Figure 7.5).

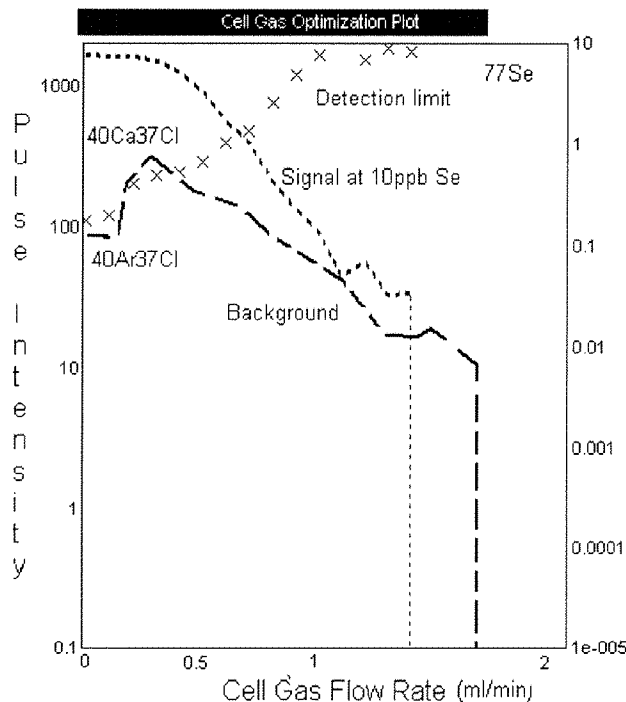


Figure 7.5. Signal profiles for background and $10 \mu\text{g l}^{-1}$ Se for ^{77}Se , in a CaCl matrix as the methane gas flow was increased.

Employing the default values of $\alpha = 0$, and $q = 0.45$, and imposing the natural abundance fingerprint of the isotopes with respect to the signal at ^{78}Se (shown by the broad lines), the magnitude of the interferences present at m/z of 77, 80, and 82 can be assessed (Figure 7.6.). The best conditions were found to be with the methane gas flow level at 0.5 ml min^{-1} , and the α and q values set to 0 and 0.7 respectively, to exclude masses of less than 60 amu, producing the scan shown in Figure 7.7. Destabilising calcium and chloride from the reaction cell reduced the isobaric interference seen at mass 77. However, this has desensitised the analysis, with signals at less than half the intensities obtained when q was set to 0.45.

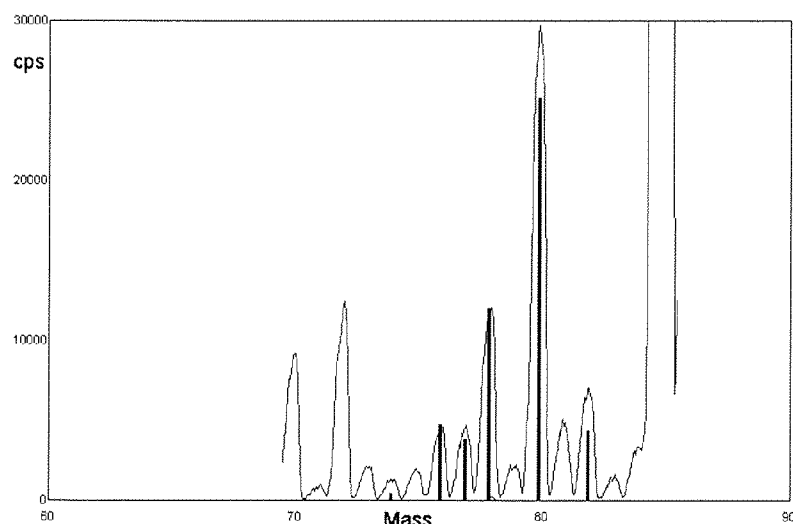


Figure 7.6. Selenium isotope scan of 1+14 dilution bovine serum with Se at $100 \mu\text{g l}^{-1}$ in 0.5% butanol, $\alpha = 0$ and $q = 0.45$, showing interferences present at m/z of 77, 80, and 82.

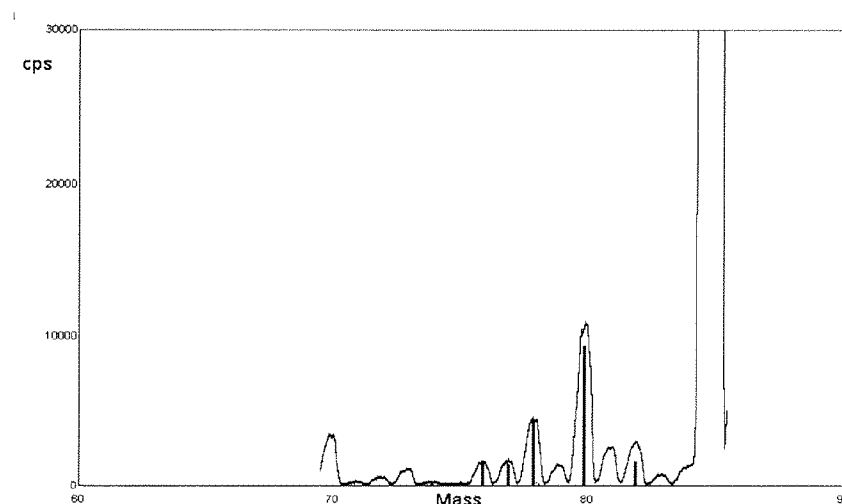


Figure 7.7. Selenium isotope scan of 1+14 dilution bovine serum with Se at $100 \mu\text{g l}^{-1}$ in 0.5% butan-1-ol, $\alpha = 0$ and $q = 0.7$, broad lines showing abundances with respect to the signal at ^{78}Se .

Mathematical equations were employed to correct for any hydrogen bromide interference on masses 80, and 82. Signal intensities at masses 80 and 82 can be divided by the blank subtracted signal increase at mass 79, obtained in the presence of 50 mg l^{-1} bromine diluted as a sample. The appropriate correction factor can be included in the scanning parameter equations (eg. $-0.97889 * Br79$ for the measurement of ^{80}Se , and $-0.99383 * Br79$ for ^{82}Se). Dependent on the operational conditions, they need to be established for each assay.

Although the argon dimers isobaric with the selenium isotopes have been eliminated, there does appear to be some interference still present in the mass region of interest (Figure 7.8). A scan of water, (with q set at 0.6), displayed a signal at mass 81, possibly due to $^{40}\text{Ar}^{40}\text{Ar}^1\text{H}$, which was reduced to 100 cps when q was set to 0.7. This would contribute to the elevation in signal at mass 81, which is disproportionate to the signal at m/z 79 given the similar natural abundances of the bromine isotopes (50.7% for ^{79}Br compared with 49.3% for ^{81}Br).

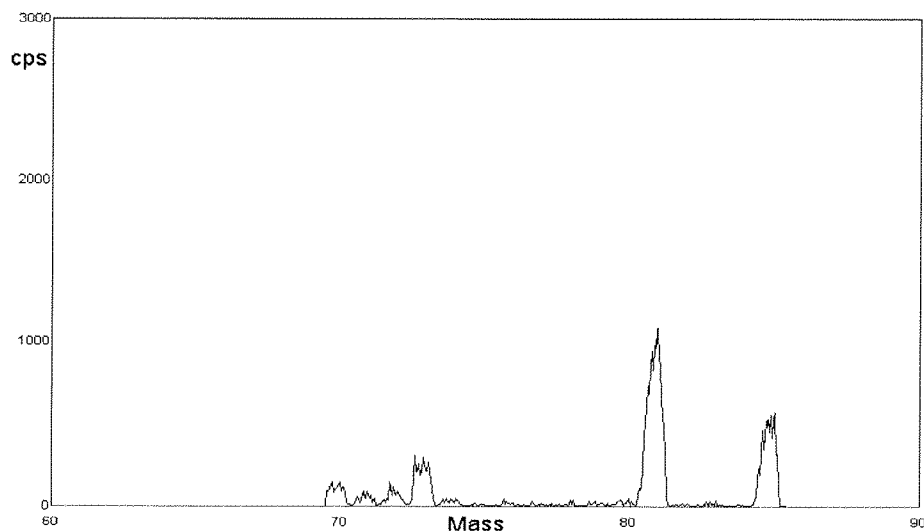


Figure 7.8. Selenium isotope scan of water, showing the presence of interferences in the analytical region of interest ($q = 0.6$).

The peak seen in Figures 7.6 and 7.7 at mass 83, evident in the presence of selenium was also enhanced by butanol. Sloth and Larsen¹³⁸ ascribed this peak to selenium hydride ($^{82}\text{Se}^1\text{H}$). The signal intensity at m/z 83 does rise with selenium concentration, although the changes are not proportional, and verification of the presence of hydrides of the other

isotopes from mass scans is prevented by the mass distribution of these isotopes. However, the signal was also elevated in the presence of bromine - indicative of $^{81}\text{Br}^1\text{H}_2$ formation.

The use of deuterated methane, demonstrated that the hydride production was not a product of the methane gas reacting with the selenium¹³⁸, and must therefore be a reaction product formed from the elements derived from the sample matrix. Due to the additional effect of bromine, the signal at mass 83 cannot be used to impose a correction equation on selenium measurement, but the production of selenium hydride may be adequately compensated for by the calibration curve itself. This was confirmed by the ability of the assay to produce selenium concentrations differing by less than 3% between measurements, obtained on monitoring ^{76}Se , ^{77}Se , ^{78}Se and ^{80}Se (with bromine correction imposed). This would be with respect to each selenium isotope differing in the amount reacting to form the hydride and the elevation of signal due to the presence of hydride of the isotope at the lower mass. Selenium values obtained on ^{82}Se determination (with bromine correction) were found to be about 10% higher, with consistently greater internal variation between the 3 replicates within an analysis. This would suggest that the bromide correction was not adequate in compensating for the interference experienced at this mass.

In consideration of these points, the isotope monitored was ^{78}Se . The signal for ^{76}Se was also determined to act as a check on selenium measurement. The percentage bias between selenium concentrations measured by the two isotopes was found to be $0.8\%\pm2.1\%$ on analysis of 100 sera. Although measurement of ^{80}Se enabled better sensitivity due to it's greater abundance, it employed a correction equation derived from the count-rate obtained at mass 79 that would not be entirely due to bromine. ^{78}Se was measured without the krypton correction imposed, as the preferential reactions with the methane gas would effectively remove any krypton present.

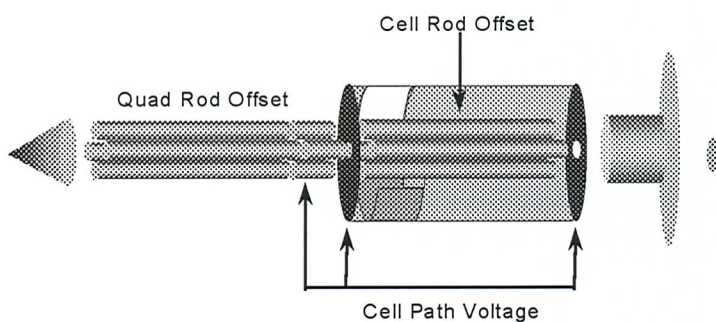
7.2.3. Use of organic solvent

The optimal nebuliser gas flow and ion lens voltage settings were determined by the auto-optimisation routines built into the software. The introduction of 0.5% v/v butan-1-ol altered the operational settings for the best sensitivity for the analyte, and the differences are listed in Table 7.4.

Table 7.4. Comparison of parameter settings for optimal conditions for ^{78}Se determination, with and without butan-1-ol, using a cross-flow nebuliser.

Parameters	Without Butanol	With 0.5% Butanol
Lens voltage	7.25	7.50
ICP RF power	1050	1075
DRC Mode NEB	0.88	0.86
DRC Mode QRO	-11.5	-15.0
DRC Mode CRO	0	0
DRC Mode CPV	-15.0	-20.0

A schematic diagram of the DRC is shown in Figure 7.9, illustrating the locations of the quadrupole rod offset (QRO), cell rod offset (CRO), and the cell path voltage (CPV).



Perkin-Elmer: DRC Theory and Operation

Figure 7.9. Schematic diagram showing cell rod offset, cell path voltage, and quad rod offset parameters.

These parameters determine the energy distribution of the ions, therefore the distribution of arrival times to the detector, and consequently the peak shape of the signal. The optimal settings for these parameters are established as part of the method development for the determination of the analyte, and are used in subsequent assays to maintain between-run consistency in mass discrimination (although, re-optimised when the detector voltages are altered). CRO voltages are restricted to -1 to +1V and that of the CPV, between -20 to -15. Higher negative voltages cause too great an acceleration of ions, that may effect reaction rates and distort peak shapes of the analyte.

The profile of the change in sensitivity of the ^{78}Se signal, as the DRC nebuliser flow rate is increased, differs dramatically in the presence of butan-1-ol. Figure 7.10. demonstrates how the organic solvent improves the quality of the sample aerosol to produce an smoother profile overall and requires a lower nebuliser gas flow rate to reach its optimum.

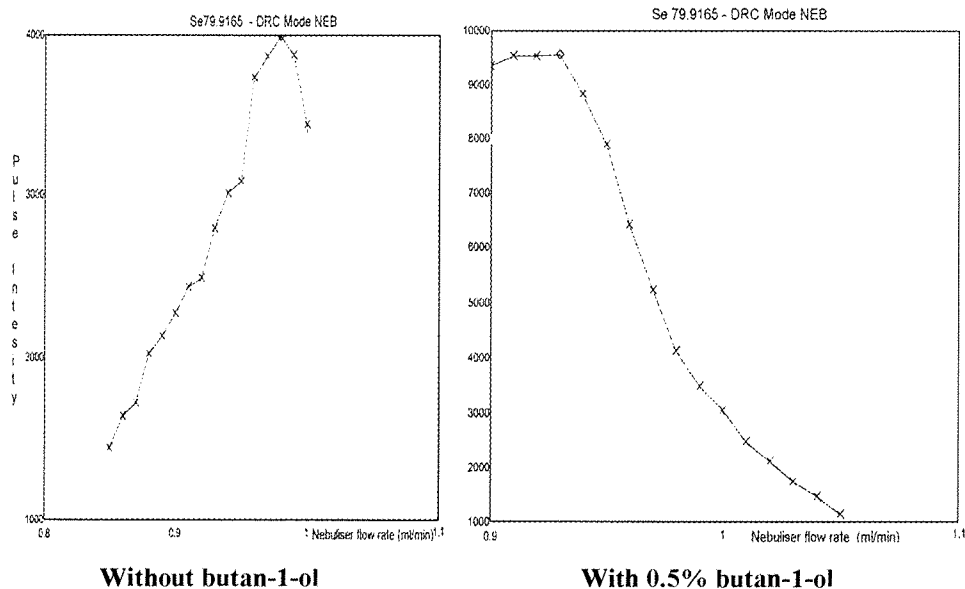


Figure 7.10. DRC nebuliser flow optimisation profiles for samples with and without butan-1-ol, showing the change in signal response with increased nebuliser flow rate.

The change in signal for the selenium isotopes with increasing butan-1-ol was monitored to determine if DRC conditions affected the signal enhancement behaviour of the solvent.

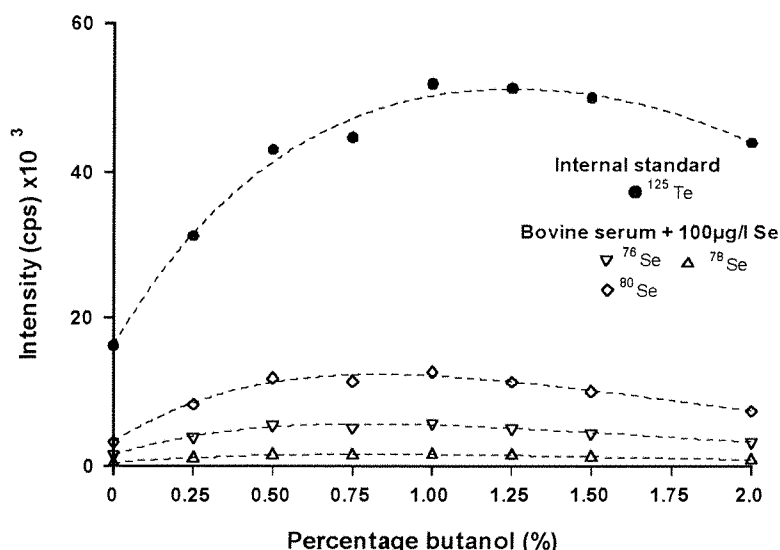


Figure 7.11. The effect of the intensity of signals at m/z ratio 76, 78, 80, and 125 with increasing concentration of butan-1-ol.

Count rates were increased 3-fold at 0.5% v/v butan-1-ol, at the start of a plateau of signal intensity that begins to decrease at 1.25% butanol (Figure 7.11.).

7.2.4. Choice of internal standard

Finding the correct internal standard for the measurement of selenium proved to be difficult because of a change in behavioural characteristics of elements in the DRC cell. Metals close in molecular weight to selenium, gallium (^{71}Ga), germanium (^{72}Ge), yttrium (^{89}Y) and niobium (^{93}Nb), as well as the more universally used internal standards of rhodium (^{103}Rh) and indium (^{115}In) were assessed. Normalisation to tellurium was also included, despite its difference in mass from selenium, because of its usefulness as an internal standard in non-DRC mode.

The presence of gallium introduced isobaric interference at mass 76 in DRC mode, while measurement of yttrium and niobium experienced a marked drift in sensitivity independent of the signal fluctuations displayed by selenium. Germanium and rhodium determination suffered from poor reproducibility, giving a mean RSD of 5% on 200,000 cps (indicative of isobaric interference). Indium and tellurium were found to be the most suitable internal standards, showing good reproducibility and accuracy of selenium analysis. Tellurium's closer ionisation efficiency with respect to selenium, made it the internal standard of choice. Similar behaviour patterns of the tellurium isotopes measured: ^{125}Te , ^{126}Te and ^{128}Te , enabled any of these to be used to normalise the count-rate obtained for selenium. ^{125}Te was monitored in subsequent selenium analysis to prevent any potential problems with excessive iodine concentrations as discussed in Section 3.12.

7.2.5. Method

Samples were prepared according to the protocol used in conventional analysis, the reagents are listed in Section 3.3.

Samples were run against a bovine serum calibration curve, spiked with 0, 10, 20, 50, 100, 200 $\mu\text{g l}^{-1}$ selenium. A 1 + 14 dilution of sample was prepared, containing 1% Triton-X-100, blood diluent solution (0.14 M ammonia, 0.003 M ethylenediaminetetra aceytic acid diammonium salt and 0.029 M ammonium dihydrogen phosphate), and tellurium at 500 $\mu\text{g l}^{-1}$ as an internal standard, added in equal volume to the sample (100 μl). The sample was made up to 1.5 ml with deionised water and 6% v/v butan-1-ol to give a

final concentration of 0.5% butanol.

The between-sample wash appeared to have a greater influence on the internal precision of selenium measurement when compared to the conventional method. The addition of blood diluent (6.7%) to the butanol / triton rinse was required to lower the precision variation of replicates within a single analysis to less than 2% RSD. The longer settling time which is required for DRC analysis (3 ms) compared to standard mode (0.2 ms), reflects the need for a long dwell time of 200-500 ms, with more than 5 sweeps per reading having little effect on the precision of analysis (Table 7.5).

Table 7.5. Percentage relative standard deviation of the analysis of five dilutions of bovine serum ($55 \mu\text{g l}^{-1}$ endogenous Se) on increasing dwell time and sweeps per reading, monitoring ^{78}Se .

Dwell time (ms)	%RSD	
	Sweeps	per reading
	5	10
100	7.3	
200	1.5	1.9
400	1.2	-
500	0.8	0.7
600	3.0	-

For the Elan 6100DRC, general practice after cleaning cones and changing injector tubes, is to condition the system by aspirating a dilute solution of the analyte or one containing calcium and chloride for 15 minutes. This avoids a marked drift in sensitivity at the beginning of an assay. Conditioning the cones for selenium analysis, was carried out by running standard addition dilutions of the bovine serum prior to the assay calibration curve, to achieve the required stability at the start of the selenium assay. Re-calibration was found to be necessary within the assay run, sometimes as often as every 20 samples.

Calibration curves obtained for bovine serum and blood can be seen in Figure 7.12. demonstrating a small reduction in regression line gradient when compared with water, due to matrix effects.

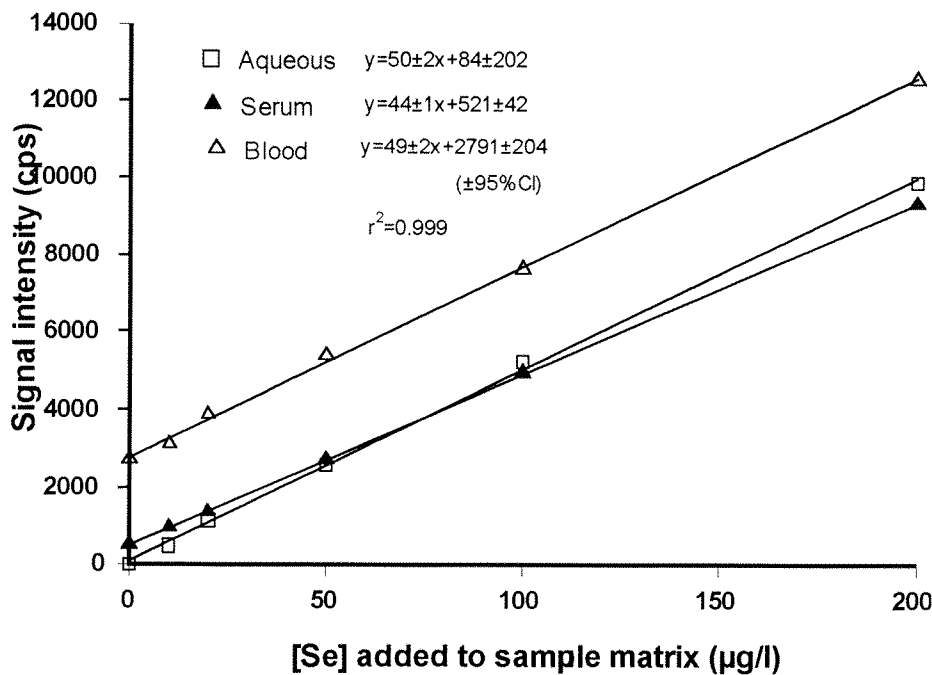


Figure 7.12. Selenium standard additions to water, bovine serum (endogenous value = $10 \mu\text{g l}^{-1}$ Se) and bovine blood ($55 \mu\text{g l}^{-1}$ Se) in 0.5% butan-1-ol, using ^{125}Te internal standard.

The sensitivity was three times greater than that obtained for the Elan 5000. This was reflected in the lower detection limit, at $0.4 \mu\text{g l}^{-1}$ ($0.005 \mu\text{mol l}^{-1}$) for measurement of ^{78}Se , calculated from three standard deviations of ten blank determinations.

7.2.6. Accuracy and precision

Reanalysis of the forty EQA samples (provided by Quebec National Institute of Public Health Laboratories and UK-TEQAS), gave a more confined spread of variation of the measured concentration with target values, when compared to analysis by the Elan 5000 (Figure 7.13.). A positive a mean bias of $+0.8 \pm 4.7 \mu\text{g l}^{-1}$ ($+0.01 \pm 0.06 \mu\text{mol l}^{-1}$) was obtained using DRC-ICP-MS, compared with $-0.8 \pm 5.5 \mu\text{g l}^{-1}$ ($-0.01 \pm 0.07 \mu\text{mol l}^{-1}$) for conventional analysis. A range of -1.7 to $0.1 \mu\text{g l}^{-1}$ for the 95% confidence interval was obtained for DRC analysis. The individual results obtained and their percentage bias from the target values is listed in Table 4 of Appendix I.

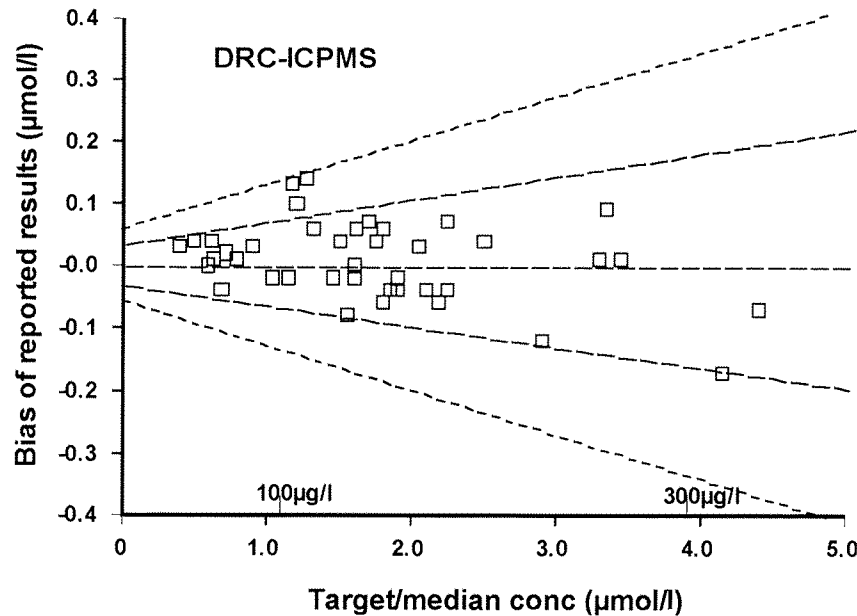


Figure 7.13. Comparison of the bias from target values, of sera determined by DRC-ICP-MS.

Analysis of certified quality control sera Seronorm (704121), and our own IQC material (Series B), displayed a positive mean bias between observed and target values of $+2.0 \mu\text{g l}^{-1}$ ($0.03 \mu\text{mol l}^{-1}$), $+2.9\%$. The between-run precision ranged from $\pm 5\%$ at $20 \mu\text{g l}^{-1}$ ($0.25 \mu\text{mol l}^{-1}$), to $\pm 3\%$ at $150 \mu\text{g l}^{-1}$ ($1.90 \mu\text{mol l}^{-1}$) and the within-run precision ranged from $\pm 4\%$ at $20 \mu\text{g l}^{-1}$ to $\pm 2\%$ at $150 \mu\text{g l}^{-1}$ (Table 7.6).

Table 7.6. Internal quality control data for serum analysis by DRC-ICP-MS.

IQC sample	Target value ($\mu\text{g l}^{-1}$)	Observed mean	Value ($\mu\text{g l}^{-1}$) ± sd	N
Level 1B	21.5	Within run 22.9 ± 0.9	Between run 22.9 ± 1.2	10
Level 2B	54.6	55.5 ± 1.6	56.2 ± 2.0	10
Level 3B	104.0	104.6 ± 2.5	107.9 ± 3.8	10
Level 4B	138.2	138.2 ± 1.6	141.8 ± 3.9	10
Seronorm	73 / 86	76.6 ± 1.5	75.0 ± 3.1	10
Nist 1598	42.4		42.0 ± 1.8	4

The reduction of background signal to less than 20cps (equivalent to $0.4 \mu\text{g l}^{-1}$ selenium) was responsible for the lowering of the detection limit and the better precision at the lower concentrations when compared with determinations made by the conventional instrument (Figure 7.14.).

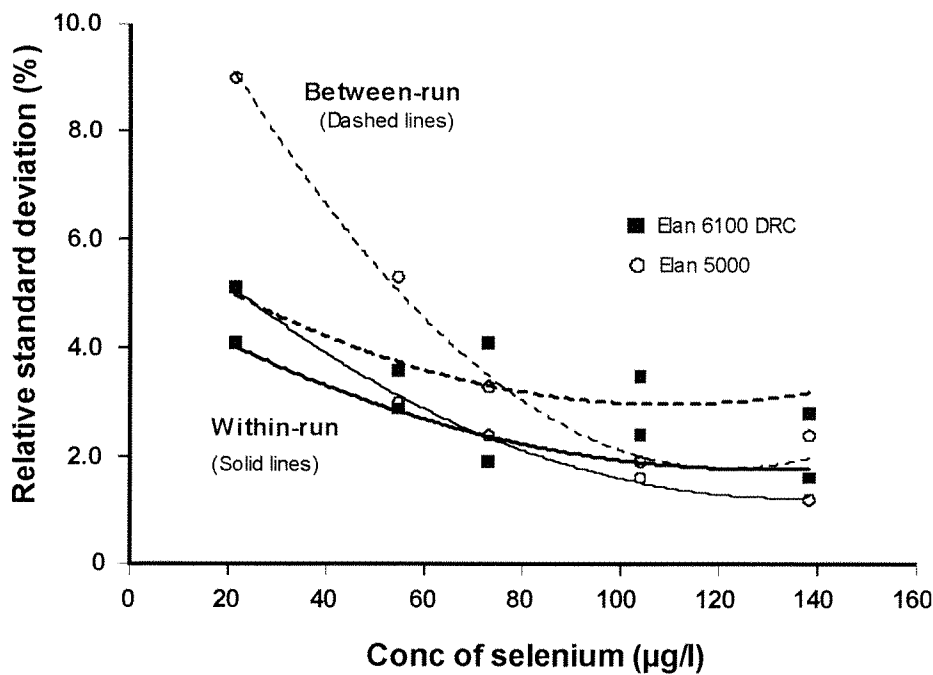


Figure 7.14. Comparison of within and between run precision data for DRC-ICP-MS with conventional ICP-MS analysis of IQC material.

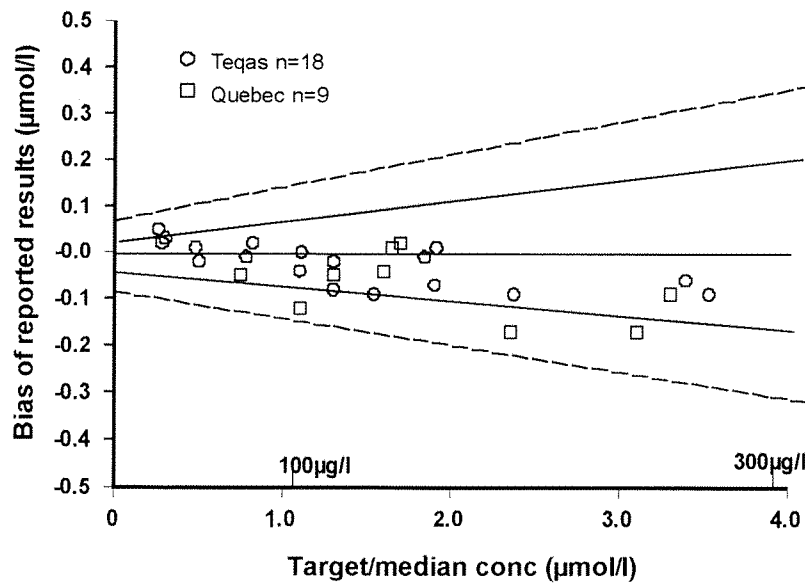


Figure 7.15. Performance in EQA schemes for selenium in serum, November 2000 to April 2001, showing proximity to target values. (Zone parameters defined by the EQA centres).

Figure 7.15. shows the bias of reported results for analysis of sera from the median/target values of the two interlaboratory comparison programs (UK-TEQAS and Quebec National Institute of Public Health Laboratories). Despite the positive bias obtained for the IQs, a small negative mean bias of $-3 \pm 5 \text{ } \mu\text{g l}^{-1}$ ($-0.04 \pm 0.06 \text{ } \mu\text{mol l}^{-1}$) was evident

for these sample. Although the analysis period covers only six months, the good agreement between the reported and target values attained, demonstrates the capability of the DRC method for producing accurate selenium determination in routine clinical analysis.

7.2.7. Whole-blood analysis

A 1 + 29 dilution of whole-blood was required for assay runs which were longer than 6 hours. The accumulation of denatured protein in the injector tube and a drift in signal sensitivity appeared to be more pronounced for whole-blood analysis using DRC-ICP-MS when compared to the conventional quadrupole instrument, which was overcome by analysing a greater dilution of the sample.

Bovine blood (Selbourne Biological Services, Alton, Hampshire) was used as an internal quality control (QcB), and when diluted 1 + 1 with the blood diluent, provided the second internal quality control sample (QcA). Two Seronorm whole-blood certified reference samples were also analysed. A comparison of the selenium concentrations of the IQC material obtained for the DRC instrument, with results measured by the Elan 5000, is presented in Table 7.7. using tellurium as the internal standard in both cases

Table 7.7. Internal quality control data for selenium in whole-blood by DRC and direct ICP-MS detection.

Quality Control Material	Target value ($\mu\text{g l}^{-1}$)	Observed Mean $\pm \text{sd} (\mu\text{g l}^{-1})$	
		ICP-MS	DRC-ICP-MS
QcA		28.4 \pm 1.8 (n=22)	26.9 \pm 2.8 (n=16)
Bovine bld (1+1)		54.6 \pm 6.6 (n=22)	54.8 \pm 4.0 (n=16)
QcB			
Bovine blood			
Seronorm level1 (404107)	80 (80-91)	79.2 \pm 8.2 (n=26)	81.5 \pm 4.8 (n=16)
Seronorm level2 (404108)	82 (82-89)	79.7 \pm 3.0 (n=26)	
Seronorm level2 (MR9067)	112		113.9 \pm 7.2 (n=19)

Analysis of the certified reference material showed good agreement between measured values and the assigned values, with a mean bias of $+1.7 \mu\text{g l}^{-1}$ ($0.02 \mu\text{mol l}^{-1}$),

1.8%. The precision appeared to be similar for the two instruments, ranging from $\pm 8\%$ RSD for between-run analysis, to $\pm 6\%$ within-run measurements for DRC analysis at 30 – 90 $\mu\text{g l}^{-1}$ (0.38 – 1.14 $\mu\text{mol l}^{-1}$), compared to $\pm 9\%$ (between-run), to $\pm 5\%$ RSD (within-run) measurements for conventional ICP-MS.

7.2.8. Conclusion

The low background signals of DRC-ICP-MS detection for conventional selenium measurement, enabled a better reproducibility at low sample concentrations, yet a greater variability was evident at the higher levels for between-run comparison with direct ICP-MS.

Differences in behavioral characteristics in a pressurised reaction cell between elements, prevented the employment of an internal standard that was close to the m/z of selenium. Despite tellurium's capability of reflecting changes in ionisation conditions, it was not possible to achieve complete compensation for instrumental drift on normalisation, and frequent re-calibration was required. The compensation capability of indium was found to be consistent with that obtained for tellurium, both metals responding to organic solvent signal enhancement. However, being isobaric with a tin isotope, a correction equation is required in the scanning parameters, increasing analysis time and introducing another variable in the analysis.

Variation in changes in signal intensities between these elements, suggests that their reaction with the DRC gas does play a more significant role than has been previously thought. Although the methane would react with the analyte at a much slower rate than that with the argon dimers, the scope for signal drift compensation by other elements is limited. Normalisation to the analyte isotope would therefore have clear advantages with regards to compensation for instrumental fluctuations for selenium analysis, and in the following chapter, the application of isotope dilution to DRC-ICP-MS determination is discussed.

CHAPTER 8

SELENIUM DETERMINATION BY ID-DRC-ICP-MS

The combination of argon-adduct removal by the methane gas and band-pass mass filtering, offers the potential of interference-free measurement of selenium isotopic ratios by dynamic reaction cell (DRC) instrumentation. Reproducibility studies carried out for the determination of both ^{78}Se : ^{77}Se and ^{78}Se : ^{74}Se ratios for the use of ID-DRC-ICP-MS were indicative of a procedure that could match, if not better, the levels of precision achieved by ^{74}Se ID analysis by direct solution nebulisation (SN) ICP-MS. However, further investigations showed that the developed ID method could not be directly transposed to DRC detection, and additional considerations with respect to operational conditions had to be addressed. These investigations are outlined in this chapter, together with an assessment of performance, which for ^{78}Se : ^{77}Se , reflected the associated analytical problems of the method presented.

8.1. Using the ^{77}Se -enriched selenium isotope standard

Isotope dilution employing the ^{77}Se -enriched selenium standard at $30\mu\text{g l}^{-1}$, produced measured ratios for the selenium isotopes, which deviated up to 10% from the calculated values. Table 8.1. lists these for each isotope, alongside the optimal blend ratio calculated for $80\mu\text{g l}^{-1}$ natural selenium, and the spike concentration required to achieve this isotopic mixture.

Table 8.1. Calculated and measured ratios for selenium isotopes at $80\mu\text{g l}^{-1}$ selenium spiked with the calculated optimal blend of ^{77}Se -enriched standard.

Isotope	^{77}Se ratio for Optimal blend	Spike ($\mu\text{g l}^{-1}$)	At $80\mu\text{g l}^{-1}\text{Se}$, $30\mu\text{g l}^{-1}^{77}\text{Se}$	
			True ratio	Measured Ratio (%deviation)
^{76}Se	0.216	50	0.31	0.28 (-10%)
^{78}Se	0.891	30	0.90	0.95 (+5%)
^{80}Se	0.878	66	1.57	1.53 (-3%)
^{82}Se	0.166	60	0.28	0.29 (-4%)

8.1.1. Instrumental scanning parameters

Generally, the measurement period for isotope ratio analysis, should be short enough to allow a scan cycle to be completed in a faster time than the period of noise fluctuation, but with a signal integration time long enough to average out the inconsistencies caused by peak hopping between analytes. In practice, this is realised by a short dwell time of about 10 ms for each isotope, and a large number of sweeps per reading, 1000 sweeps being the maximum parameter setting for the Elan 6100DRC. These data acquisition parameters (with 3 replicates per sample analysis), when applied to ^{78}Se : ^{77}Se measurement, produced 0.4% RSDs for 5 consecutive measurements of ^{77}Se -spiked serum at $80 \mu\text{g l}^{-1}$ natural selenium. Optimisation of the scanning parameters to produce the lowest variation in replicate analysis at 0.2% RSD, resulted in a dwell time of 80 ms and 100 sweeps per reading. Due to their relatively lower natural abundance, ratio determination involving ^{76}Se and ^{82}Se isotopes, gave twice the %RSD when compared to measurements made for the other isotopes.

8.1.2. Method

The protocol described in Chapter 5 for ^{74}Se isotope dilution, was applied to ^{78}Se : ^{77}Se measurement, using the ^{77}Se -enriched standard at $30 \mu\text{g l}^{-1}$ (optimal blend concentration at $80 \mu\text{g l}^{-1}$ selenium). 200 μl aliquots of sample and spike were diluted to 1.5 ml with a 1% butan-1-ol diluent. ^{77}Se -spiked serum, sodium chloride and aqueous reference solutions containing 0, 40, 80 and $160 \mu\text{g l}^{-1}$ selenium were run against each other, with selenium concentrations of test sera determined from the measured ratios.

8.1.3. Accuracy

The first problem encountered was that these calibration solutions did not produce a straight line for the measured ratios with increasing selenium. It was possible, however, to apply a parabolic curve-fit to the data, using a graphical data processing package (Fig P-the scientific figure processor, FigP Software Corporation, Durham), resulting in regression coefficient squared values of 0.998 (Figure 8.1). A variable mean deviation in ^{78}Se : ^{77}Se ratios was evident for the calibration solutions, which decreased with selenium concentration and appeared to be matrix dependant (Table 8.2).

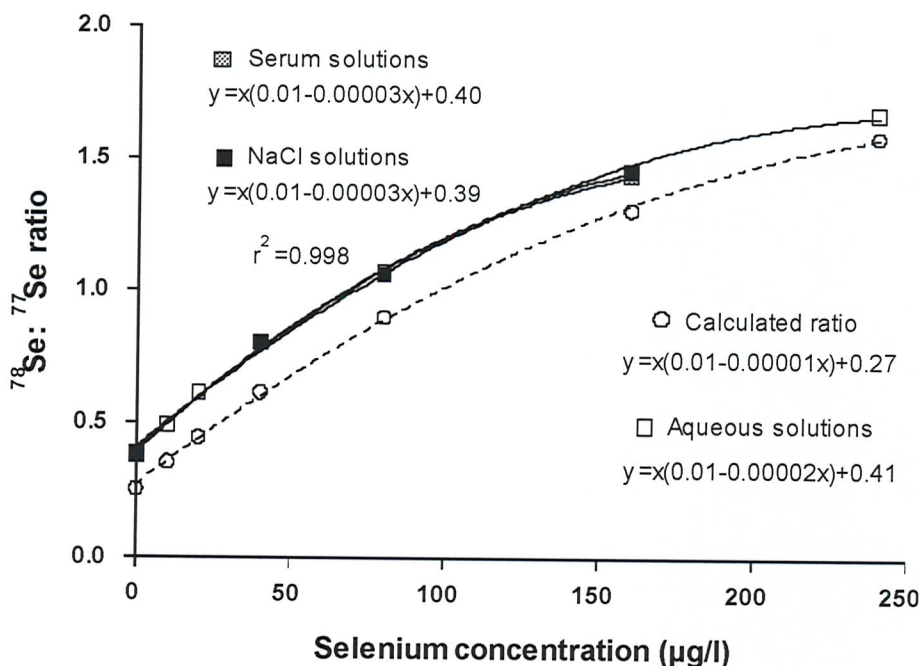


Figure 8.1. Comparison of ^{78}Se : ^{77}Se ratios obtained for bovine serum, sodium chloride and aqueous reference solutions at 0, 40, 80, 160 $\mu\text{g l}^{-1}$ selenium.

Table 8.2. Comparison of aqueous, sodium chloride and serum ratio values obtained for ^{78}Se : ^{77}Se measurement.

Reference Solution	Expected Ratios ^{78}Se : ^{77}Se	Measured ratio values	^{78}Se : ^{77}Se
0	0.255	Aqueous 0.384	NaCl 0.383
40	0.618	0.802	0.802
80	0.899	1.066	1.066
160	1.306	1.455	1.454

The capability of the reference solution equations in predicting accurate sample selenium content, was found to be limited to concentrations which fell within the calibration range. A plot of determined selenium values across a wider range of concentrations, demonstrated how the 0 /80 /160 parabolic curve was not representative of the curve fit at concentrations greater than 200 $\mu\text{g l}^{-1}$ (Figure 8.2.). Increasingly negative bias of the calculated values of 45 sera (consisting of 40 EQA and 5 IQC) from target values was

evident at higher concentrations. Similar characteristics were observed for ^{80}Se : ^{77}Se IDMS analysis, with a better reference solution correction obtained on the analysis of ^{80}Se without the bromine correction employed.

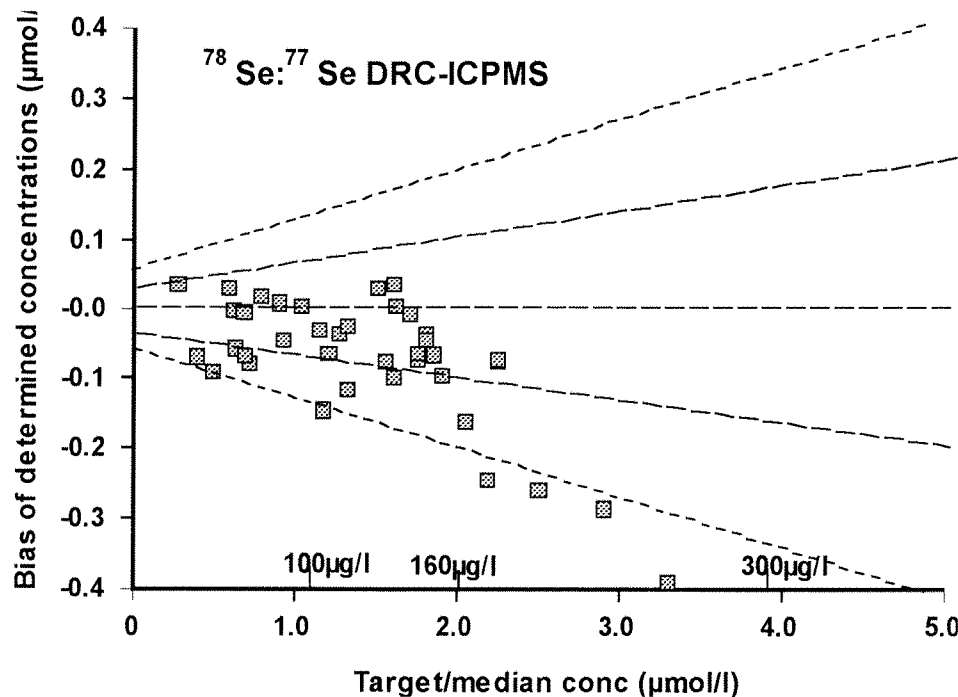


Figure 8.2. Bias from target values of serum samples determined by ^{78}Se : ^{77}Se DRC-IDMS with serum calibration.

8.1.4. Conclusion

On application of DRC, destabilisation of the major interferences, improved the accuracy of ^{78}Se : ^{77}Se ratio measurement sufficiently to enable selenium determination by ^{78}Se : ^{77}Se IDMS. However, the requirement of a parabolic curve-fit and the use a ratio correction that is specific for the concentration of the analysed samples, makes this technique difficult to apply to the routine analysis of samples.

8.2. Using the ^{74}Se -enriched selenium isotope standard

8.2.1. Scanning parameters

Internal precision of replicate measurements and deviation from the calculated ratio was found to be influenced by the q value selected for the ^{74}Se ratio of each isotope. As q

changed from 0.25 (recommended value for non-DRC mode), to 0.74 (q value used in conventional DRC selenium analysis), the signal intensity for ^{74}Se decreased in relation to the count rate obtained for the other isotopes, effectively increasing the observed ratio, as shown in Table 8.3.

Table 8.3. Change of the isotopic ratios obtained by ^{74}Se IDMS, with increasing q value, employing $100 \mu\text{g l}^{-1} {^{74}\text{Se}}$ spike (internal precision of analysis is given in brackets).

q value	$^{76}\text{Se}:{^{74}\text{Se}}$ value (sd)	$^{77}\text{Se}:{^{74}\text{Se}}$ value (sd)	$^{78}\text{Se}:{^{74}\text{Se}}$ value (sd)	$^{80}\text{Se}:{^{74}\text{Se}}$ value (sd)	$^{82}\text{Se}:{^{74}\text{Se}}$ value (sd)
	<i>True ratio</i> 0.69	<i>True ratio</i> 0.37	<i>True ratio</i> 1.01	<i>True ratio</i> 2.04	<i>True ratio</i> 0.35
0.25	0.75 (0.3)	0.46 (0.6)	1.24 (0.3)	3.01 (0.2)	0.49 (0.9)
0.45	0.76 (0.3)	0.49 (0.3)	1.25 (0.3)	2.61 (0.2)	0.47 (0.5)
0.5	0.76 (0.4)	0.50 (0.5)	1.27 (0.3)	2.65 (0.3)	0.48 (0.7)
0.6	0.77 (0.7)	0.52 (0.6)	1.29 (0.4)	2.65 (0.3)	0.51 (0.7)
0.6 varied	0.98 (0.8)	0.70 (0.7)	1.54 (0.6)	3.97 (0.7)	0.79 (0.9)
0.7	0.79 (0.5)	0.55 (0.7)	1.35 (0.1)	2.76 (0.3)	0.53 (0.7)
0.7 varied	0.99 (0.6)	0.77 (0.5)	2.02 (0.3)	4.63 (0.5)	0.92 (0.7)
0.74	0.79 (0.3)	0.57 (0.7)	1.37 (0.8)	2.83 (0.4)	0.55 (0.7)

Shaded region denotes varied q values: to maintain the same lower mass cut-off for analysis with all isotopes.

When the selected q was varied in order to maintain a consistent lower mass cut-off, as described in Section 7.2.2. (eg. $q=0.74$ for ^{74}Se , $q=0.72$ for ^{76}Se , $q=0.71$ for ^{77}Se , $q=0.70$ for ^{78}Se , $q=0.68$ for ^{80}Se , and $q=0.67$ for ^{82}Se , to enable a cut-off at 60amu), the measured ratio increased appreciably and replicate variation was raised. It appears that the low settling time of 0.2 msec selected for isotope dilution analysis, does not provide sufficient time for the electronics of the instrument to respond to the parameter settings between isotope measurement.

The q value determines the signal intensities of the isotopes - the lower the value, the greater the count-rate, and consequently the better the internal precision of measurement. However, at $q=0.25$, appreciable blanks were obtained which were reduced to less than 250cps on raising the value to 0.45 for the isotopes measured, and less than 100 cps at $q=0.7$, the setting selected for standard addition. A constant q value at 0.7 was employed for subsequent isotopic ratio determination.



The optimal scanning parameters were consistent with that found for SN-ICP-MS. A 10ms dwell time, 1000 sweeps per reading and 3 replicates per analysis, gave RSDs of 0.2% for 5 replicate analyses at $80\mu\text{g l}^{-1}$ selenium, monitoring ^{78}Se : ^{74}Se on spiking with $100\mu\text{g l}^{-1}$ ^{74}Se -enriched standard. The 0/40/80/160 calibration solutions produced linear regression lines ($r^2 > 0.999$).

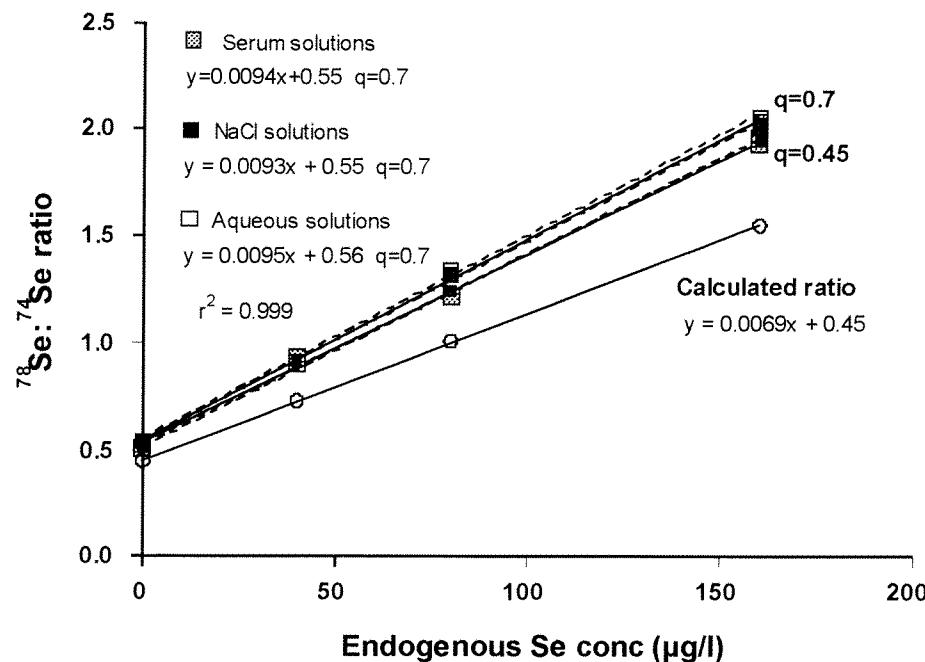


Figure 8.3. Comparison of ^{78}Se : ^{74}Se isotopic ratios obtained for serum, sodium chloride and aqueous reference solutions at 0,40,80,160 $\mu\text{g l}^{-1}$ spiked with ^{74}Se standard at $100\mu\text{g l}^{-1}$, with q at 0.45 and 0.7.

8.2.2. Accuracy and precision

Differences in regression line characteristics between NaCl and serum solution calibrations, were reduced by using a more dilute salt solution of 70 mmol l^{-1} sodium chloride, resulting in a 1% variation in concentration levels for the sera (Table 8.4.). The concentrations obtained for internal quality control and 40 EQA sera determination, employing the sodium chloride correction are given in Table 8.4. and Figure 8.6., respectively. The individual concentrations for the EQA samples are listed in Table 6 of Appendix I.

Table 8.4. Internal quality control data for serum analysis by ID-DRC-ICP-MS.

IQC sample	Target value ($\mu\text{g l}^{-1}$)	Observed	Value ($\mu\text{g l}^{-1}$)			N
		Serum calibration Mean \pm sd	Sodium chloride Mean	Calibration \pm sd	(%RSD)	
Level 1B	21.5	Within run 22.0 \pm 0.5	Within run 22.1 \pm 0.5 (2.1)	Between run 21.3 \pm 0.9 (4.2)		10
Level 2B	54.6	54.0 \pm 1.1	54.8 \pm 1.1 (2.0)	54.8 \pm 0.9 (1.6)		10
Level 3B	104.0	107.3 \pm 1.0	106.2 \pm 1.0 (1.0)	106.0 \pm 2.4 (2.3)		10
Level 4B	138.2	138.8 \pm 3.9	137.4 \pm 3.9 (2.9)	140.3 \pm 2.6 (1.8)		10
Seronorm	73 / 86	71.6 \pm 2.1	71.6 \pm 2.1 (2.1)	73.1 \pm 1.8 (2.5)		10
Nist 1598	42.4			43.4 \pm 1.5 (3.4)		10

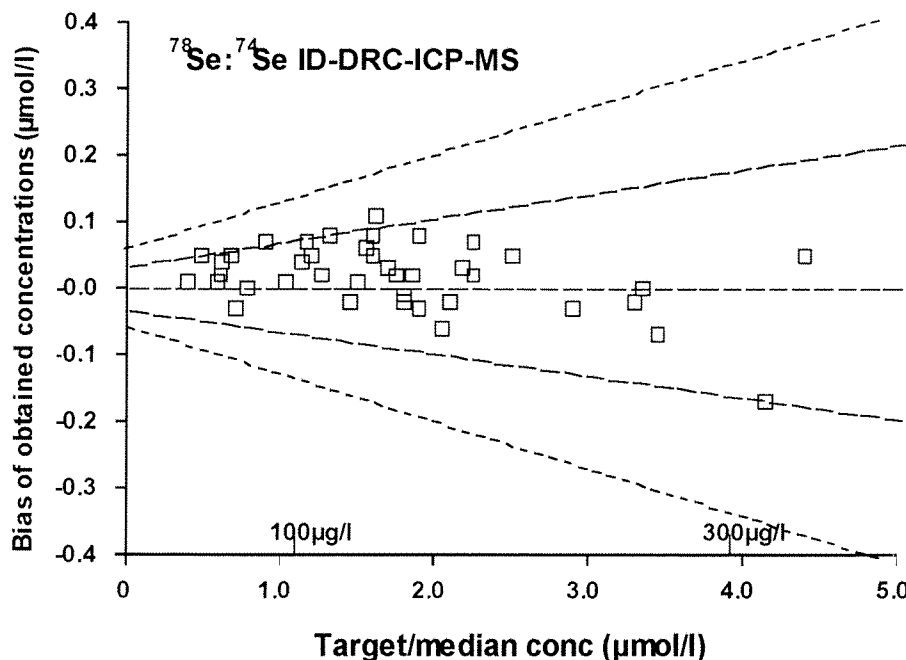


Figure 8.4. Comparison of the bias from target values, of serum samples determined by ID-DRC-ICP-MS, using ^{74}Se -enriched standard at $100 \mu\text{g l}^{-1}$, with NaCl (70mmol l^{-1}) calibration.

A positive mean bias of $1.6 \pm 4.0 \mu\text{g l}^{-1}$ ($0.02 \pm 0.05 \mu\text{mol l}^{-1}$) was obtained on determination of the EQA concentrations by DRC analysis. An equivalent spread of bias to that obtained by ID-SN-ICP-MS, signifies that isotope dilution overcame the problems experienced by standard addition analysis using DRC. A 1% RSD variation in mass bias ratio, seen during a day's assay run of 6 hours, was compensated for by analysis of the reference solutions at intervals of 10 test samples.

8.2.3. Conclusion

The application of DRC analysis to ID determination, lowers signal intensities of the measured isotopes by half, in relation to standard mode operation of the Elan 6100. This is mainly due to the band pass filtering, defined by the q value selected in the scanning parameters. At $q=0.7$, precision of $^{78}\text{Se} : ^{74}\text{Se}$ ratio measurement is equivalent to that obtained in standard mode (0.2%RSD), and lowering the q setting may enable greater precision to be achieved through the increase in count rate. The effect on accuracy would need to be assessed, as altering the band pass filtering would increase the risk of potential interference at the masses being monitored. Nevertheless, more work needs to be carried out with respect to understanding what effect the presence of the reaction cell gas has on the detection of the selenium isotopes. The effect of selenium hydride formation, found to be at 10% of total selenium under the conditions stated, needs to be investigated.

In practise, a greater level of accuracy for selenium determination, was prevented by the analytical drift evident in the assays carried out. This has also been experienced by analytes other than selenium. Studies carried out on lead isotope ratio measurement, in the presence of methane to enable a 3-fold increase in sensitivity by collisional focussing, exhibited differential changes in signal between the isotopes. This does question whether the stability required by high precision analysis can be achieved in DRC mode of detection, although it may be the case, that careful selection of operational conditions and scanning parameters can overcome this situation, and further investigation is necessary.

CHAPTER 9

COMPARISON OF ICP-MS METHODOLOGIES

In this chapter, a direct comparison is given of the performance of the methodologies presented in this thesis, namely SN- ICP-MS, HG-ICP-MS and DRC-ICP-MS applied to conventional analysis and ID. The quality of analysis was found to be influenced by the extent to which polyatomic species in the plasma, originating from the argon support gas and matrix components of the samples, have been reduced or eliminated. This was accomplished by the use of an organic solvent in SN-ICP-MS, by a reactive gas in DRC-ICP-MS and by separation of the analyte as the hydride in HG-ICP-MS. Low selenium sensitivity was overcome by the signal enhancement effect produced by the organic solvent for both direct and DRC-ICP-MS, and the effective concentration of the sample on production of the hydride gas with HG-ICP-MS.

HG-ICP-MS assessment is confined to conventional analysis, as isotope dilution by this technique was found to be unworkable at the early stages of method development. An assessment of selenium determination by ICP-MC-MS was prevented by the problems of sample introduction. These could not be resolved in the limited time available on this instrument, and the technique is therefore excluded from this comparison.

9.1. Methodology

Instrumentation, operating conditions, reagents and protocol details are compared in Appendix II.

For conventional analysis, sample preparation consisted of a simple 1 + 14 dilution of the sera with a diluent containing Triton-X-100 and an ammonia/EDTA/phosphate solution to improve sample nebulisation, and butan-1-ol to give a working concentration of 0.5% butan-1-ol. A similar sample preparation was required for IDMS, employing a 1 + 7 dilution of the sample in 1.0% butan-1-ol. To compensate for instrumental fluctuations, the internal standard added was tellurium for conventional analysis and an isotopically enriched selenium standard for ID measurement. Samples were run against calibration solutions consisting of 0 – 200 $\mu\text{g l}^{-1}$ selenium standard additions to bovine serum (conventional analysis), and sodium chloride reference solutions containing 0, 80, 160 $\mu\text{g l}^{-1}$ selenium (IDMS).

The requirement for dissolution of the sample for the analysis by HG-ICP-MS requires a more time-consuming sample preparation. Digestion with a mixture of nitric and sulphuric acids, enabled the selenium to be dissociated from the organic material, with the oxidation of the selenium to the tetravalent and hexavalent forms. Conversion to Se(IV) was carried out using hydrochloric acid. The hydride, generated on reaction of the analyte with sodium tetrahydroborate, was released into an argon gas flow and introduced into the plasma of the ICP-MS for quantification. The signals for ^{77}Se , ^{78}Se , and ^{82}Se were monitored without normalisation to an internal standard.

9.2. Assessment of analytical performance

Conventional analysis of selenium by direct solution nebulisation ICP-MS has proved to be precise and accurate for the measurement of the analyte in serum, as demonstrated by its good performance in the two EQA schemes. It is in reference to this method that the performance of the other techniques is described.

9.2.1. Calibration and sensitivity

Analysis by DRC-ICP-MS proved to be the most sensitive of the methods for measurement of selenium at mass 78, giving rise to a 3-fold improvement in signal response over SN- ICP-MS detection, using the Elan 5000 (Figure 9.1.).

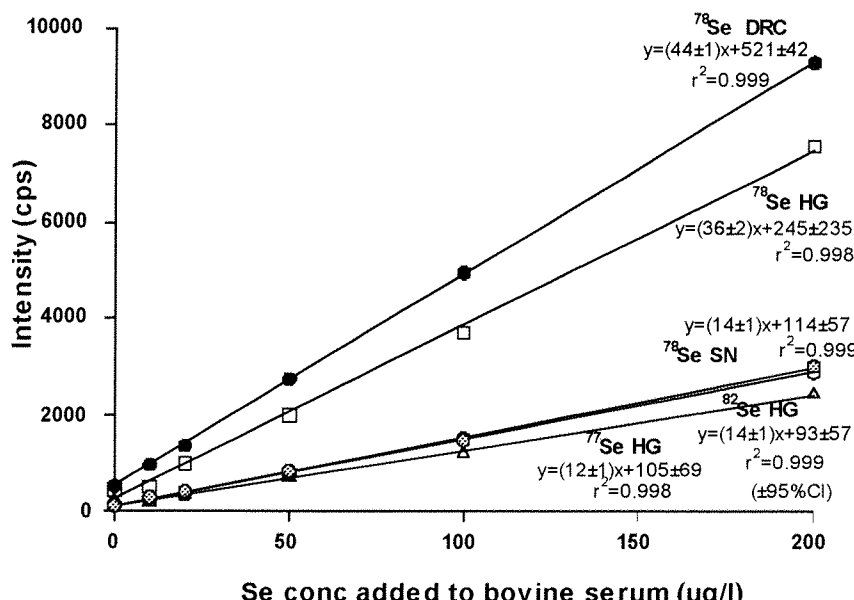


Figure 9.1. Standard addition calibration curves obtained for conventional analysis carried out by hydride generation and DRC-ICP-MS compared to direct (SN) ICP-MS analysis.

A 2-fold improvement was achieved by hydride generation analysis, although this increase in sensitivity did not directly translate into precision, illustrated by a correlation coefficient squared of 0.998, for the linear regression.

A greater difference from the calculated $^{78}\text{Se} : {}^{74}\text{Se}$ ratio value, was obtained for DRC analysis at 1.32, compared to that found for direct ID-MS measurement at 1.08, on the addition of $100 \mu\text{g l}^{-1}$ ${}^{74}\text{Se}$ to $80 \mu\text{g l}^{-1}$ natural selenium. This 24% increase in deviation from the calculated ratio of 1.01, reflects the greater mass bias experienced by the selenium isotopes in DRC mode, imposed by the band-pass mass filtering. A small increase in gradient was evident on the determination of $^{78}\text{Se} : {}^{74}\text{Se}$ ratio with increasing selenium concentrations by DRC-ICP-MS (Figure 9.2.), which implies a better differentiation between concentrations.

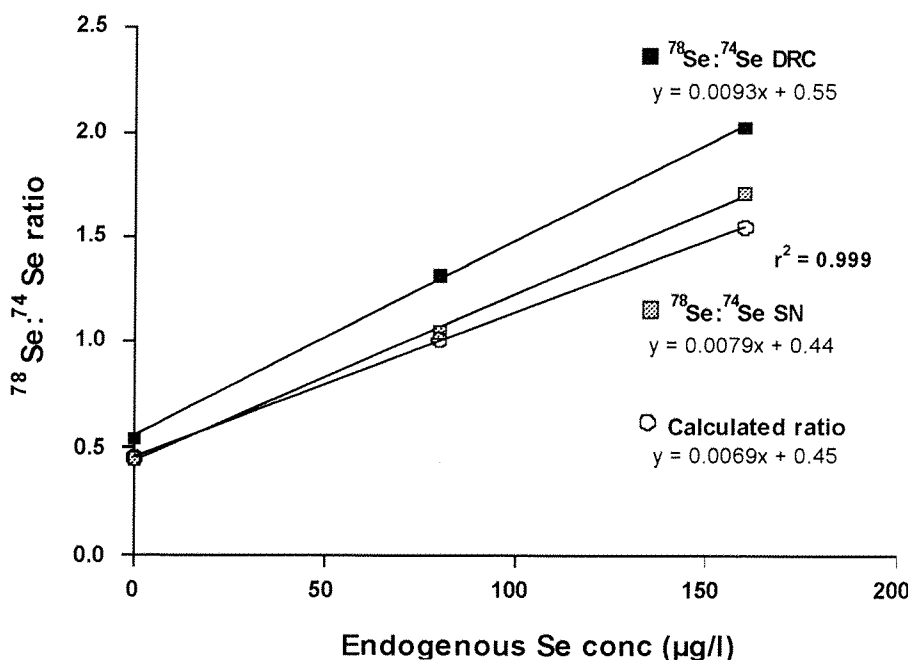


Figure 9.2. Measured isotopic ratios as a function of increasing levels of selenium for direct (SN) and DRC-ICP-MS analysis, using $100 \mu\text{g l}^{-1}$ ${}^{74}\text{Se}$ spike (NaCl calibration).

9.2.2. Detection limits

The ratio of signal response to noise determines the detection limit of a method. Hydride generation, conventional and isotope dilution analysis by SN- ICP-MS, gave a detection limit of $2 \mu\text{g l}^{-1}$ ($0.025 \mu\text{mol l}^{-1}$), calculated from three standard deviations of ten

blank determinations. This was reduced to $0.4 \mu\text{g l}^{-1}$ ($0.005 \mu\text{mol l}^{-1}$) with DRC-ICP-MS, due to the lower background signals, although a detection limit of $1.5 \mu\text{g l}^{-1}$ ($0.019 \mu\text{mol l}^{-1}$) was obtained when ID was applied.

9.2.3. Accuracy and precision

Analytical accuracy was determined by the use of internal quality control material, external quality assessment samples, and certified materials. The reference method was validated using four IQC sera, consisting of bovine serum spiked with selenium, of which the target values were established by HG-AAS to be $24, 55, 103, 148 \mu\text{g l}^{-1}$ (series A). Additional IQC samples were prepared for work carried out on ID and DRC-ICP-MS, with comparable values of $22, 55, 104, 138 \mu\text{g l}^{-1}$ selenium (Series B). Certified reference material consisted of a lyophilised serum of human origin, Seronorm (Lot:704121) and of bovine serum NIST 1598. The Seronorm reference material assigned analytical values of 73 and $86 \mu\text{g l}^{-1}$ selenium for the sample (results obtained from two reference laboratories), and $42.4 \pm 3.5 \mu\text{g l}^{-1}$ selenium for NIST 1598.

Analysis of certified quality control sera Seronorm (704121) and NIST 1598, and our own IQC material, showed little bias difference between the methods. A mean bias between observed and target values ranged from $-0.5 \mu\text{g l}^{-1}$ ($-0.006 \mu\text{mol l}^{-1}$) obtained by HG-ICP-MS, to $+2.0 \mu\text{g l}^{-1}$ ($+0.025 \mu\text{mol l}^{-1}$) determined by conventional DRC-ICP-MS (Tables 9.1. and 9.2.).

Table 9.1. Internal quality control data for serum determination by conventional analysis using SN-ICP-MS (Series A IQCs employed).

	Target value ($\mu\text{g l}^{-1}$)	Observed Value ($\mu\text{g l}^{-1}$)
IQC sample		Mean \pm sd
Level 1	23.7	22.2 ± 2.0
Level 2	54.5	54.7 ± 2.7
Level 3	102.7	103.4 ± 2.0
Level 4	147.7	149.9 ± 3.8
Seronorm	73 / 86	74.7 ± 2.6
Nist 1598	42.4	42.4 ± 1.3
Mean Bias	($\mu\text{g l}^{-1}$)	0.6

Table 9.2. Internal quality control data for serum determination by HG-ICP-MS, IDMS, conventional and ID analysis using DRC-ICP-MS (Series B IQCs employed).

IQC sample	Target value	IDMS	Observed Values		Mean \pm sd ($\mu\text{g l}^{-1}$)		
			DRC		Hydride 77Se	Generation 78Se	ICP-MS 82Se
			Conventional	IDMS			
Level 1B	21.5	21.1 ± 1.2	22.9 ± 1.2	21.3 ± 0.9	22.8 ± 3.3	22.4 ± 3.3	22.2 ± 2.9
Level 2B	54.6	53.4 ± 1.2	56.2 ± 2.0	54.8 ± 0.9	51.7 ± 4.8	51.9 ± 2.8	52.0 ± 2.5
Level 3B	104.0	105.3 ± 2.2	107.9 ± 3.8	106.0 ± 2.4	99.9 ± 2.4	100.0 ± 3.5	98.8 ± 3.5
Level 4B	138.2	137.5 ± 2.4	141.8 ± 3.9	140.3 ± 2.6	143.4 ± 4.4	142.6 ± 5.0	141.4 ± 3.9
Seronorm	73 / 86	72.0 ± 1.9	75.0 ± 3.1	73.1 ± 1.8	74.0 ± 3.2	73.3 ± 3.7	74.2 ± 4.9
Nist 1598	42.4	43.3 ± 1.9	42.0 ± 1.8	43.4 ± 1.5	41.3 ± 4.4	40.7 ± 3.9	41.5 ± 4.1
Mean Bias	($\mu\text{g l}^{-1}$)	-0.2	2.0	0.9	-0.1	-0.5	-0.5

Analytical precision was demonstrated by the percentage relative standard deviation obtained for the analysis of ten sample preparations, the reproducibility of analysis on a day to day basis, and the regression fit of data obtained for standard addition calibrations.

A comparison of within-run reproducibility in Figure 9.3, shows similar precision variation of $\pm 5\%$ RSD at $20 \mu\text{g l}^{-1}$ ($0.25 \mu\text{mol l}^{-1}$), to $\pm 1.5\%$ RSD at $150 \mu\text{g l}^{-1}$ ($1.9 \mu\text{mol l}^{-1}$) selenium, for standard addition analysis, with the exception of hydride generation. IDMS analysis, both with and without DRC, demonstrated a consistent variation of $\pm 2\%$ RSD throughout the concentration range.

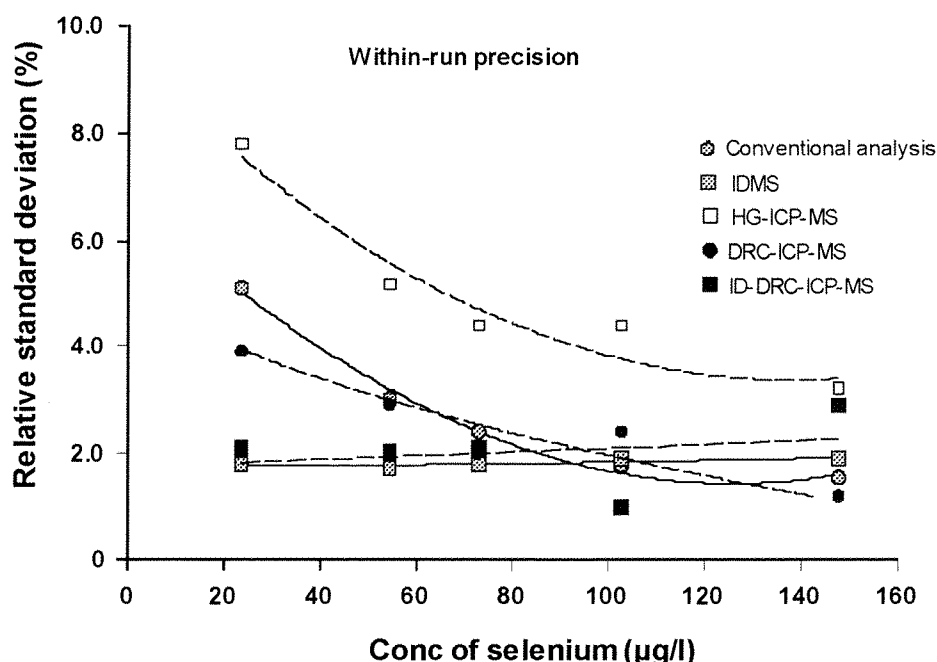


Figure 9.3. Comparison of within-run precision data for conventional and ID analysis by direct SN-ICP-MS and DRC, and for HG-ICP-MS analysis.

The reproducibility of analysis by the hydride generation method for between-run determination, again did not reach the level of precision demonstrated by the other techniques, and DRC analysis appeared to display more inconsistency at higher concentrations (Figure 9.4). Over the concentration range, ID-DRC-ICP-MS gave the overall lowest relative standard deviation.

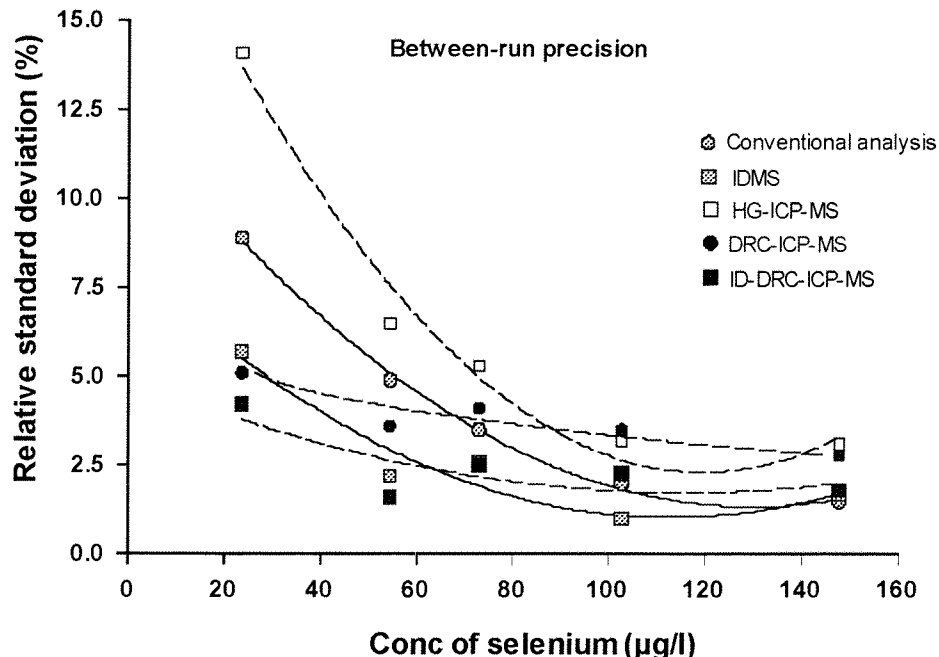
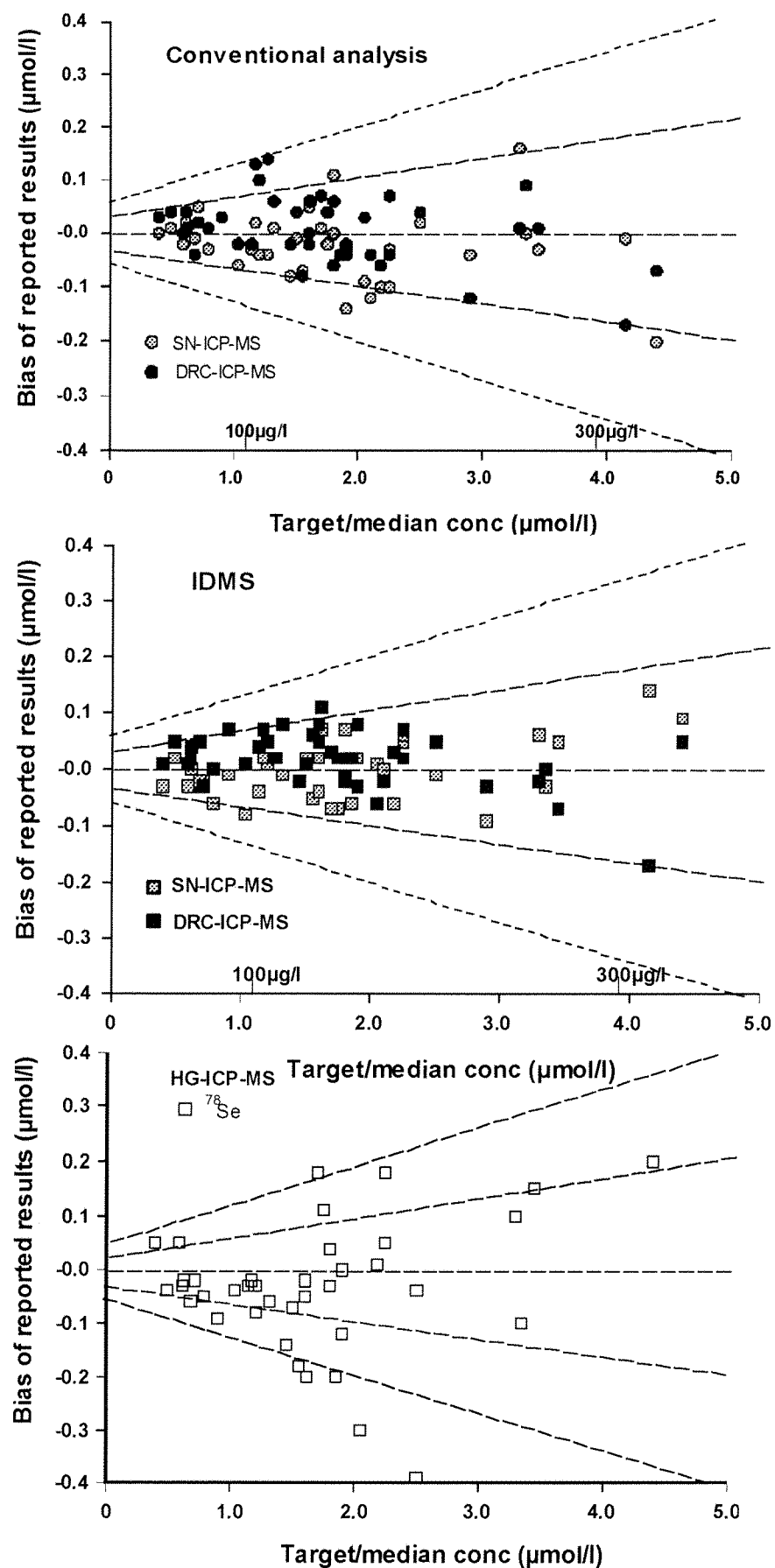


Figure 9.4. Comparison of between-run precision data for conventional and ID analysis by direct SN-ICP-MS and DRC, and for HG-ICP-MS analysis.

9.2.4. Intra-laboratory comparison of EQA samples

The analysis of 40 samples provided by the two EQA centres, enabled an assessment on accuracy of the methods investigated. With the exception of HG-ICP-MS, all techniques well exceeded the minimum requirements for an acceptable analytical performance of not less than 60% within the inner zone and 80% within the outer zone.

Comparison of the bias from the target values can be seen in Figure 9.5., with the reduction of the overall spread of mean bias: $0.0 \pm 4.0 \mu\text{g l}^{-1}$ ($-0.00 \pm 0.05 \mu\text{mol l}^{-1}$) for ID analysis, compared with $-0.8 \pm 5.5 \mu\text{g l}^{-1}$ ($-0.01 \pm 0.07 \mu\text{mol l}^{-1}$) for conventional analysis by SN-ICP-MS. For isotope dilution analysis 98% of the results were within the inner zone.



Figures 9.5. Comparison of the bias from target values, of sera determined by conventional and ID analysis by direct (SN) and DRC-ICP-MS, and HG-ICP-MS.

A positive mean bias of $1.6 \pm 4.0 \mu\text{g l}^{-1}$ ($0.02 \pm 0.05 \mu\text{mol l}^{-1}$) was obtained on determination of the EQA concentrations by ID-DRC-ICP-MS analysis.

For hydride generation, 55-65% of the values were within the inner zone and 84% were within the outer zone, for the three isotopes. The spread of bias was found to be $-4.0 \pm 10.3 \mu\text{g l}^{-1}$ ($-0.05 \pm 0.13 \mu\text{mol l}^{-1}$) for ^{78}Se , reflecting the inability of the technique to achieve the accuracy obtained by solution nebulisation.

9.3. Conclusion

The order of both precision and accuracy of analysis was found to be:

ID-DRC-ICP-MS \cong ID-SN- ICP-MS $>$ DRC-ICP-MS \cong SN-ICP-MS $>>$ HG-ICP-MS

OVERALL CONCLUSIONS AND SUGGESTIONS FOR FURTHER WORK

A method has been developed for the direct analysis of selenium by ICP-MS, in which the spectral interferences normally experienced by low-resolution detection have been reduced sufficiently to enable precise and accurate determination in serum. The reliability of this routine method was demonstrated by the good performance achieved in external quality control programmes over a period of three years. The versatility of the procedure has been shown by its application to the analysis of more complicated matrices of whole-blood and erythrocytes, and low level analysis in protein association investigations.

The potential of isotope dilution analysis was investigated with a view to improving both the reproducibility and accuracy of the developed method. This has been achieved by the measurement of $^{78}\text{Se} : ^{74}\text{Se}$ ratio, with the suppression of the argon-adduct interference at mass 78, and the signal enhancement of both isotopes accomplished by the use of an organic solvent. The enhanced precision over conventional analysis was due to the internal standardisation being carried out by an isotope of the analyte (^{74}Se), which experienced the same changes in signal sensitivity due to instrumental fluctuations and ionisation efficiency, as the selenium isotope being measured (^{78}Se).

The method features a series of calibrating solutions, rather than being reliant on a specific concentration solution as is common practise for mass bias correction in isotope dilution analysis. This has enabled the simplification of the data processing associated with IDMS, since it provides an equation from which a range of selenium concentration can be accurately calculated. The use of an aqueous salt matrix for calibration, which matched the suppression of signal response to that obtained by serum, removes the uncertainty associated with the endogenous selenium concentration for the calibrating serum. Validated using certified reference materials, the method is shown to be more accurate and capable of greater precision than conventional standard addition methodology applied to ICP-MS analysis.

HG-ICP-MS is representative of the established methodology used for selenium determination by ICP-MS detection. The technique requires time consuming sample preparation, and is less reliable, producing data of a poorer quality compared to that of direct ICP-MS. In assessing the method, attention was focused on isotope dilution analysis, which was found to be impracticable for both ^{78}Se : ^{77}Se and ^{78}Se : ^{74}Se measurement. Analysis using ^{74}Se -enriched standard was susceptible to memory effects, and spiking with ^{77}Se -enriched standard gave poor reproducibility and showed a large positive bias on selenium concentrations.

Reaction cell technology, which has only recently become commercially available and is relatively expensive, was found to be capable of matching the precision by conventional and ID, ICP-MS detection. Isotope dilution measurement by this technique offers the potential for higher accuracy than that achieved by conventional analysis, due to the reduced background signals. The full potential was not realised in the limited studies carried out, in which the impact of the chemistry and physics involved in the pressurised reaction cell on selenium detection needs to be addressed. The matrix dependency of the individual isotopes and how they are altered by changes in scanning parameters, need to be examined.

Destabilisation of the argon-adducts by DRC instrumentation, enables the measurement of ^{80}Se and ^{76}Se isotopes, and allows a number of isotopic combinations for ID analysis. Employment of ^{76}Se and ^{78}Se -enriched standards would offer the prospect of better precision, due to the optimal blend consisting of a more even proportion of spike to natural isotope arising from the less marked differences in natural isotopic abundance. The assessment of the performance of ^{80}Se : ^{78}Se , ^{80}Se : ^{76}Se and ^{78}Se : ^{76}Se ID, may also provide information towards understanding the behaviour of these isotopes during DRC detection.

Multicollector magnetic field instrumentation provides simultaneous detection of analytes within the sample and the ability to destabilise interfering polyatomic ions. However, the sample introduction system of the ICP-MC-MS was unsuitable for the direct analysis of clinical samples. Analysis of digested sera would need to be investigated to determine whether the advantages of this technique improve on the levels of accuracy and precision presented in this thesis, despite the additional sample preparation required.

The development of these procedures was governed by their application to routine analysis of clinical samples, with limited sample volume and a relatively short analysis time. The presented method using standard addition calibration by solution nebulisation ICP-MS provides the quality of analysis necessary for clinical interpretations to be made.

The investigations described in the thesis have been directed towards developing a method using low resolution quadrupole instrumentation for which greater precision and accuracy can be acquired for selenium measurement in clinical samples. This has been achieved by isotope dilution. The described procedure is as straightforward as conventional quantitative analysis, with the advantages associated with ID, demonstrating a better reproducibility and accuracy for selenium determination by low resolution ICP-MS.

References

1. Schwarz K, Foltz C. Selenium as an integral part of factor 3 against dietary necrotic liver disease. *J. Am. Chem. Soc.* 1957, 59, 3292-3.
2. Rotruck J, Pope A, Ganther H, Swanson A, Hafeman D, Hoekstra W. Selenium: biochemical role as a component of glutathione peroxidase. *Science* 1973, 179, 588-90.
3. Beck M, Levander O. Dietary oxidative stress and the potentiation of viral infection. *An. Rev. Nutr.* 1998, 18, 93-116.
4. Coombs G, et al. Selenium and carcinogenesis. Symposium presented by American Institute of Nutrition. *Fed. Proc.* 1985, 44, 2561-89.
5. Levander O. A global view of human selenium nutrition. *Ann. Rev. Nutr.* 1987, 7, 227-50.
6. Allan C, Lacourciere G, Stadtman T. Responsiveness of selenoproteins to dietary selenium. *Ann. Rev. Nutr.* 1999, 19, 1-16
7. Behne D, Kyriatopoulos A, Meinhold H, Kohrb J. Identification of type I iodothyronine 5' deiodinase as a selenoenzyme. *Biochem. Biophys. Res. Comm.* 1990, 73, 1143-1149.
8. Contempre B, Vanderpass J, Dumont J, Nyo B, Diplock A. Effect of selenium supplementation on thyroid hormone metabolism in a iodine and selenium deficient population. *Clin. Endocrinol.* 1992, 36, 579-83.
9. Scott R, MacPherson A, Yates R, Hussain B, Dixon J. The effect of oral selenium supplementation on human sperm motility. *Br. J. Urol.* 1998, 82, 76-80.
10. Strauss E. Selenium's role in infertility explained. *Science* 1999, 285, 1339.
11. Barrington J, Lindsay P, James D, Smith S, Roberts A. Selenium deficiency and miscarriage: a possible link. *Br. J. Obstret. Gynaecol.* 1996, 103, 130-132.
12. Robinson M, Rea H, Friend G, Stewart R, Snow P, Thomson C. On supplementing the selenium intake of New Zealanders. Prolonged metabolic experiments with daily supplements of selenomethionine, selenite and fish. *Br. J. Nutr.* 1978, 39, 589-600.
13. Schroeder H, Frost D, Balassa J. Essential trace metals in man: selenium. *J. Chronic Dis.* 1970, 23, 227-43.
14. Thorn J, Robertson J, Buss D, Bunton N. Trace nutrients: Selenium in Bristish food. *Br. J. Nutr.* 1978, 39, 391-6.
15. Barclay M, MacPherson A, Dixon J. Selenium content of a range of UK foods. *J. Food Comp. Anal.* 1995, 8, 307-18.

16. Diplock A. Indexes of selenium status in human population. *Am. J. Nutr.* 1993, 57, 256S-8S.
17. Burk R. Selenium in man. In: 'Trace metals in human health and disease,' Vol 2. eds. Prased A, Oberlea D. *publ.* Academic Press, New York 1976, pgs. 105-33.
18. Levander O. Considerations on the assessment of selenium status. *Fed. Proc.* 1985, 44, 2579-83.
19. Report of a WHO expert committee. Selenium. In: ' Trace elements in human nutrition and health. 1996, 1, 105-22.
20. Pyrzynska K. Speciation analysis of some organic selenium compounds. A review. *Analyst* 1996, 121, 77R-83R.
21. Petrovic V, Buzadzic B, Saicic Z, Spasic M. Selenium metabolism with a special interest in Se-dependant glutathione peroxidase. Serbian academy of sciences and arts. Scientific meeting - conference on selenium. Belgrade 1995.
22. Combs G, Combs S. The nutritional biochemistry of selenium. *Ann. Rev. Nutr.* 1984, 4, 257-80.
23. Sandholm M. Function of erythrocytes in attaching selenite into specific plasma proteins. *Acta pharamacol. Toxicol.* 1975, 36, 321-27.
24. Patterson B, Zech L. Development of a model for selenite metabolism in humans. *J. Nutr.* 1992, 122, 709.
25. Swanson C, Patterson B, Levander O, Veillon C et al. Human ^{74}Se -selenomethionine metabolism: a kinetic model. *Am. J. Clin. Nutr.* 1991, 54, 917.
26. Sandholm M. The initial fate of a trace amount of intravenously administered selenite. *Acta pharamacol. Toxicol.* 1973, 33, 1-5.
27. Suzuki K, Shiobara Y, Itoh M, Ohmichi M. Selective uptake of selenite by red blood cells. *Analyst* 1998, 123, 63-67.
28. Burk R, Brown D, Seely R, Scaief C. Infience of dietary and injected selenium on whole-body retention, route of excretion, and tissue retention of $^{75}\text{SeO}_3^{2-}$ in the rat. *J. Nutr.* 1972, 102, 1049-56.
29. Alaejos M, Romero C. Urinary selenium concentrations. *Clin. Chem.* 1993, 39, 2040.
30. Gammelgaard B, Jons O. Determination of selenite and selenate in human urine by ion chromatography and ICP-MS. *J. Anal. At. Spectrom.* 2000, 15: 945-49.
31. Goyer R, Cherian M. Tissue and cellular toxicology of metals. *Clinical chemistry and chemical toxicology of metals.* ed. Brown S. 1977 Elsevier, North-Holland Biochemical Press. 89-103.

32. Davies T. Hair analysis and selenium shampoos. *Lancet* 1982, 2, 935.
33. Nichol C, Herdman J, Sattar N, O'Dwyer P, O'Reilly D, Littlejohn D. Changes in the concentrations of plasma selenium and selenoproteins after minor elective surgery. *Clin. Chem.* 1998, 44, 1764-66.
34. Harrison I, Littlejohn D. Determination of selenium in human hair and nail by ETA-AAS. *J. Anal. At. Spectrom.* 1995, 10, 215-1.
35. Yi Sun, Haozhi Li. Determination of trace selenium in human plasma and hair with ternary inclusion compound fluorescent. *Analyst* 2000, 125, 2326-29.
36. Ge K, Young G. The epidemiology of selenium deficiency in the etiological studies of endemic diseases in China. *Am. J. Clin. Nutr.* 1993, 57, 2595-2635.
37. Yang G. Endemic selenium intoxication of humans in China. *Am. J. Clin. Nutr.* 1983, 37, 872-881.
38. Lombeck I. The evaluation of selenium state in children. *J. Inher. Metab. Dis.* 1983, 6, Suppl 1, 83-84.
39. Bratter P. Maternal selenium status influences the concentration and binding form of iodine in human milk. Sixth international symposium on metal ions in biology and medicine. *ICP Inf. Newsletter* 2000, 26, 315.
40. Rij A, Thomson C, McKenzie J, Robinson M. Selenium deficiency in TPN. *Am. J. Clin. Nutr.* 1979, 32, 2076-85.
41. Reilly C, Barnett J, Patterson C, Tirigg U, Latham S, Marrinan A. Trace element nutrition status and dietary intake of children with phenylketonuria. *Am. J. Clin. Nutr.* 1990, 52, 152-65.
42. McConnel K, Broghamer J, Blotcky A, Hurt O. Selenium levels in human blood and tissues in health and disease. *J. Nutr.* 1975, 105, 1026.
43. Look M, Rocksroh J, Rao G, Kneivzer K et al. Serum Se, plasma GSH, and erythrocyte GSH-Px levels in asymptomatic vs symptomatic human immunodeficiency virus 1(HIV-1) infection. *Eur. J. Clin. Nutr.* 1997, 51, 266-272.
44. MAFF UK:1997 Total diet study: Al, As, Cd, Cr, Cu, Pb, Hg, Ni, Se, Sn and Zn. Food surveillance information sheet no.191, 1999.
45. Rayman M. Dietary selenium: a time to act. *BMJ.* 1997, 314, 387-388.
46. Lloyd B. Selenium in relation to heart disease. Southampton Univ., MPhil thesis. 1987.
47. Arnold L. The influence of geochemistry on selenium in soils and plants of England and Wales. Ph.D. thesis. London, Imperial College of Science and Technology, 1990.

48. Thomson C, Rea H, Doesburg V, Robinson M. Selenium concentrations and glutathione peroxidase activities in whole-blood of New Zealand residents. *Brit. J. Nutr.* 1977, 37, 457-460

49. Thomson B, Stevens S, Van Rij A, Wade C, Robinson M. Selenium and vitamin E supplementation activities of GSH-Px in human tissues. *Am. J. Clin. Nutr.* 1988, 48, 316-23.

50. Rayman M. The importance of selenium to human health. *Lancet* 2000, 356, 233-241.

51. Sheehan T, Halls D. Measurement of selenium in clinical specimens. *Ann. Clin. Biochem.* 1999, 36, 301-315.

52. Watkinson J. Fluorometric determination of selenium in biological material with 2,3-diamino-naphthalene. *Anal. Chem.* 1966, 38, 92-7.

53. Welz B, Melcher M, Neve J. Determination of selenium in human body fluids by HG-AAS. *Pure. Appl. Chem.* 1987, 59, 929-36.

54. McLaughlin K, Dadgar D, Smyth M, McMaster D. Determination of selenium in blood plasma and serum by flow injection HG-AAS. *Analyst* 1990, 115, 275-8.

55. Saeed K, Thomassen Y, Langmyhr F. Direct ETA-AAS determination. *Anal. Chim. Acta* 1979, 110, 285-9.

56. Schlemmer G, Welz B. Palladium and magnesium nitrates, a more universal modifier for GF-AAS. *Spectrochim. Acta* 1986, 41B, 1157-65.

57. Ek P, Hulden S, Johansson E, Lilje fors T. A continuous HG system for ICP-MS using separately nebulised internal standards. Applications of plasma source mass spectrometry. The Royal Soc. of Chem., Cambridge. 1991, 178-198.

58. Rayman M, Abou-Shakra F, Ward N. Determination of selenium in blood serum by HG-ICP-MS. *J. Anal. At. Spectrom.* 1996, 11, 61-8.

59. Ko F, Yang M. On-line removal of interferences via anion-exchange column separation for the detection of Ge, As, and Se in biological samples by ICP-MS. *J. Anal. At. Spectrom.* 1996, 11, 413-20.

60. Townsend A. The determination of As and Se in standard reference materials using sector field ICP-MS in high resolution mode. *Fresenius' J. Anal. Chem.* 1999, 364, 521-26.

61. Douthitt C. Magnetic sector ICP-MS: Comprehensive Bibliographies of HR-ICP-MS and MC-ICP-MS. *ICP Inform Newsletter* 1999, 2, 87-119.

62. Tanner S, Baranov V. Theory, design and operation of a Dynamic reaction cell for ICP-MS. *Atomic Spectroscopy* 1999, 20, 2, 45-52.

63. Heuzen A, Hoekstra T, Van Wingerden B. Precision and accuracy attainable with ID analysis applied to ICP-MS: Theory and experiments. *J. Anal. At. Spectrom.* 1989, 4, 483-89.

64. Handbook of ICP-MS. 1993, *ed.* Jarvis K, Gray A, *publ.* Houk R. Blackie, Glasgow.

65. Hougse N, Houk R. Review: Fundamental aspects of ion extraction in ICP-MS. *Spectrochim. Acta Part B*, 1996, 51, 779-815.

66. Houk R. Mass spectrometry of ICPs. *Anal. Chem.* 1986, 58, 97A.

67. Delves HT. Biomedical applications of ICP-MS. *Chemistry in Britain*. 1988, 1009-12.

68. Bacon J, Crain J, Van Vaeck L, Williams J. Atomic spectrometry update. *J. Anal. At. Spectrom.* 1999, 14, 1633-59.

69. Bacon J, Crain J, Van Vaeck L, Williams J. Atomic mass spectrometry. *J. Anal. At. Spectrom.* 2000, 15, 1025-53.

70. Duckworth H, Barber R, Venkatasubramanian V. *eds.* Mass Spectrometry. Cambridge University Press 1986, 124-29.

71. Fieldmann I, Tittes W, Jakubowski N, Stuewer D. Performance characterises of ICP spectrometry with high mass resolution. *J. Anal. At. Spectrom.* 1994, 9, 1008-14.

72. Rodushkin I, Odman F, Olofsson R, Axelsson M. Determination of 60 elements in whole blood by sector field ICP-MS. *J. Anal. At. Spectrom.* 2000, 15, 937-44.

73. Emteborg H, Tian X, Adams F. Quality assurance of arsenic, lead, tin and zinc in copper alloys using axial ICP-TOF-MS. *J. Anal. At. Spectrom.* 1999, 14, 1567-72.

74. Busch K, Glish G, McLuckey. Mass spectrometry – Techniques and applications of tandem mass spectrometry. 1988 VCH publishers, 15-52.

75. Uchida H, Ito T. Inductively coupled nitrogen plasma mass spectrometry assisted by adding argon to the outer gas. *J. Anal. At. Spectrom.* 1995, 10, 843-848

76. Goosen J, Moens L, Dams R. A mathematical correction method for spectral interferences on selenium in ICP-MS. *Talanta* 1994, 41, 187-93.

77. Evans E, Ebdon L. Effect of organic solvents and molecular gases on polyatomic ion interferences in ICP-MS. *J. Anal. At. Spectrom.* 1990, 5, 425-430.

78. Goosens J, Vanhaecke F, Moens L, Dams R. Elimination of interferences in the determination of arsenic and selenium in biological samples by ICP-MS. *Anal. Chimica Acta* 1993, 280, 137-143.

79. Olivas R, Quetel C, Donard O. Sensitive determination by selenium by ICP-MS with flow injection and hydride generation in the presence of organic solvents. *J. Anal. At. Spectrom.* 1995, 10, 865-870.

80. Lorente L, Gomez M, Camara C. Improvement of selenium determination in water by ICP-MS through the use of organic compounds as matrix modifiers. *Spectrochim. Acta Part B* 1997, 52, 1825-1838.

81. Gammelgaard B, Jones O. Determination of selenium in urine by ICP-MS: interferences and optimisation. *J. Anal. At. Spectrom.* 1999, 14, 867-874.

82. Abou-Shakra F, Rayman M, Ward I, Hotton V, Bastian G, J. Enzymic digestion for the determination of trace elements in blood serum by ICP-MS. *Anal. At. Spectrom.* 1997, 12, 429-433.

83. Tanner S. Characterisation of ionisation and matrix suppression in IC 'Cold' plasma MS. *J. Anal. At. Spectrom.* 1995, 10, 905-921.

84. Rea H, Thomson C, Campbell D, Robinson M. Relationship between erythrocyte selenium concentration and glutathione peroxidase (EC1.11.19) activities of New Zealand residents and visitors. *Br. J. Nutr.* 1989, 42, 201-208.

85. McMaster D, Bell N, Anderson P, Love A. Automated measurement of 2 indicators of human selenium status, and applicability to population studies. *Clin Chem.* 1990, 36, 211-216.

86. Butler J, Thomson C, Whanger P, Robinson M. Selenium distribution in blood fractions of New Zealand women taking organic or inorganic selenium. *Am. J. Clin. Nutr.* 1991, 53, 748-54.

87. O. Mestek, M. Suchanek, Z. Vodickova, B. Zemanova, T. Zima. Comparison of the suitability of various atomic spectroscopic techniques for the determination of selenium in human whole-blood. *J. Anal. At Spectrom.* 1997, 12, 85-89.

88. Prohaska C, Steffan I, Torvenyi A, Pomazal K. Optimisation of different atomic spectrometric methods for the determination of selenium in blood and blood fractions. *J. Anal. At. Spectrom.* 2000, 15, 335-340.

89. B. Radziuk, and Y. Thomassen. Chemical modification and spectral interferences in Se determination using Zeeman-effect ETA-AAS. *J. Anal. At Spectrom.* 1992, 7, 397-403.

90. Carnick G, Manning D, Slavin W. Determination of selenium in biological materials with platform furnace AAS and Zeeman background correction. *Analyst* 1983, 108, 1297-1312.

91. Deagen J, Butler J, Zachara A, Whanger P. Determination of the distribution of selenium between GSHPx, selenoprotein P, and albumin in plasma. *Anal Biochem.* 1993, 208, 176-81.

92. Harrison I, Littlejohn D, Fell G. Distribution of selenium in human blood plasma and serum. *Analyst* 1996, 121, 189-94.

93. Akesson B, Bellow T, Burk R. Purification of selenoprotein P from human plasma. *Biochim. Biophys. Acta* 1994, 1204, 243-49.

94. Whanger P. Metabolism of Se in humans. *J. Trace Elem. Exp. Med.* 1998, 11, 227-40.

95. Stadtman T. Selenium-dependent enzymes. *Annu. Rev. Biochem.* 49, 93-110.

96. Takahashi K, Avissar N, Whitin J, Cohen H. Purification and characterisation of human plasma GSHPx: a selenoglycoprotein distinct from the known cellular enzyme. *Arch. Biochem. Biophys.* 1987, 256, 677-88.

97. Takahashi K, Cohen H. Selenium-dependent GSHPx protein and activity: Immunological investigation on cellular and plasma enzymes. *Blood* 1986, 68, 640-645.

98. Maddipati K, Gasporski C, Marnett L. Characterisation of the hydroperoxide-reducing activity of human plasma. *Arch. Biochem. Biophys.* 1987, 254, 9-17.

99. Read R, Bellow T, Yang J, Hill K, Palmer I, Burk R. Selenium and aminoacid composition of selenoprotein P, the major selenoprotein in rat serum. *J. Biol. Chem.* 1990, 265, 17899-905.

100. Yang J, Morrison-Plummer, Burk R. Purification and quantitation of a rat selenoprotein distinct from GSHPx using monoclonal antibodies. *J. Biol. Chem.* 1987, 262, 13372-75.

101. Burk R, Hill K, Read R, Bellow T. Response of rat selenoprotein P to selenium administration and the fate of its selenium. *Am. J. Physiol.* 264, E26-E30.

102. Hill K, Lloyd R, Yang J, Read R, Burk R. The cDNA for rat SeP contains 10 TGA codons. *J. Biol. Chem.* 266, 10050-10053.

103. Daher R, Van Lente F. Cocan Calvin A bound selenoprotein in human serum analysed by graphite furnace. *Clin. Chem.* 1994, 40, 62.

104. Persson-Moschos M, Huang W, Srikumar T, Akesson B. Selenoprotein P in serum as a biochemical marker of selenium status. *Analyst*. 1995, 120, 833-836.

105. Herman J. The properties of a rat serum protein labelled by the injection of sodium selenite. *Biochim Biophys. Acta*. 1977, 500, 61-70.

106. McKay E, Laurell C. The interaction of heparin with plasma proteins. *J. Lab. Clin. Med.* 1980, 95, 69-80.

107. Gordon D, Leinart A, Cousins R. Portal copper transport in rats by albumin. *Am. J. Physiol.* 1987, 252, E327-E333.

108. Schuitemaker L. The distribution of selenium among human serum proteins. Unpublished research project. Southampton General Hospital, 1998.
109. Fassett J, Paulsen P. ID-MS for accurate elemental analysis. *Anal Chem.* 1989, 61, 643A-648A.
110. Dixon A. Radiogenic isotope geology. 1997 *publ.* Cambridge University Press, 28-31.
111. Heumann K, Baier K, Beer F, Kifmann R, Schindlemeier W. Mass spectrometric ID analysis of trace amounts of halides. *Adv. Mass Spectrom.* 1980, 8, 318-324.
112. Heuzen A, Hoekstra T, Van Wingerden B. Precision and accuracy attainable with ID analysis applied to ICP-MS: Theory and experiments. *J. Anal. At. Spectrom.* 1989, 4, 483-489.
113. Catterick T, Fairman B, Harrington C. Structured approach to achieving high accuracy measurements with ID ICP-MS. *J. Anal. At. Spectrom.* 1998, 13, 1009-1013.
114. Lam J, McLaren J, Methven B. Determination of Cr in biological tissues by ICP-MS. *J. Anal. At. Spectrom.*, 1995, 10, 551-554.
115. Wu J, Boyle E. Low blank preconcentration techniques for the determination of Pb, Cu and Cd in small volume seawater samples by ID-MS. *Anal. Chem.* 1997, 69, 2464-2470.
116. Gregoire D. Determination of Boron in fresh and saline waters by ICP-MS. *J. Anal. At. Spectrom.* 1990, 5, 623-626.
117. Henrion A. Reduction of systematic errors in quantitative analysis by ID-MS: an iterative method. *Fresenius J. Anal. Chem.* 1994, 350, 657-658.
118. Buckley W, Budac J, Godfrey D, Koenig K. Determination of selenium by ICP-MS utilising a new hydride generation sample introduction system. *Anal. Chem.* 1992, 64, 724.
119. Tao H, Lam W, McLaren J, Determination of selenium in marine certified reference materials by HG-ICP-MS. *J. Anal. At. Spectrom.* 1993, 8, 1067-73.
120. Ohata M, Ichinose T, Furuta N. ID analysis of Se in human blood serum by using high-power nitrogen microwave - induced plasma mass spectrometry coupled with a HG technique. *Anal. Chem.* 1998, 70, 2726-2730.
121. Turner J, Hill S, Evans E, Fairman B, Wolff Brice C. Accurate analysis of selenium in water and serum using ETV-ICP-MS with isotope dilution. *J. Anal. At. Spectrom.* 2000, 15, 743-746.
122. DeBievre P, Debus G. Precision mass spectrometric ID analysis. *Nucl. Instrum. Methods* 1965, 32, 224-228.

123. Guidelines for achieving high accuracy in ID-MS. RSC Analytical Committee. LGC 1999.
124. Potts P. A Handbook of silicate rock analysis. 1987 *publ.* Blackie.
125. IUPAC., Isotopic composition of the elements 1989. Pure Appl. Chem. 1991, 63, 991-1002
126. Yoshinaga J, Shirasaki T, Oishi K, Morita M. ID analysis of Se in biological materials by nitrogen microwave-induced plasma mass spectrometry. Anal. Chem. 1995, 67, 1568-1574.
127. Quijano M, Gutierrez M, Conde M, Camara C. Optimisation of flow injection HG-ICP-MS for the determination of Se in water and serum. J. Anal. At. Spectrom. 1995, 10, 871- 74.
128. Welz B, Melcher M. Determination of selenium in human body fluids by HG-AAS -optimisation of sample decomposition. Anal. Chim. Acta 1984, 165, 131-40.
129. Bye R, Lund W. Optimal conditions for the reduction of selenate to selenite by hydrochloric acid. Fresenius Z Anal Chem. 1988, 332, 242-44.
130. Lloyd B, Holt P, Delves HT. Determination of selenium in biological samples by HG and AAS. Analyst 1982, 107, 927-33.
131. Selenium by HG ICP-MS. Unpublished method. Laboratory of the Government Chemist 1999.
132. Bowman J, Fairman B, Catterick T. Development of a multi-element HG ICP-MS procedure for the simultaneous determination of arsenic, antimony, and selenium in waters. J. Anal. At. Spectrom. 1997, 12, 313-16.
133. Santosa S, Mokudai H, Tanaka S. Automated continuous-flow HG with ICP-MS detection for the determination of trace amounts of selenium (IV), and total antimony, arsenic and germanium in sea-water. J. Anal. At. Spectrom. 1997, 12, 409-15.
134. Smaele T, Vercauteren J, Moens L, Dams R. Higher sensitivities for metal speciation. HP Peak 1999, 2, 10-11.
135. Janghorbani M, Ting W. Comparison of pneumatic nebulisation and HG ICP-MS for isotopic analysis of selenium. Anal. Chem. 1989, 61, 701-8.
136. Taylor P, DeBievre P, Walder A, Entwistle A. Validation of the analytical linearity and mass discrimination correction model exhibited by a MC-ICP-MS by means of a set of synthetic uranium isotope mixtures. J. Anal. At. Spectrom. 1995, 10, 395-97.
137. Hirata T. Lead isotopic analysis of NIST standard reference materials using MC-ICP-MS with a modified external correction method for mass discrimination effect. Analyst 1996, 121, 1407-1411.

138. New Dynamic Reaction Cell Technology. Special Issue. *Atomic Spectroscopy* 1999, 20, 45-77.
139. Denoyer E, Tanner S, Voelkopf U. A new dynamic reaction cell for reducing ICP-MS interferences using chemical resolution. *Spectroscopy* 1999, 14, 43-54.
140. Sloth J, Larsen E. The application of ICP dynamic reaction cell mass spectrometry for measurement of selenium isotopes, isotope ratios and chromatographic detection of selenoamino acids. *J. Anal. At. Spectrom.* 2000, 15, 669-72.
141. Tanner S, Baranov V, Vollkopf U. A dynamic reaction cell for ICP-MS. *J. Anal. At. Spectrom.* 2000, 15, 1261-69.

APPENDIX I

Table 1. Measurement of selenium in serum solutions by direct ICP-MS and HG-AAS

Sample	Target value $\mu\text{mol l}^{-1}$	ICP-MS Indium $\mu\text{mol l}^{-1}$	ICP-MS Tellurium $\mu\text{mol l}^{-1}$	HG-AAS result $(\mu\text{mol l}^{-1})$	%Difference ICP-MS (Indium)	from target HG-AAS	HG-AAS - ICP-MS $(\mu\text{mol l}^{-1})$
Se1	1.75	1.74	1.73	1.80	-0.6	2.9	0.06
Se2	2.18	2.02	2.08	1.94	-7.3	-11.0	-0.08
Se3	1.90	1.85	1.87	1.80	-2.6	-5.3	-0.05
Se4	2.90	2.84	2.86	2.84	-2.1	-2.1	0.00
Se5	1.50	1.55	1.49	1.56	3.3	4.0	0.01
Se6	1.60	1.59	1.65	1.76	-0.6	10.0	0.17
Se7	3.35	3.33	3.35	3.39	-0.6	1.2	0.06
Se8	3.30	3.12	3.46	3.34	-5.5	1.2	0.22
Se9	1.80	1.75	1.91	1.66	-2.8	-7.8	-0.09
Se10	2.25	2.19	2.22	2.27	-2.7	0.9	0.08
Se11	4.15	3.81	4.14	4.08	-8.2	-1.7	0.27
Se12	1.55	1.48	1.48	1.49	-4.5	-3.9	0.01
Se13	1.85	1.71	1.81	1.68	-7.6	-9.2	-0.03
Se14	1.60	1.55	1.66	1.52	-3.1	-5.0	-0.03
Se15	1.70	1.67	1.71	1.61	-1.8	-5.3	-0.06
Se16	2.50	2.36	2.52	2.27	-5.6	-9.2	-0.09
Se17	2.25	2.13	2.15	2.20	-5.3	-2.2	0.07
Se18	1.80	1.82	1.80	1.69	1.1	-6.1	-0.13
Se19	2.05	2.07	2.08	1.92	1.0	-6.3	-0.15
Se20	1.62	1.62	1.68	1.52	0.0	-6.2	-0.10
Se21	3.45	3.42	3.42	3.34	-0.9	-3.2	-0.08
Se22	2.10	2.10	1.98	1.94	0.0	-7.6	-0.16
Se23	1.45	1.46	1.38	1.36	0.7	-6.2	-0.10
Se24	1.90	1.90	1.76	1.76	0.0	-7.4	-0.14
Se25	4.40	4.31	4.02	4.28	-2.1	-2.7	-0.03
Teqas1	0.72	0.70		0.68	-2.8	-5.6	-0.02
Teqas2	0.49	0.51		0.54	4.1	10.2	0.03
Teqas3	0.72	0.70		0.68	-2.8	-5.6	-0.02
Teqas4	0.81	0.84		0.86	3.7	6.2	0.02
Teqas5	1.04	1.04		0.97	0.0	-6.7	-0.07
Teqas6	0.97	0.97		0.99	0.0	2.1	0.02
Teqas7	0.84	0.80		0.81	-4.8	-3.6	0.01
Teqas8	0.49	0.51		0.51	4.1	4.1	0.00
Teqas9	0.62	0.62		0.62	0.0	0.0	0.00
Teqas10	0.84	0.81		0.75	-3.6	-10.7	-0.06
Teqas11	1.08	1.01		1.01	-6.5	-6.5	0.00
Teqas12	0.74	0.73		0.75	-1.4	1.4	0.02
(n=37)			Bias $(\mu\text{mol l}^{-1})$	Average	-0.04	-0.06	-0.01
				%bias	-1.8	-2.8	
				sd	3.2	5.3	
				Range	-8.2 to 4.1	-11.0 to 10.2	

Measurement of selenium in serum solutions by IDMS and conventional analysis using ^{77}Se -enriched and ^{74}Se -enriched standards.

Table 2A. Measurement of ^{78}Se : ^{77}Se ratio

Sample	Target value $\mu\text{mol l}^{-1}$	ICP-MS result $\mu\text{mol l}^{-1}$	Aqueous mb80 corrected $\mu\text{mol l}^{-1}$ %bias	Aqueous mb40,80,160 $\mu\text{mol l}^{-1}$ %bias	Serum mb80 corrected $\mu\text{mol l}^{-1}$ bias	Serum mb40,80,160 $\mu\text{mol l}^{-1}$ %bias
Se1	1.75	1.74	1.72 -1.7	1.74 -0.6	1.78 1.7	1.83 4.6
Se2	2.18	2.02	2.02 -7.3	2.04 -6.4	2.09 -4.1	2.16 -0.9
Se3	1.90	1.85	1.84 -3.2	1.85 -2.6	1.90 0.0	1.96 3.2
Se4	2.90	2.84	2.78 -4.1	2.81 -3.1	2.89 -0.3	3.00 3.4
Se5	1.50	1.55	1.50 0.0	1.51 0.7	1.54 2.7	1.59 6.0
Se6	1.60	1.59	1.60 0.0	1.62 1.3	1.65 3.1	1.70 6.2
Se7	3.35	3.33	3.40 1.5	3.44 2.7	3.55 6.0	3.71 10.7
Se8	3.30	3.12	3.24 -1.8	3.28 -0.6	3.38 2.4	3.53 7.0
Se9	1.80	1.75	1.81 0.6	1.83 1.7	1.87 3.9	1.93 7.2
Se10	2.25	2.19	2.19 -2.7	2.21 -1.8	2.27 0.9	2.35 4.4
Se11	4.15	3.81	3.89 -6.3	3.95 -4.8	4.08 -1.7	4.28 3.1
Se12	1.55	1.48	1.47 -5.2	1.49 -3.9	1.52 -1.9	1.56 0.6
Se13	1.85	1.71	1.68 -9.2	1.70 -8.1	1.74 -5.9	1.79 -3.2
Se14	1.60	1.55	1.56 -2.5	1.58 -1.3	1.61 0.6	1.66 3.7
Se15	1.70	1.67	1.74 2.4	1.75 2.9	1.79 5.3	1.85 8.8
Se16	2.50	2.36	2.44 -2.4	2.47 -1.2	2.53 1.2	2.62 4.8
Se17	2.25	2.13	2.17 -3.6	2.19 -2.7	2.25 0.0	2.33 3.6
Se18	1.80	1.82	1.80 0.0	1.82 1.1	1.86 3.3	1.92 6.7
Se19	2.05	2.07	1.98 3.4	2.00 -2.4	2.05 0.0	2.12 3.4
Se20	1.62	1.62	1.58 -2.5	1.60 -1.2	1.63 0.6	1.69 4.3
Se21	3.45	3.42	3.44 -0.3	3.49 1.2	3.59 4.1	3.75 8.7
Se22	2.10	2.10	2.10 0.0	2.12 1.0	2.17 3.3	2.24 6.7
Se23	1.45	1.46	1.40 -3.4	1.41 -2.8	1.44 -0.7	1.48 2.1
Se24	1.90	1.90	1.78 -6.3	1.79 -5.8	1.83 -3.7	1.89 -0.5
Se25	4.40	4.31	4.05 -8.0	4.11 -6.6	4.25 -3.4	4.46 1.4
Teqas1	0.72	0.70	0.68 -5.6	0.68 -5.6	0.69 -4.2	0.76 2.7
Teqas2	0.49	0.51	0.46 -6.1	0.45 -8.2	0.47 -4.1	0.49 0.0
Teqas3	0.72	0.70	0.65 -9.7	0.65 -9.7	0.66 -8.3	0.66 -8.3
Teqas4	0.81	0.84	0.77 -4.9	0.77 -4.9	0.78 -3.7	0.78 -3.7
Teqas5	1.04	1.04	1.08 3.8	1.08 3.8	1.10 5.8	1.10 5.8
Teqas6	0.97	0.97	1.02 5.2	1.02 5.2	1.03 6.2	1.02 5.2
Teqas7	0.84	0.80	0.85 1.2	0.85 1.2	0.86 2.4	0.86 2.4
Teqas8	0.49	0.51	0.40 -18.4	0.39 -20.4	0.41 -16.3	0.42 -14.3
Teqas9	0.62	0.62	0.67 8.1	0.65 4.8	0.68 9.7	0.70 12.9
Teqas10	0.84	0.81	0.88 4.8	0.88 4.8	0.89 6.0	0.88 4.8
Teqas11	1.08	1.01	1.09 0.9	1.09 0.9	1.11 2.8	1.11 2.8
Teqas12	0.74	0.73	0.76 2.7	0.76 2.7	0.77 4.1	0.77 4.1
	(n=37)	Average % Bias	-2.4	-1.9	0.5	3.1
		sd	4.9	5.0	4.8	5.1
		range	-18.4 to 8.1	-20.4 to 5.2	-16.3 to 9.7	-14.3 to 12.9

Table 2B. Measurement of ^{78}Se : ^{74}Se ratio.

Sample	Target value $\mu\text{mol l}^{-1}$	ICP-MS Result $\mu\text{mol l}^{-1}$	Aqueous mb80corrected $\mu\text{mol l}^{-1}$ %bias		Aqueous mb40,80,160 $\mu\text{mol l}^{-1}$ %bias		Serum mb80 corrected $\mu\text{mol l}^{-1}$ %bias		Serum mb40,80,160 $\mu\text{mol l}^{-1}$ bias	
Se1	1.75	1.74	1.69	-3.4	1.72	-1.7	1.67	-4.6	1.74	-0.6
Se2	2.18	2.02	2.01	-7.8	2.04	-6.4	1.99	-8.7	2.06	-5.5
Se3	1.90	1.85	1.82	-4.2	1.85	-2.6	1.80	-5.3	1.87	-1.6
Se4	2.90	2.84	2.79	-3.8	2.82	-2.8	2.76	-4.8	2.85	-1.7
Se5	1.50	1.55	1.49	0.7	1.51	0.7	1.47	-2.0	1.53	2.0
Se6	1.60	1.59	1.56	-2.5	1.59	-0.6	1.55	-3.1	1.61	0.6
Se7	3.35	3.33	3.34	-0.3	3.38	0.9	3.32	-0.9	3.40	1.5
Se8	3.30	3.12	3.20	-3.0	3.24	-1.8	3.18	-3.6	3.26	-1.2
Se9	1.80	1.75	1.75	-2.8	1.78	-1.1	1.73	-3.9	1.80	0.0
Se10	2.25	2.19	2.12	-5.8	2.15	-4.4	2.10	-6.7	2.17	-3.6
Se11	4.15	3.81	3.86	-7.0	3.90	-6.0	3.84	-7.5	3.93	-5.3
Se12	1.55	1.48	1.48	-4.5	1.51	-2.6	1.46	-5.8	1.53	-1.3
Se13	1.85	1.71	1.66	-10.3	1.69	-8.6	1.64	-11.4	1.71	-7.6
Se14	1.60	1.55	1.60	0.0	1.63	1.9	1.58	-1.3	1.65	3.1
Se15	1.70	1.67	1.66	-2.4	1.69	-0.6	1.65	-2.9	1.71	0.6
Se16	2.50	2.36	2.48	-0.8	2.51	0.4	2.46	-1.6	2.54	1.6
Se17	2.25	2.13	2.18	-3.1	2.21	-1.8	2.16	-4.0	2.23	-0.9
Se18	1.80	1.82	1.74	-3.3	1.77	-1.7	1.72	-4.4	1.79	-0.6
Se19	2.05	2.07	1.99	-2.9	2.02	-1.5	1.97	-3.9	2.04	-0.5
Se20	1.62	1.62	1.67	3.1	1.70	4.9	1.65	1.9	1.72	6.2
Se21	3.45	3.42	3.48	0.9	3.52	2.0	3.45	0.0	3.54	2.6
Se22	2.10	2.10	2.03	-3.3	2.06	-1.9	2.01	-4.3	2.08	-1.0
Se23	1.45	1.46	1.43	-1.4	1.46	0.7	1.41	-2.8	1.48	2.1
Se24	1.90	1.90	1.83	-3.7	1.86	-2.1	1.81	-4.7	1.88	-1.1
Se25	4.40	4.31	4.37	-0.7	4.41	0.2	4.35	-1.1	4.45	1.1
Teqas1	0.72	0.70	0.77	6.9	0.77	6.9	0.69	-4.2	0.69	-4.2
Teqas2	0.49	0.51	0.59	20.4	0.45	-8.2	0.52	6.1	0.49	0.0
Teqas3	0.72	0.70	0.81	12.5	0.81	12.5	0.73	1.4	0.73	1.4
Teqas4	0.81	0.84	0.86	6.2	0.86	6.2	0.79	-2.5	0.79	-2.5
Teqas5	1.04	1.04	1.19	14.4	1.19	14.4	1.11	6.7	1.11	6.7
Teqas6	0.97	0.97	1.04	7.2	1.04	7.2	0.96	-1.0	0.96	-1.0
Teqas7	0.84	0.80	0.94	11.9	0.94	11.9	0.87	3.6	0.87	3.6
Teqas8	0.49	0.51	0.61	24.5	0.47	-4.1	0.54	10.2	0.51	4.1
Teqas9	0.62	0.62	0.71	14.5	0.71	14.5	0.63	1.6	0.63	1.6
Teqas10	0.84	0.81	0.87	3.6	0.87	3.6	0.76	-6.0	0.79	-6.0
Teqas11	1.08	1.01	1.15	6.5	1.15	6.5	1.07	-0.9	1.07	-0.9
Teqas12	0.74	0.73	0.78	5.4	0.78	5.4	0.71	-4.1	0.71	-4.1
	(n=37)	Average			1.6			1.1		
		% Bias			7.9			5.8		
		sd			-10.3 to 24.5			-8.6 to 14.5		
		range						-11.4 to 10.2		

Table 3. Measurement of selenium in serum solutions by IDMS and conventional analysis

Sample	Target value $\mu\text{mol l}^{-1}$	ICP-MS Result* $\mu\text{mol l}^{-1}$	%bias	IDMS result $\mu\text{mol l}^{-1}$	%bias
Se1	1.75	1.73	-1.1	1.68	-4.0
Se2	2.18	2.08	-4.6	2.12	-2.8
Se3	1.90	1.87	-1.6	1.92	1.1
Se4	2.90	2.86	-1.4	2.81	-3.1
Se5	1.50	1.49	-0.7	1.52	1.3
Se6	1.60	1.65	3.1	1.62	1.3
Se7	3.35	3.35	0.0	3.32	-0.9
Se8	3.30	3.46	4.8	3.36	1.8
Se9	1.80	1.91	6.1	1.87	3.9
Se10	2.25	2.22	-1.3	2.30	2.2
Se11	4.15	4.14	-0.2	4.29	3.4
Se12	1.55	1.48	-4.5	1.50	-3.2
Se13	1.85	1.81	-2.2	1.79	-3.2
Se14	1.60	1.66	3.8	1.56	-2.5
Se15	1.70	1.71	0.6	1.63	-4.1
Se16	2.50	2.52	0.8	2.49	-0.4
Se17	2.25	2.10	-6.7	2.31	2.7
Se18	1.80	1.80	0.0	1.78	-1.1
Se19	2.05	2.08	-4.4	2.06	0.5
Se20	1.62	1.68	3.7	1.69	4.3
Se21	3.45	3.42	-0.9	3.50	1.4
Se22	2.10	1.98	-5.7	2.10	0.0
Se23	1.45	1.38	-5.5	1.43	-1.4
Se24	1.90	1.76	-7.4	1.98	4.2
Se25	4.40	4.20	-4.5	4.49	2.0
Teqas 517	0.71	0.76	7.0	0.69	-2.8
Teqas 518	0.62	0.63	1.6	0.62	0.0
Teqas 519	1.21	1.17	-3.3	1.23	1.7
Teqas 523	0.49	0.50	2.0	0.51	4.1
Teqas 524	0.61	0.63	3.3	0.58	-4.9
Teqas 525	1.20	1.16	-3.3	1.21	0.8
Teqas 526	0.90	0.93	3.3	0.89	-1.1
Teqas 527	1.03	0.97	-5.8	0.95	-7.8
Teqas 528	1.14	1.11	-2.6	1.10	-3.5
Teqas 529	1.32	1.33	0.8	1.31	-0.8
Teqas 530	0.59	0.57	-3.4	0.56	-5.1
Teqas 531	1.17	1.19	1.7	1.19	1.7
Teqas 537	0.79	0.76	-3.8	0.73	-7.6
Teqas 553	0.39	0.39	0.0	0.36	-7.7
Teqas 554	0.68	0.67	-1.5	0.66	-2.9
(n=40)	Av % Bias		-0.6		-0.8
	sd		3.6		3.3
	range		-7.4 to 7.0		-7.7 to 4.3

* Tellurium as internal standard

Table 4. Measurement of selenium in serum solutions by HG-ICP-MS and conventional SN-ICP-MS analysis

Sample	Target value $\mu\text{mol l}^{-1}$	ICP-MS result $\mu\text{mol l}^{-1}$	77Se result $\mu\text{mol l}^{-1}$	%bias	78Se result $\mu\text{mol l}^{-1}$	%bias	82Se result $\mu\text{mol l}^{-1}$	%bias
Se1	1.75	1.73	1.89	7.8	1.86	6.3	1.77	0.9
Se2	2.18	2.08	2.15	-1.6	2.19	0.6	2.08	-4.7
Se3	1.90	1.87	1.91	0.7	1.90	0.2	1.85	-2.7
Se4	2.90	2.86	2.52	-13.1	2.51	-13.5	2.53	-12.9
Se5	1.50	1.49	1.48	-1.4	1.43	-4.8	1.37	-8.4
Se6	1.60	1.65	1.60	-0.3	1.58	-1.0	1.48	-7.5
Se7	3.35	3.35	3.29	-1.8	3.25	-3.0	3.11	-7.2
Se8	3.30	3.46	3.39	2.8	3.40	3.0	3.27	-1.0
Se9	1.80	1.91	1.85	3.0	1.84	2.1	1.73	-3.9
Se10	2.25	2.22	2.42	7.5	2.43	8.0	2.28	1.2
Se11	4.15	4.14	4.08	-1.6	4.02	-3.0	3.85	-7.2
Se12	1.55	1.48	1.31	-15.7	1.37	-11.6	1.34	-13.2
Se13	1.85	1.81	1.62	-12.2	1.65	-11.0	1.58	-14.5
Se14	1.60	1.66	1.61	0.9	1.55	-3.1	1.46	-9.1
Se15	1.70	1.71	1.93	13.6	1.88	10.5	1.78	4.9
Se16	2.50	2.52	2.54	1.6	2.46	-1.6	2.33	-6.7
Se17	2.25	2.15	2.32	3.3	2.30	2.3	2.19	-2.8
Se18	1.80	1.80	1.83	1.6	1.77	-1.7	1.69	-6.0
Se19	2.05	2.08	1.75	-14.6	1.75	-14.5	1.66	-19.0
Se20	1.62	1.68	1.32	-18.2	1.42	-12.2	1.32	-18.2
Se21	3.45	3.42	3.57	3.5	3.60	4.3	3.41	-1.3
Se22	2.10	1.98	1.70	-18.9	1.69	-19.7	1.62	-22.7
Se23	1.45	1.38	1.38	-4.6	1.31	-9.7	1.28	-11.7
Se24	1.90	1.76	1.71	-10.1	1.78	-6.1	1.83	-3.6
Se25	4.40	4.26	4.59	4.4	4.60	4.6	4.61	4.7
Teqas 517	0.71	0.76	0.70	-1.7	0.69	-2.9	0.77	8.9
Teqas 518	0.62	0.63	0.65	4.4	0.60	-2.9	0.65	5.0
Teqas 519	1.21	1.17	1.19	-2.0	1.13	-6.9	1.17	-3.3
Teqas 523	0.49	0.50	0.49	0.2	0.45	-8.0	0.49	1.0
Teqas 524	0.61	0.63	0.56	-8.3	0.58	-5.1	0.61	12.8
Teqas 525	1.20	1.16	1.23	2.9	1.17	-2.1	1.20	3.5
Teqas 526	0.90	0.93	0.84	-7.0	0.81	-10.1	0.90	-4.4
Teqas 527	1.03	0.97	1.02	-1.1	0.99	-4.1	1.03	0.8
Teqas 528	1.14	1.11	1.02	-10.3	1.11	-2.8	1.14	-7.5
Teqas 529	1.32	1.33	1.32	0.4	1.26	-4.4	1.32	-0.7
Teqas 530	0.59	0.57	0.66	12.3	0.64	8.1	0.59	14.5
Teqas 531	1.17	1.19	1.18	0.7	1.15	-1.5	1.17	1.9
Teqas 537	0.79	0.76	0.67	-14.9	0.74	-6.2	0.79	-5.8
Teqas 553	0.39	0.39	0.44	12.0	0.44	12.6	0.39	6.9
Teqas 554	0.68	0.67	0.69	0.8	0.62	-9.1	0.68	1.8
(n=40)		Average %	-1.87		-3.0		-3.1	
		Bias sd	8.2		7.1		8.3	
		Range	-18.9 to 13.6		-19.7 to 12.6		-22.7 to 14.5	

**Table 5. Measurement of selenium in serum solutions by DRC-ICP-MS
 ^{78}Se : ^{74}Se ID-DRC-ICP-MS, and conventional SN-ICP-MS analysis.**

Sample	Target value $\mu\text{mol l}^{-1}$	ICP-MS Result* $\mu\text{mol l}^{-1}$ %bias		DRC-ICP-MS Result $\mu\text{mol l}^{-1}$ %bias		ID-DRC-ICP-MS ^{78}Se : ^{74}Se $\mu\text{mol l}^{-1}$ %bias	
Se1	1.75	1.73	-1.1	1.79	2.3	1.77	1.1
Se2	2.18	2.08	-4.6	2.21	-2.8	2.21	1.4
Se3	1.90	1.87	-1.6	1.88	-1.1	1.87	-1.6
Se4	2.90	2.86	-1.4	2.78	-4.1	2.87	-1.0
Se5	1.50	1.49	-0.7	1.54	2.7	1.51	0.7
Se6	1.60	1.65	3.1	1.58	-1.3	1.65	3.1
Se7	3.35	3.35	0.0	3.44	2.7	3.35	0.0
Se8	3.30	3.46	4.8	3.31	0.3	3.28	-0.6
Se9	1.80	1.91	6.1	1.74	-3.3	1.79	-0.6
Se10	2.25	2.22	-1.3	2.21	-1.8	2.27	0.9
Se11	4.15	4.14	-0.2	3.98	-4.1	3.98	-4.1
Se12	1.55	1.48	-4.5	1.47	-5.2	1.61	3.9
Se13	1.85	1.81	-2.2	1.81	-2.2	1.87	1.1
Se14	1.60	1.66	3.8	1.60	0.0	1.68	5.0
Se15	1.70	1.71	0.6	1.77	4.1	1.73	1.8
Se16	2.50	2.52	0.8	2.54	1.6	2.55	2.0
Se17	2.25	2.10	-6.7	2.32	3.1	2.32	3.1
Se18	1.80	1.80	0.0	1.86	3.3	1.78	-1.1
Se19	2.05	2.08	-4.4	2.08	1.5	1.99	-2.9
Se20	1.62	1.68	3.7	1.68	3.7	1.73	6.8
Se21	3.45	3.42	-0.9	3.46	0.3	3.38	-2.0
Se22	2.10	1.98	-5.7	2.06	-1.9	2.08	-1.0
Se23	1.45	1.38	-5.5	1.44	-1.4	1.43	-1.4
Se24	1.90	1.76	-7.4	1.86	-2.1	1.98	4.2
Se25	4.40	4.20	-4.5	4.30	-1.6	4.45	1.1
Teqas 517	0.71	0.76	7.0	0.73	2.8	0.68	-4.2
Teqas 518	0.62	0.63	1.6	0.63	1.6	0.66	6.5
Teqas 519	1.21	1.17	-3.3	1.35	11.6	1.23	1.7
Teqas 523	0.49	0.50	2.0	0.53	8.2	0.54	10.2
Teqas 524	0.61	0.63	3.3	0.65	6.6	0.63	3.3
Teqas 525	1.20	1.16	-3.3	1.30	8.3	1.25	4.2
Teqas 526	0.90	0.93	3.3	0.93	3.3	0.97	7.8
Teqas 527	1.03	0.97	-5.8	1.01	-1.9	1.04	1.0
Teqas 528	1.14	1.11	-2.6	1.12	-1.8	1.18	3.5
Teqas 529	1.32	1.33	0.8	1.38	4.5	1.40	6.1
Teqas 530	0.59	0.57	-3.4	0.59	0.0	0.60	1.7
Teqas 531	1.17	1.19	1.7	1.30	11.1	1.24	6.0
Teqas 537	0.79	0.76	-3.8	0.80	1.3	0.79	0.0
Teqas 553	0.39	0.39	0.0	0.42	7.7	0.40	2.6
Teqas 554	0.68	0.67	-1.5	0.64	-5.9	0.73	7.4
(n=40)	Av % Bias	-0.6		1.3		1.9	
	sd	3.6		4.2		3.3	
	range	-7.4 to 7.0		-5.9 to 11.6		-4.2 to 10.2	

*Tellurium as internal standard

APPENDIX II

1. INSTRUMENTAL OPERATING CONDITIONS

The following instrumental conditions were common to conventional SN-ICP-MS, ID-SN-ICP-MS and HG-ICP-MS. Variations specific for each of the techniques are described separately.

SN-ICP-MS

Data system	IBM Personal System/ 2 Model 70 386 computer
Autosampler	Gilson 221
Torch	Standard demountable quartz torch with 2.0mm id alumina injector tube
Neubuliser	Cross-flow
Plasma gas flow rate	15.00 l min ⁻¹
Sampling / skimmer cone	Platinum/Nickel

Conventional SN-ICP-MS (Elan 5000)

rf power	1000 W
Autosampler wash solution	0.05%v/v Triton-X-100, and 0.5% butan-1-ol.
Auxiliary gas flow rate	0.8 l min ⁻¹
Nebuliser gas flow rate	0.92 l min ⁻¹
Sample uptake rate	0.8 ml min ⁻¹ (by peristaltic pump)
Measurements	80 ms dwell time, 75 sweeps/reading, 1 reading/ replicate, 3 replicates
Masses	78 and 128 (⁷⁸ Kr and ¹²⁸ Xe correction removed)
Calibration Method	Additions Calibration

ID-SN-ICP-MS (Elan 6100DRC)

rf power	1200 W
Autosampler wash solution	0.05%v/v Triton-X-100, 1% butan-1-ol, and 6.7% blood diluent.
Auxiliary gas flow rate	1.0 l min ⁻¹
Nebuliser gas flow rate	0.8 – 0.9 l min ⁻¹ (Optimised daily for ⁷⁴ Se)
Lens voltage	8-11V (Optimised daily for ⁷⁴ Se)
Sample uptake rate	Peristaltic pump setting -18
Measurements	10 ms dwell time, 1000 sweeps/reading, 1 reading/ replicate, 3 replicates
Masses	74 and 78 (⁷⁴ Ge and ⁷⁸ Kr correction removed)

HG-ICP-MS

Elan 5000 coupled to FIAS-200 Flow Injection System (Perkin-Elmer, Beaconsfield)

Autosampler	AS-90
Between sample wash-out time	10 s
rf power	1250 W
Nebuliser gas flow rate	0.95 l min ⁻¹
Measurements	200 ms dwell time, 1 sweeps/reading, 54 reading/ replicate, 2 replicates
Masses	77, 78 and 82
Calibration Method	Additions Calibration
FIAS program:	

Program step	Start Read	Time (sec)	Speed (rpm) Pump1	Speed (rpm) Pump2	Valve Position
Pre-sample		10	100	0	1
1		5	100	0	1
2		3	0	0	1
3		1	0	70	2
4	X	11	0	70	2
5		1	0	0	1
6		0	0	0	1
7		0	0	0	1
8		0	0	0	1
Post-run		10	100	0	1

DRC -ICP-MS (Elan 6100DRC)

Data system	Elan software Version 2.3.2. Windows NT.	
rf power	1200 W	
Auxiliary gas flow rate	1.0 l min ⁻¹	
Nebuliser gas flow rate	0.8 – 0.9 l min ⁻¹	(Optimised daily)
Lens voltage	8-11 V	(Optimised daily)
Detector mode	Pulse counting	
Sample uptake rate	Peristaltic pump setting	-18
Wash solution	0.5% butan-1-ol, 0.05% Triton-X100, 6.7% blood diluent.	
DRC parameters:	Methane gas flow rate	0.5 ml min ⁻¹
	Cell rod offset	0V
	Quadrupole rods offset	-16V
	Cell potential voltage	-20V

Conventional DRC-ICP-MS

Measurements	500ms dwell time, 5 sweeps/reading, 1 reading/ replicate, 3 replicates
Masses	76, 78 and 125 (⁷⁸ Kr correction removed)
Calibration Method	Additions Calibration
<i>q</i> parameter	0.72 for ⁷⁶ Se, 0.7 for ⁷⁸ Se, 0.44 for ¹²⁵ Te
Settling time	3ms

ID-DRC-ICP-MS

Measurements	10ms dwell time, 1000 sweeps/reading , 1 reading/ replicate, 3 replicates
Masses	⁷⁴ Se (⁷⁴ Ge correction removed)
	⁷⁶ Se, ⁷⁷ Se
	⁷⁸ Se (⁷⁸ K correction removed)
	⁸⁰ Se, ⁸² Se (with ⁷⁹ Br correction)
<i>q</i> parameter	0.7
Settling time	0.2ms

2. REAGENTS FOR ICP-MS METHODOLOGY.

These reagents were common to conventional SN-ICP-MS, ID-ICP-MS, HG-ICP-MS and DRC-ICP-MS. Variations specific for each of the techniques are described separately.

Distilled, then de-ionised water	-Milli-Q system, Millipore, Watford, Hertfordshire.
Nitric acid "Aristar" (16 mol l ⁻¹)	- Merck, Poole, Dorset .
Calibration	
Selenium solution, at 1020 mg l ⁻¹	- Sigma-Aldrich, Poole, Dorset.
Bovine serum	-Selbourne Biological Services, Alton, Hampshire.
Sample diluents:	
Triton-X-100	-Merck, Poole, Dorset.
Butan-1-ol 'Certified quality'	-Fisher Scientific Ltd.
Modifier solution: 1% v/v ammonia, 1.16 g l ⁻¹ (NH ₄) ₂ H ₂ EDTA, and 0.33% v/v ammonium phosphate, all of "Aristar" purity, Merck, Poole, Dorset.	
Disposable test tubes (RT25: 65x10mm)	- Merck, Poole, Dorset
Autosampler tray, coded: 28 (Maximum tube capacity of 108)	- Gilson, Anachem, Luton, Bedfordshire
Certified reference materials:	
Seronorm lyophilised serum samples Nist 1598	-Nycomed Pharma Diagnostics, Oslo, Norway. -National Institute of Standards and Technology.

Conventional ICP-MS

Internal standard solution: Tellurium (1 mg ml⁻¹) - Merck, Poole, Dorset

ID-ICP-MS

Stable isotopes:

Enriched ⁷⁴Se/4 isotope standard -AEA Technology, Nuclear Science, Didcot.
2.0 mg of the enriched isotope was digested in 200 μ l concentrated nitric acid and the solution was made up to 100 ml in a volumetric flask, to give a selenium stock solution of 20 μ g ml⁻¹ Se in 0.1% HNO₃.
Sodium Chloride "Analar" -Merck, Poole, Dorset.

HG-ICP-MS

Digestion:

Nitric acid "Aristar" (16 mol l⁻¹) - Merck, Poole, Dorset.
Sulphuric acid "Primar" (18 mol l⁻¹) -Fisons, Loughborough, Leicestershire.
Hydrochloric acid "Primar" (11 mol l⁻¹) -Fisons, Loughborough, Leicestershire.

Digestions were carried out on a Grant QBT block heater (Grant Instruments, Cambridge)

Borosilicate test tubes
Plastic tubes (10ml) -Teklab, Sacriston, Durham.

Hydride generation reductant:

0.02% m/v sodium tetrahydroborate -‘Spectrosol’, BDH. Poole, Dorset.
Sodium hydroxide - Fisons, Loughborough, Leicestershire.

3. STANDARD AND SAMPLE PREPARATION

Conventional ICP-MS

Working standards containing 0, 10, 20, 50, 100, 200 $\mu\text{g l}^{-1}$ selenium, in 0.1% v/v nitric acid, were diluted with the basal bovine serum in equal volume, directly in the autosampler tube. Test sera samples were dispensed with '0' aqueous standard. 100 μl aliquots of 1% Triton X-100, blood diluent and tellurium were added, and the solution was made up to 1.5 ml with deionised water and 6% v/v butan-1-ol to give a final concentration of 0.5% butanol. Reagent blanks are prepared in the same way, with deionised water replacing the serum. A summary of sample preparation is given in Table 6.

Table 6. Reagent volumes used for sample dilution for conventional and ID-ICP-MS analysis

Reagent	Conventional ICP-MS	Volume (μl)	Isotope Dilution ICP-MS	Volume (μl)
Calibrating serum	Bovine serum	100		
NaCl			140 mmol l^{-1} (70 mmol l^{-1} for DRC)	200
Aqueous Standard	0 – 200 $\mu\text{g l}^{-1}$ 0 $\mu\text{g l}^{-1}$ for test + QC	100	0, 80, 160 $\mu\text{g l}^{-1}$ 0 $\mu\text{g l}^{-1}$ for test + QC	200
Serum (QC/test)		100		200
Tellurium	100 $\mu\text{g l}^{-1}$ in 1% HNO_3	100	100 $\mu\text{g l}^{-1}$ in 1% v/v HNO_3	200
^{74}Se standard				
Triton-X-100	1% v/v	100	1% v/v	100
Blood Diluent		100		100
Butan-1-ol	6% v/v	125	6% v/v	250
Deionised water		875		450

ID-ICP-MS

200 μl serum samples were diluted with 100 μl 1% v/v Triton X-100 and blood diluent, and 250 μl 6% v/v butan-1-ol, directly into the autosampler tubes. Three matrix-matched calibration solutions were prepared by diluting NaCl in the same way as the serum samples, spiked at selenium concentrations of 0, 80, 160 $\mu\text{g l}^{-1}$. 200 μl ^{74}Se -enriched standard was added to every dilution, and the volume made up to 1.5 ml with deionised water (Table 6). The calibration and reagent blank solutions containing sodium chloride solution, were analysed at the beginning of the assay and at intervals of five samples in duplicate. All signal intensities were blank subtracted. The regression line equations obtained from the mean values of the enclosing sets of calibrating solutions were used to convert the measured ^{78}Se : ^{74}Se isotopic ratios of the test samples to concentrations.

HG-ICP-MS

Matrix matched standards were prepared by pipetting an equal volume (100 μl) of the appropriate aqueous standard (0–200 $\mu\text{g l}^{-1}$ Se) with bovine serum, and 100 μl serum test samples were aliquoted into thick-walled glass tubes in duplicate, with water replacing the serum in the reagent blanks. Aliquots of 250 μl of nitric acid, and 200 μl 25% v/v sulphuric acid were added to each tube, which were then placed in the heating-block set at 130°C for 1 hour. On the addition of 300 μl hydrochloric acid (30% v/v), the solutions were heated for a further 15 minutes. When cool, the digests were quantitatively transferred into preweighed 10 ml plastic tubes and the volume was made up to 6.0 ml with deionised water, by weight. 10% v/v hydrochloric acid was used as the carrier solution and the reductant was 0.2% m/v sodium tetrahydroborate in 0.05% m/v sodium hydroxide, made up on the day of analysis. The nebuliser and FIAS carrier gas (set at 200 ml min^{-1}) were introduced into the ICP plasma via a vapour adapter piece.

PUBLICATIONS IN SUPPORT OF CANDIDATURE

The following papers are based on work presented in this thesis:

Sieniawska C, Mensikov R, Delves HT.

Determination of total selenium in serum, whole blood and erythrocytes by ICP-MS
Journal of Analytical Atomic Spectrometry 1999; 14:109-112.

Delves HT, Sieniawska C.

Simple method for the accurate determination of selenium in serum by using ICP-MS.
Journal of Analytical Atomic Spectrometry 1997; 12:387-389.

The following published papers were included in the bound thesis. These have not been digitised due to copyright restrictions, but the links are provided.

<https://doi.org/10.1039/a806307i>

<https://doi.org/10.1039/a608027h>